Seismic response of earth dams: some recent developments*

George Gazetas

Rensselaer Polytechnic Institute, Troy, New York, USA, and National Technical University, Athens, Greece

The paper focuses on theoretical methods for estimating the dynamic response of earth dams to earthquake ground excitation. Following an outline of the historical developments in this field, the basic concepts/models for response analysis are introduced and their salient features, advantages and limitations are elucidated. The major phenomena associated with, and factors influencing, the response are identified and studied. Particular emphasis is accorded to inhomogeneity due to dependence of soil stiffness on confining pressure, nonrectangular canyon geometry, and nonlinear-inelastic soil behaviour. Several new formulations that have evolved over the last five years are outlined and characteristic results provide considerable insight into the problem. The simplicity of some of these formulations is underlined and attempts are made to compare their predictions with measurements from full-scale, natural and man-made, forced vibration tests. The basic validity as well as the limitations of the proposed analysis methods is demonstrated and topics of needed further research are suggested.

1. INTRODUCTION

The last few years have witnessed a renewed interest in understanding the seismic behaviour of earth and rockfill dams and embankments. Several new analytical/numerical formulations have been developed for predicting the response, and laboratory-based procedures have evolved for assessing the overall safety of such dams against strong potential earthquakes. At the same time the pool of available well documented case histories and of results from full-scale vibration tests have been significantly increasing, to the point that it may now be feasible to calibrate our procedures using actual measurements.

This paper focuses primarily on *new theoretical methods for estimating deformations, strains, accelerations and stresses* generated in earthfill/rockfill dams in response to earthquake ground shaking. Linear, nonlinear and inelastic formulations are presented along with characteristic results and comparative studies. A substantial effort is also devoted into assessing the capability of these methods to reproduce the recorded seismic response of several actual large dams. It is thereby shown that the developed methods can serve as useful design tools, provided their advantages and limitations are well understood. Considerable insight is gained into the mechanics of the problem and the role of several material, geometric and excitation parameters is elucidated. The paper concludes with suggested areas and topics of needed further research and attention.

2. HISTORICAL PERSPECTIVE

2.1 The pseudo-static approach

Not too many years ago the standard seismic design method for earth dams was based on the erroneous assumption that dams are *absolutely rigid bodies* fixed on their foundation and thus experiencing a uniform acceleration equal to the underlain-ground acceleration. The latter was specified in seismic codes in terms of a single peak value (typically in the range of 0.05 g to 0.20 g even for regions of the highest seismicity) and was taken as acting pseudo-statically in one-direction, giving rise to a horizontal inertia-like force on a potential slide mass. Slope instability was envisioned as the only possible mode of failure and it was not considered likely to occur unless the pseudo-static factor of safety of the trial slide mass happened to be smaller than unity.

It is now clearly understood that earth dams behave as deformable rather than rigid bodies; their response to seismic base shaking is dictated by the properties of the constituent materials, the geometry, and the nature of the base motion. Early convincing evidence of such behaviour has come from full-scale forced-vibration tests[50] and from observations of response during earthquakes[76], although it had been theoretically anticipated much earlier[68].

Other serious drawbacks of the pseudo-static procedure have been thoroughly discussed by Seed[94]. First, the horizontal inertia forces do not act permannently and in one direction but rather fluctuate rapidly in both magnitude and direction; thus, even if the factor of safety dropped momentarily below unity the slope would not necessarily experience a gross instability but might merely undergo some permanent (sliding) deformations – a notion aforesaid by Terzaghi[103] and materialized by Newmark[71]. This idea of performance controlled by magnitude of deformations rather than by limiting values of pseudostatic factors of safety has been exploited and evolved into a full-fledged standard practical procedure of assessing the seismic safety of dams and embankments consisting of nonliquefiable soils.

Another problem with the pseudo-static method is that it considers classical slope instability as the *sole* potential

* Keynote Address presented at the 2nd International Conference on Soil Dynamics and Earthquake Engineering, 28 June/3 July 1985.

0261–7277/87/010002–46 $2.00

mode of failure. In fact, over the years, several other types of seismic damage have been observed in earth dams and embankments all over the world. They include: (a) liquefaction flow failures triggered by the development of excess porewater pressures in contractive saturated fine cohesionless zones of the dam; (b) longitudinal cracks occurring near the crest due to shear sliding deformations and large tensile strains during lateral oscillations; (c) differential crest settlements and loss of free board possibly resulting from lateral sliding deformations or soil densification; (d) transverse cracks caused by tensile strains from logintudinal oscillations or by different lateral response near the abutments and near the central crest zone; and (e) piping failures through cracks in cohesive soil zones.

2.2 First stage of development of basic dynamic models

Fifty years ago (1936) Mononobe[68] was perhaps the first to consider earth dams as deformable bodies and to introduce the ingredients of what has come to be called the '*shear wedge*' or '*shear beam*' model. However, it was not until 20 years later that this model was fully explored and achieved the status of a complete engineering theory, following the work of Hatanaka and of Ambraseys. Hatanaka[41,42] demonstrated that bending-type rocking deformations are negligible compared to those in simple shear, and proposed a design method using a 'seismic coefficient' computed from the fundamental mode shape of a shear wedge in a rectangular canyon, and an underlain homogeneous elastic soil layer.

The developed shear-beam (shear-wedge) model was exploited in the 1960's and 1970's to interpret the results of full-scale tests, to conduct parameter studies aimed at gaining a better understanding of the problem, and to obtain 'seismic coefficients' for use in design.

Table 1 summarizes in chronological order the most significant developments and studies related to the shear-beam concept.

Important developments in the 1960's include the first rather successful test of the shear-beam model in light of full-scale vibration measurements on Bouquet Dam[50,51]. Predicted values for the first five natural frequencies were only about 10–20 percent higher than those actually measured; but the predicted pattern of oscillation amplitudes at each of these frequencies (i.e., the mode shapes) could hardly match the observed pattern of rapidy decreasing amplitudes with depth from the crest (Fig. 1). This discrepancy was blamed on the shear-beam assumption by noting that[51] 'on vertical section through the dam, the [measured] deflected shape of the dam is

Table 1. *Evolution of developments related to the shear-beam concept (partial list)*

Author(s) [Reference]	Contribution
Mononobe[68] 1936	first introduced the 1-D shear beam model for earth dams
Hatanaka[41,42] 1952, 1955	showed that shearing deformations are predominant; performed 2-D shear-beam analysis for dam in rectangular canyon; developed rational design procedure with use of response spectrum
Ambraseys[7,8] 1960	extended shear-beam model to account for truncated-wedge shape, rectangular canyon, and underlying elastic layer (simplified solution)
Keightly[50,51] 1963, 1966	lumped-mass shear-beam model to interpret results of full-scale tests
Martin[59] 1965	parameter studies with 1-D shear beam model; solution for modulus proportional to the cubic root of depth from crest
Seed and Martin[93] 1966	
Ambraseys and Sarma[9] 1967	used 1-D shear beam to obtain 'seismic coefficients' on potential slide blocks
Okamoto *et al.*[76] 1969	presented complete records of response of the Sannokai Dam during several earthquakes; interpretation with 1-D shear beam
Frazier[28] 1969	2-D lumped-mass shear beam model of Bouquet Canyon Dam
Petrofski *et al.*[81] 1972	2-D lumped-mass shear beam model of Mavrovo Dam
Okamoto[77] 1973	1-D shear-beam model including radiation damping through the underlying soil deposit
Sarma[91] 1979	simplified 1-D shear model of dam underlain by elastic layer deforming only in shear
Makdisi and Seed[56] 1979	simplified hand-calculation procedure based on 1-D shear beam and equivalent linearization
Abdel-Ghaffar and Scott[1,2] 1979	used 1-D and 2-D shear-beam models to compare with results of full-scale tests and of earthquake shaking
Gazetas[31] 1980	lateral and longitudinal stability of earth dams using 2-D shear beam models
Gazetas[32,33] 1981, 1982	developed analytical 1-D shear-beam model with modulus increasing as the 2/3 power of depth; extensive calibration through case histories
Gazetas[34,35] 1981	extension of shear-beam concept to study longitudinal and vertical response of homogeneous and inhomogeneous earth dams; comparison with recorded response of actual dams
Gazetas and Abdel-Ghaffar[38] 1981	used results from full-scale measurements in 12 dams to verify inhomogeneous shear-beam models
Abdel-Ghaffar and Koh[4,5] 1981	extension of shear-beam concept to logitudinal vibrations of earth dams with modulus increasing with depth from the rest
Ohmachi[73,74] 1981, 1982	simplified 3-D model: dam divided through vertical cross-sections into inter-connected superelements responding as 1-D shear beams
Gazetas *et al.*[36,37] 1981, 1982	developed a 'linear' and a 'strain-compatible piecewise linear' non-stationary random vibration formulations based on the inhomogeneous shear beam model
Abdel-Ghaffar and Koh[6] 1982	3-D model based on Galerkin formulation using linear eigenmodes as basic functions
Oner[78] 1984	simple expression for fundamental natural period of earth dams accounting in a semi-empirical way for canyon geometry and inhomogeneity
Elgamal *et al.*[27] 1984	developed simplified inelastic Galerkin-type formulations using linear
Prevost *et al.*[84] 1985	shear-beam 1-D and 2-D eigenmodes as the basis functions
Dakoulas and Gazetas[19,20,21] 1985	generalized the 1-D inhomogeneous shear-beam to account for modulus increasing as an arbitrary power m of depth: $G \sim z^m$
Dakoulas and Gazetas[22] 1985	extended shear-beam concept to obtain close-form solution for lateral vibrations of dam in semi-cylindrical canyon
Dakoulas and Gazetas[19,23] 1985	simplified nonlinear 1-D shear beam model; comparison with equivalent linear finite-element analysis

similar to the shape of a cantilever beam [deforming] in bending,' rather than in shear.

Similar conclusions were drawn by Okamoto *et al.*[76] who analysed 'complete' records of the response of the Sannokai earth dam during five distant earthquakes. Once more, values predicted with the shear model for the first two natural frequencies were in accord with the measurements. However, discrepancies were again noted between mode shapes (Fig. 1). In fact, the unexpectedly sharp decay with depth of the recorded first resonant shape led Okamoto and his co-workers to suspect that this shape corresponded to the second, rather than the first, natural mode[76]. Later, however, when ever stronger recorded motions exhibited a similar pattern of mode shapes, they rejected their initial interpretation[77]. Instead, they correctly attributed the failure of the model used to explain what was actually observed in the field *not* to any inadequancy of the shear-beam concept but rather to 'the nonuniform rigidity of the embankment... because of the different [amount of] consolidation within the dam body...'[77].

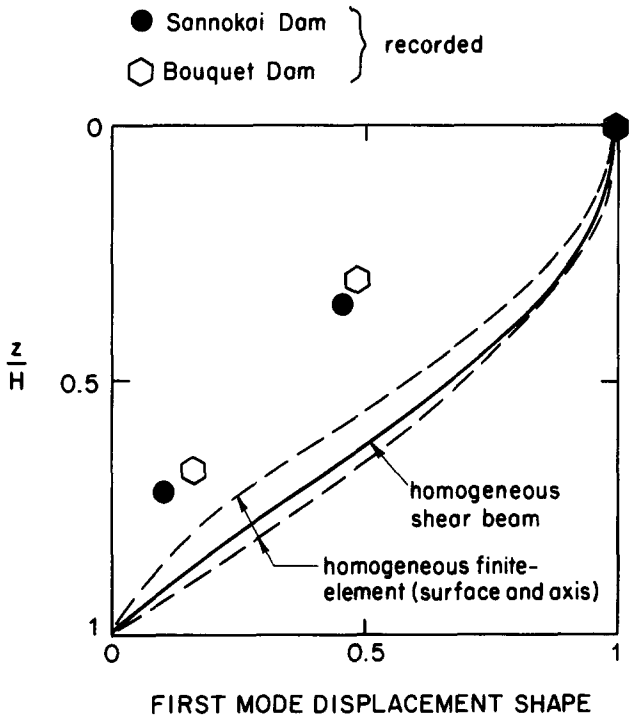

Fig. 1. The early (homogeneous) models invariably failed to explain the observed fundamental mode shapes of actual dams

The 1960's also witnessed the first implementation and subsequent wide-spread use of the *finite-element method* in studying the seismic response of earth dams[10–12]. However, at least two finite-difference studies[47,63] had earlier recognized the 2-Dimensional (2-D) nature of dynamic deformations experienced by infinitely long embankment dams subjected to vertical *S*-waves, under plane-strain conditions.

Table 2 summarizes in chronological order some of the most important studies making use of finite-element procedures for the seismic response of earth dams.

The early popularity of the finite-element method stemmed chiefly from two factors: (a) its capability for handling any number of zones with different materials, whereas the shear-beam model assumed that the elastic properties of the dam could be represented by an average value; and (b) its capability of rationally reproducing the 2-D dynamic stress and displacement field during earthquake shaking, whereas the simplifying assumption of uniform horizontal shear stresses in shear-beam analyses seemed to violate the physical requirement of vanishing stresses on the two faces of the dam.

Nevertheless, early comparative studies of the two basic dynamic earth dams models suggested that their

Table 2. Evolution of developments based on finite-element discretization (partial list)

Author(s) [Reference]	Contribution
Ishizaki and Hatakeyama[47] 1962	2-D plane-strain analysis of lateral vibration using a finite-difference discretization
Medvedev and Sinitsym[63] 1965	plane-strain finite-difference analysis
Clough and Chopra[10,11] 1966, 1967	first introduced the finite-element method for 2-D plane-strain analysis; viscoelastic soil behaviour
Dibaj and Penzien[25] 1967	2-D finite element model of dam subjected to horizontally travelling waves
Chopra and Perumalswami[13] 1969	2-D finite-element model of dam supported on homogeneous elastic halfspace
Mathur[62] 1969	2-D finite-element analysis of dam and soil layer over bedrock
Seed *et al.*[97] 1969	2-D finite-element response analyses to assess the causes of failure the Sheffield dam
Ghaboussi and Wilson[108] 1973	modelled the soil as a poroelastic medium and studied the dam-reservoir interaction
Idriss *et al.*[46] 1973	incorporated the iterative 'equivalent linear' scheme in a 2-D variable-damping finite-element code (QUAD-4)
Seed *et al.*[98] 1973	2-D 'equivalent-linear' finite-element response analyses to assess the causes of failure of the Lower San Fernando Dam
Singh *et al.*[100] 1978	2-D finite-elements along with stochastic equivalent linearization
Martinez and Bielak[61] 1980	combined 2-D finite-element discretization of mid-section with Fourier expansion in longitudinal direction to obtain response of dam in symmetric canyons
Romo *et al.*[90] 1980	2-D equivalent linear finite-element analyses to compare with recorded seismic motion of the El Infiernillo and La Villita Dams
Zienkiewicz *et al.*[107] 1980	2-D finite-element visco-plasticity effective-stress model for estimating permanent deformations and porewater pressure buildup from a single analysis
Vrymoed[106] 1981 Tsiatas and Gazetas[104] 1982	2-D finite-element equivalent-linear analyses to compare with recorded motion of Oroville Dam
Dakoulas[19] 1985	comparative studies of 2-D finite-element and 1-D shear-beam models
Mansuri *et al.*[58] 1983	2-D finite-element model with soil treated as a poroelastic material, and empirically allowing for pore pressure buildup due to shear straining
Prevost *et al.*[85] 1985	2-D finite-element model with soil behaviour obeying multi-surface kinematic plasticity theory
Makdisi *et al.*[57] 1982	developed 3-D finite-element formulation using prismatic longitudinal
Mejia *et al.*[64,65] 1982, 1983	elements with six faces and eight nodes; use in case history involving Oroville Dam

differences could be reconciled[12,77]. Predicted values of natural frequencies were in general agreement, with differences being within 10%. Moreover, the shear-beam-computed distributions of modal displacements with depth were not far from the average between the distributions along the axis and along the faces of the dam computed with finite elements. As a consequence, these early finite-element models were also equally unsuccessful in reproducing the aforementioned modal displacement shapes measured in the field, at Bouquet[51] and Sannokai[73] dams.

Further developments in the 1960's related to finite-elements include attempts to study the effects of excitation by horizontally travelling waves[25] and the effects of interaction between a dam section and an underlain homogeneous halfspace or stratum[13,62]. At the same time, finite-element analyses are being used in investigations of the seismic failures of actual dams.

2.3 Development of procedures for assessing seismic safety

While substantial progress was being made towards developing rational methods of dynamic response analysis, much of the attention in the late 1960's and the 1970's focused on developing reliable procedures and criteria of assessing the stability and safety of earth dams during strong shaking. The pseudo-static limiting-equilibrium was clearly inadequate, due to its aforementioned several deficiences.

Some of these deficiences were largely overcome by the '*sliding displacement*' method which assesses the dynamic stability of an embankment in terms of potential permanent deformations. The basic elements of the procedure were proposed by Newmark[71] who envisaged that, whenever the inertia forces on a potential slide mass exceed its yield resistance, sliding movements occur; when the inertia forces are reversed, the movements stop and may even be reversed. The method has been subsequently used and refined by several researchers[30,56,92,96,45,17] and, in its present form, requires a comparison of the time history of the average induced acceleration with the yield acceleration of a potential slide mass. The former is computed from plane-strain or shear beam type of response analyses; the latter is calculated pseudo-statically using the undrained cyclic strength of the soil. Permanent displacements, assumed to occur whenever the induced accelerations exceed the yield acceleration, are simply evaluated by a double integration procedure.

Despite its several pitfalls from a theoretical point of view (chief among which is the uncoupling between 'induced' accelerations and 'resulting' sliding deformations) the method has proved to be useful in cases where the yield resistance of the soil can be reliably determined and does not exhibit any appreciable decrease with time during an earthquake. Compacted cohesive clays, dry sands and very dense saturated sands may belong in this category of soils since they experience *no* significant pore-pressure buildup during cyclic loading, retaining most of their static undrained shear strength.

However, the overall stability of dams constructed of such materials has proved satisfactory in numerous earthquakes throughout the world, as they have withstood very strong shaking with no major stability problems[96]. On the contrary, dams constructed of loose or medium dense saturated sands have experienced severe damage and failures due to build-up of pore water pressures and the resulting loss of strength (liquefaction). To evaluate the seismic stability of such embankments Seed and coworkers[94,96] developed an analysis procedure which involves the following essential steps: (a) estimating the initial static stresses in the embankment, by means of finite element analyses; (b) determining the dynamic soil properties such as shear modulus, Poisson ratio and damping as functions of the strain level; (c) computing the stresses induced in the embankment by the design ground excitation, using plane-strain finite-element analyses and the dynamic soil characteristics determined in step b; (d) subjecting in the laboratory representative soil samples to the combined effects of the initial static and the induced cyclic stresses to determine the generation of pore pressures and the ensuing reduction in strength and development of 'potential' strains: and (e) performing slope stability analyses and semi-empirically converting the strain potentials to a set of 'compatible' deformations. The stability and performance of the dam are judged from the results of these stability analyses and/or the size and distribution within the dam of the 'compatible' deformations.

This procedure has been employed to explain several cases of liquefaction failures (most notably those of the Sheffield and Lower San Fernando Dams), several cases in which large deformation have occurred (e.g., Upper San Fernando and Chabot Dams in the 1971 San Fernando earthquake; Dry Canyon Dam in the 1952 Kern County earthquake), as well as cases of dams which performed well in various earthquakes. The method has been recommended by several agencies concerned with the safety of earth dams, such as the California Department of Water Resources, the Corps of Engineers, and the International Commission on Large Dams.

In recent years some potential limitations of the aforementioned liquefaction evaluation procedure have been discussed in the literature[14,15,26,67,82]. The criticisms refer mainly: (a) to the definition of 'liquefaction' as that stage in a cyclic laboratory test when a peak pore pressure ratio of 100%, or a permanent strain of 5% develop momentarily; and (b) to the associated undrained cyclic triaxial stress-controlled testing of anisotropically consolidated specimens that is used for evaluating such a 'liquefaction' potential. With respect to (a), it has been argued[14,15,82] that development of 100% pore pressure ratio does not necessarily leads to zero shear strength and a noncontractive sand will only experience a limited amount of shear strain and may start exhibiting dilative behaviour beyond this stage of loading. Instead, 'liquefaction flow' can only occur in contractive sands and silty sands, and it is driven by (static or dynamic) shear stresses which exceed the 'undrained steady-state' shear strength[82]. In earth dams such a 'liquefaction flow' may be triggered by porewater pressure buildup which, in turn, is primarily controlled by the induced seismic shear strains[26,66]. With respect to (b), a particular limitation of the cyclic triaxial tests stems from the fact that the plane of maximum intial shear stress (at 45° from the horizontal) always coincides with the plane of maximum cyclic shear stress. In addition, the orientation of the major principal stress may rotate intermittently by 90° during each cycle. In reality, however, it is more likely that the principal stress directions rotate randomly during shaking, and only

momentarily could the planes of maximum static and dynamic shear stress coincide. New laboratory procedures have been under development, in response to these critisims of the current state-of-the-art methodology[66,67]. However, further discussion of these procedures is beyond the scope of this paper.

2.4 Recent developments

Since about 1980 a substantial amount of published research has focused on refining, expanding, and verifying the basic dynamic models developed in the 1960's for predicting the seismic response of earth dams. As a result, several improved analytical models have appeared with the use of which parameter studies have been performed to elucidate the importance of such factors as the canyon geometry and material inhomogeneity. The bank of published 'complete' records of earthquake response of actual earth dams have also increased significantly; such records have been frequently utilized in the past few years for the necessary calibration of developed theoretical formulations. Finally, the aforementioned 'liquefaction' procedure of Seed has been critically reappraised and new laboratory testing concepts have been introduced in attempts to develop an alternative approach to this outstanding geotechnical/earthquake problem.

A detailed exposition of these recent developments will be presented in the sequel. Tables 1 and 2 include a listing of some of the related publications along with a brief statement of their main contribution. Moreover, new promising procedures for nonlinear-inelastic response that have not yet been published are also put forward in this paper; results from these procedures reveal a potential for efficiently and realistically reproducing the key features of the inelastic response of earth dams to very strong earthquake shaking.

3. BASIC APPROACH – SIMPLIFYING ASSUMPTIONS AND FACTORS INFLUENCING THE RESPONSE

A clear trend in recent theoretical studies has been to develop analytical-numerical models that are computationally efficient and cost-effective, while being capable of realistically simulating one or more aspects of the physics of the problem. The desire for relatively simple methods is, of course, not new in geotechnical/earthquake engineering. It has, however, taken a special dimension in this case since earth dams are large 3-dimensional (3-D) structures of complicated geometry, consisting of various types of nonlinearly behaving materials. Furthermore, the prediction of the appropriate ground motions to be used as design excitations involves considerable uncertainties. Hence, a complete detailed evaluation of their dynamic response using elaborate 3-D and inelastic formulations, requiring a large amount of input data and excessive computer storage and time, may not be presently justified even for final design calculations.

The '*shear-wedge*' or '*shear-beam*' concept has served as the basis for many of the newly develpped models, and will thereby take prominent place in the subsequent presentation. In its basic original (pre-1980) form the shear-beam model involved the following major simplifying assumptions:

(a) Only horizontal lateral displacements and simple shearing deformations take place;
(b) Displacements and shear stresses and stains are uniformly distributed along horizontal planes across the dam;
(c) The dam consists of a homogeneous material which behaves as a linear visco-elastic solid and is described by a constant shear modulus, damping ratio, and mass density;
(d) The dam is either infinitely long or built in a rectangular canyon and is subjected to a *synchronous* (in-phase) rigid-base lateral motion.

Research efforts, described in this paper, have attempted to relax one or more of these simplifying assumptions, while retaining to the extent possible the basic simplicity of the model.

Of the foregoing assumptions, only (a) and (b) are exclusive to the shear-beam model. Hence, it must first be shown that they are reasonable engineering approximations, if the model is to become a reliable analytical tool.

With regard to assumption (a) it is noted that, in reality, every element in a dam subjected to horizontal base shaking will experience not only horizontal displacements and shearing stresses/strains, but also vertical displacements and normal stresses/strains as a result of wave reflections on the inclined surfaces of the dam. This is true even when plane-strain conditions prevail. Nevertheless, comparisons with 2-D finite-element solutions consistently show that vertical displacements and normal stresses are indeed secondary and may in most cases be neglected.

Assumptions (b) appear at first to be rather sweeping: a uniform shear-stress distribution would violate the physical requirement for vanishing stresses at the traction-free inclined surfaces of a dam. Nonetheless, several 2-D finite-element studies [e.g., Refs 10 and 19] have shown that stresses and strains follow an essentially uniform distribution across the dam, except in a small region by each traction-free surface where shear stresses decline to zero. Furthermore, it can be persuasively argued that not all of assumptions (b) are necessary. As it will be shown in the following section, when proper account is taken of the dependence of soil stiffness on the mean normal stress, it is sufficient to only assume that either strains or shear stresses are uniformly distributed across the dam – a much milder and hence fairly realistic assumption.

Assumptions (c) and (d) are not crucial for the shear model; they were invoked only in earlier stages of development of the shear beam as well as of the 2-D plane-strain model. Work published mainly in the 1980's (in addition to some limited work in the 1970's) has relaxed most of these assumptions by quantitatively evaluating the role of the following factors/phenomena:

- material inhomogeneity due to the dependence of soil stiffness on the static confining pressure
- nonrectangular canyon geometry
- excitation by longitudinal and by vertical rigid-base motion
- nonlinear and inelastic soil behaviour during strong earthquake shaking

- interaction between the dam and the supporting soil-rock system

The first three of these factors/phenomena have been investigated extensively and satisfactory solutions (using both shear-beam and 2-D finite-elements) are now available for a variety of situations. On the other hand, methods to reliably predict the nonlinear-inelastic response are scarce; fortunately, this has been recently an area of very active research and some promising developments are reported in this paper. Finally, the problem of interaction between an earth dam and the supporting alluvium has received some scattered attention over the years, but will be only briefly touched upon herein.

We start first with a systematic comparative study between compatible shear-beam and finite-element methods. It is shown that the former method predicts natural frequencies, modal shapes, and seismic response histories which are, generally, in very good accord with the results of the latter. The aforementioned assumptions (b) are evaluated and shown to be adequate approximations of reality, except perhaps for very high-frequency components of motion. Having thus established the validity of the shear-beam model, we proceed by using it to study the effects of material inhomogeneity, canyon geometry, and nonlinear-inelastic soil behaviour.

The simplicity of the shear-beam model has allowed in many cases the development of analytical closed-form expressions. Such expressions are particularly valuable for preliminary calculations in the conceptual design stage. However, they are often accurate enough to be used for final design calculations, alone or in combination with a few computer runs of sophisticated numerical codes. They are valuable for inexpensively performing parametric calculations and helping the engineer develop insight and feeling for the problem. Finally, such simple analytical solutions provide a valid reference against which the analyst can check and understand the results of complex computer programs, thereby avoiding the 'black box' syndrome.

4. EVALUATION OF SHEAR-BEAM MODEL THROUGH COMPARISONS WITH PLANE FINITE-ELEMENT ANALYSES

4.1 Necessary assumptions of shear-beam model

Refer to the sketch of a cross-section of an infinitely-long earth dam shown in Fig. 2. The dam is subjected to a horizontal rigid-base excitation described by an acceleration $\ddot{u}_g(t)$, under conditions of plane deformation. Assume that only horizontal shearing deformations develop, i.e., invoke assumption (a) of the previous section. Only one additional assumption is made: that the horizontal displacements are uniform across the dam. Denoting by u the displacement relative to the base, it follows that

$$u = u(z;t) = \text{independent of } y \tag{1}$$

No restrictive assumption is made regarding the stresses, and the upstream and downstream slopes need not be identical. However, only linear (elastic or viscoelastic) behaviour is considered in this section.

Consider the dynamic equilibrium of a horizontally sliced element having width equal to $y_u + y_d \simeq 2B \cdot z/H$ and thickness dz. The resultant inertia force (per unit length in the longitudinal direction) is equal to

$$I_z = \rho[\ddot{u}(z;t) + \ddot{u}_g(t)] \frac{2B}{H} \cdot z \, dz \tag{2}$$

while the net shearing force on the two horizontal planes equals

$$\begin{aligned} S_z &= -\frac{\partial}{\partial z}\left[\int_{-y_u}^{y_d} \tau(y,z;t)\,dy\right]dz \\ &= -\frac{\partial}{\partial z}\left[\int_{-y_u}^{y_d} G_s(y,z)\cdot\frac{\partial u(z;t)}{\partial z}\cdot dy\right]dz \\ &= -\frac{\partial}{\partial z}\left[\frac{\partial u(z;t)}{\partial z}\int_{-y_u}^{y_d} G_s(y,z)\,fy\right]dz \\ &= -\frac{\partial}{\partial z}\left[G(z)\frac{\partial u(z;t)}{\partial z}z\right]\frac{2B}{H}\,dz \end{aligned} \tag{3}$$

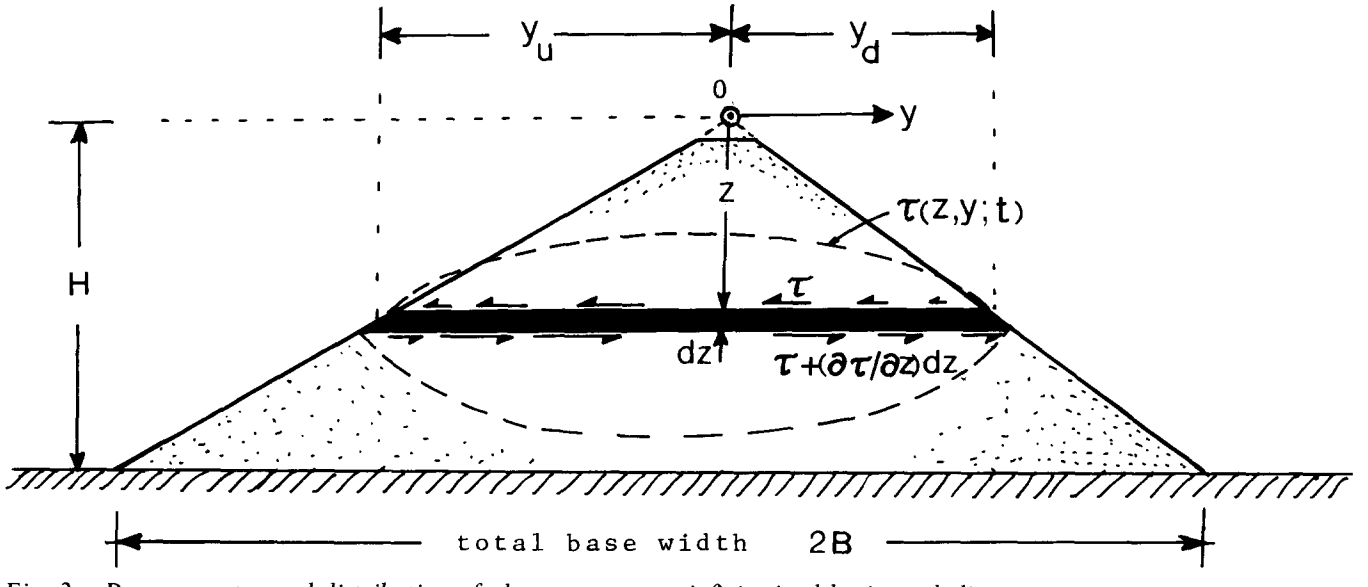

Fig. 2. Dam geometry and distribution of shear stresses on infinitesimal horizontal slice

in which: $G_s = G_s(y,z)$ = the shear modulus of a soil element at a particular location (y,z); and $G = G(z)$ = the average shear modulus on a horizontal plane across the dam, i.e.

$$G(z) = \frac{1}{y_u + y_d} \int_{-y_u}^{y_d} G_s(y,z)\,dy \tag{4}$$

Dynamic equilibrium leads to $I_z + S_z = 0$, from which:

$$\rho(\ddot{u} + \ddot{u}_g) = \frac{1}{z}\frac{\partial}{\partial z}\left[G(z)\cdot z \cdot \frac{\partial u}{\partial z}\right] \tag{5}$$

Equation (5) is indeed the 'shear-wedge' or triangular 'shear-beam' equation for the general case that the average shear modulus G is a function of z [Refs 7, 33]. This concludes the proof that the shear-beam model does *not* require uniform shear stresses or uniform shear moduli across the dam. Uniform displacements or shear strains is a sufficient condition.

Substantial numerical evidence can be cited to show that this latter assumption of uniform shear strains is indeed a realistic engineering approximation. As an example: Fig. 3a portrays the distribution of peak values of shear strains across the mid-height in three idealized dam sectiosn subjected to four historic recorded motions.

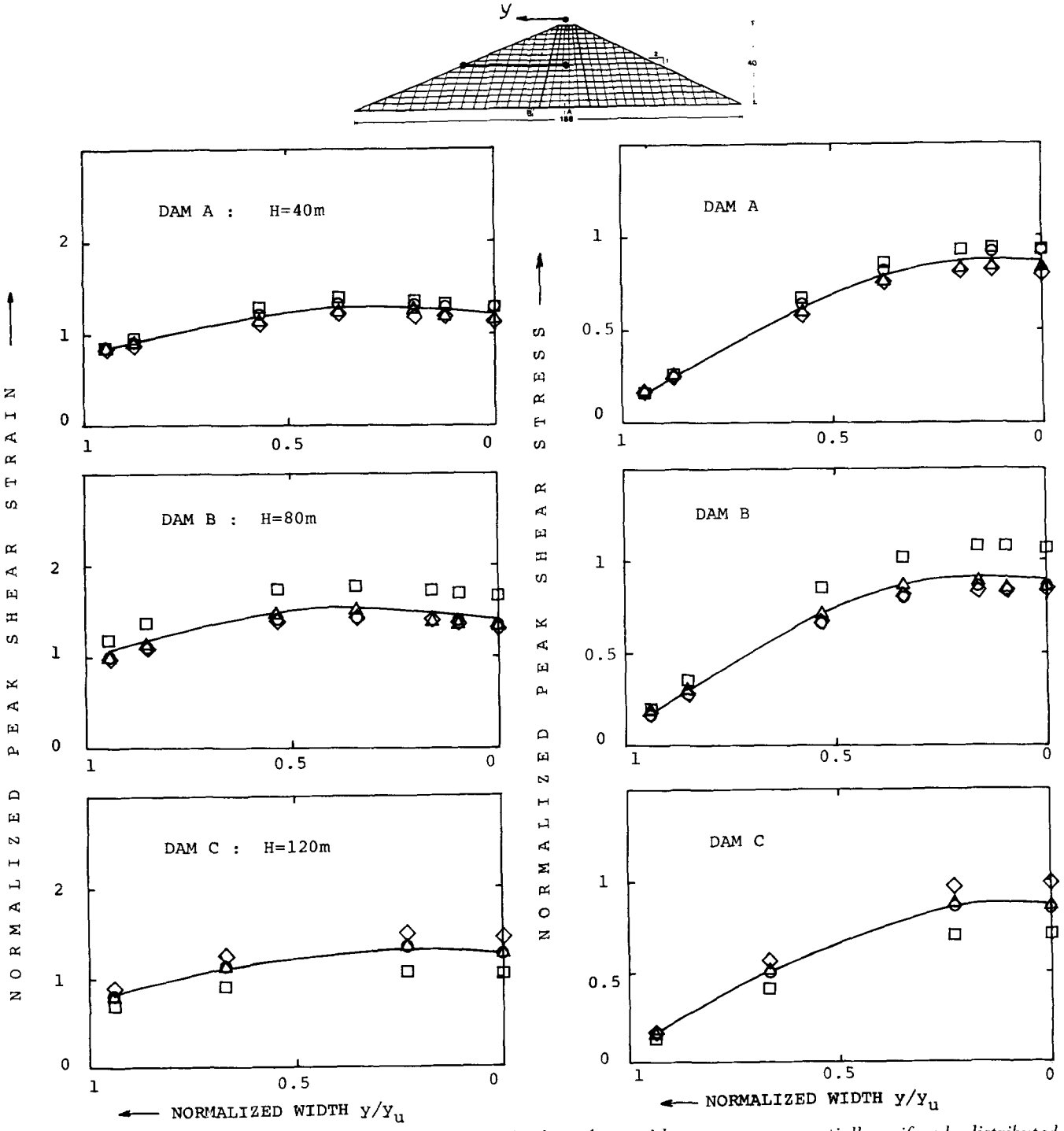

Fig. 3. The finite-element computed peak shear strains in three dams without core are essentially uniformly distributed across the dam, in supoort of the shear-beam concept. Peak shear stresses, being uniform across the middle third of the dam, decrease almost linearly to zero at the surface. (Excitations: four historic records; line represents the average)

The heights of the dams are 40 m, 80 m and 120 m, respectively, and their upstream and downstream slopes are invariably 1:2.5 and 1:2. The properties and geometry of these dams are representative of earthfill dams which are either uniform or made up of zones having very similar shear stiffnesses. The shear moduli G_s are proportional to the square root of confining pressure. The four accelerograms (Eureka NE, 1954; El Centro SE, 1940; subbasement 1901 Ave. of Stars NW, 1971; Taft NE, 1952) differ substantially in frequency characteristics, and details, but have all been scalled to a 0.20 g peak acceleration. It is evident in this figure that peak shear strains computed from plane-strain finite-element analyses are almost uniformly distributed across the dam. Moreover, as it will be shown later in the paper, the shear-strain histories of points across the dam appear to be very nearly 'in phase', and thereby the uniformity assumption is approximately valid at any time during ground shaking.

Since G_s is not constant but tends (along with confining pressure) to zero at the sloping surfaces, the distribution of shear stresses across the dam is not nearly as uniform as that of strains. As seen in Fig. 3b, the peak shear stresses induced in all the aforementioned three dams by each of the four accelerograms tend to vanish at the stress-free surface. Hence, the shear beam model does not violate the boundary conditions of the problem, as it was believed in earlier studies.

But what about rockfill dams which usually comprise a (relatively) very soft core? Are the shear-beam assumptions still reasonable? The answer is 'probably yes' – although in this case it is stresses, rather than strains, which do not exhibit any substantial variations across the dam. This can be seen, for example, in Fig. 4 which portrays the distributions of peak shear strains and stresses in two 120 m-tall dam sections subjected to the aforesaid four accelerograms. As sketched in this figure, in Dam D the average core modulus G_{core} is 1/2 of the average shell modulus G_{shell}; in Dam E: $G_{core} = (1/4)\, G_{shell}$. Notice that peak strains, while being uniform within each constituent material, change abruptly at the core-shell interface. In fact, the stains experienced in each zone are essentially inversely proportional to their respective moduli. This is consistent with Fig. 4b in which shear stresses hardly change across the interface.

So it appears that for dams comprising zones of significantly differing stiffnesses, assuming *uniform shear stresses*, rather than strains, is the appropriate necessary assumption. Although this is not as accurate as the previous assumption of uniform strains for dams with

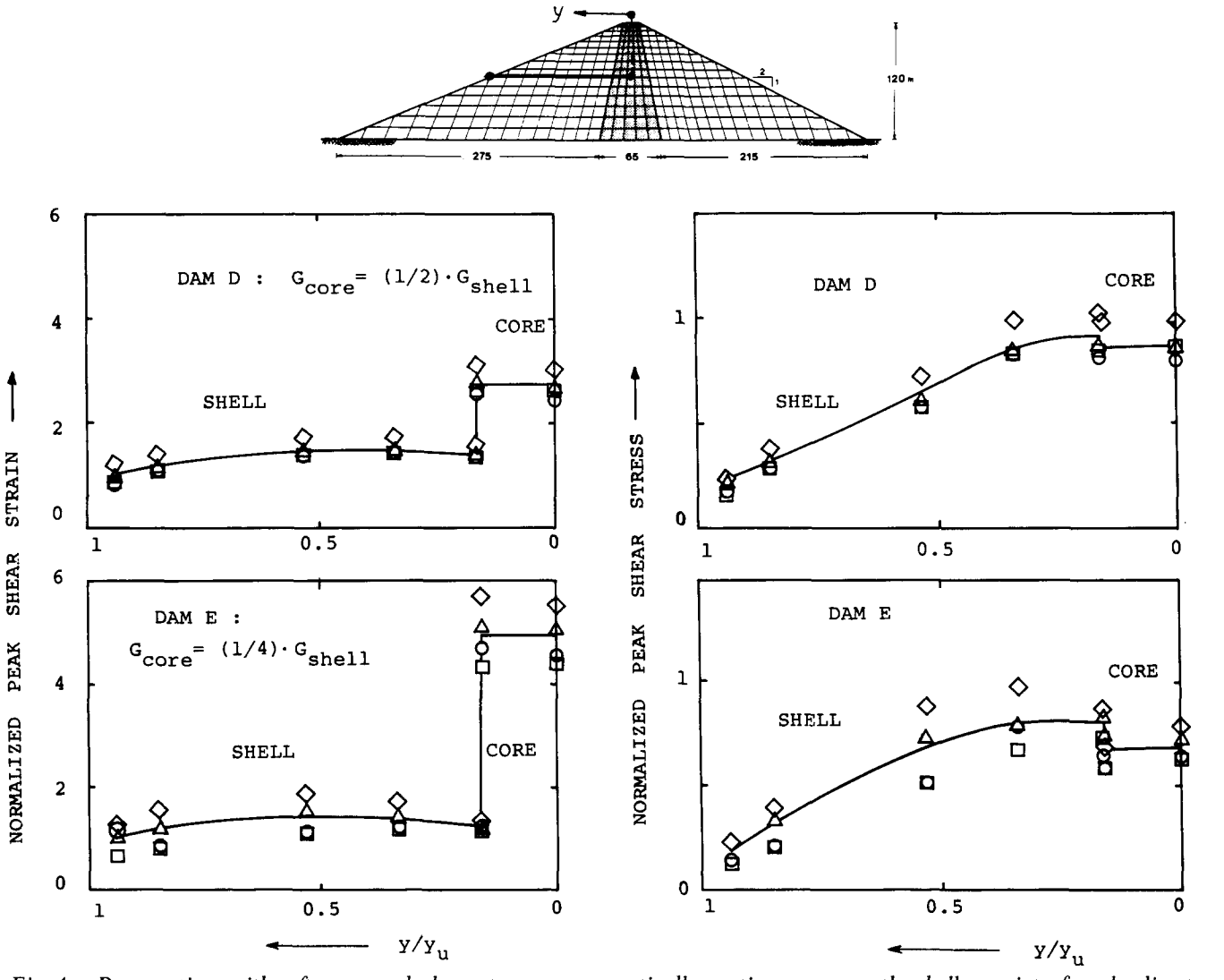

Fig. 4. Dam sections with soft core: peak shear stresses are practically continuous across the shell-core interface, leading to discontinuous peak strains, in proportion to local shear moduli (Excitations: four historic records; line represents the average)

uniform materials, it may still be considered as a reasonable approximation; indeed the shear-beam predicted stresses are very close to the average across-the-dam values of stresses computed from plane finite-element analyses, as will be seen later.

In conclusion, the assumptions of the shear beam model are realistic engineering approximations for uniform as well as for zoned earth/rockfill dams.

4.2 Comparison of shear-beam and finite-element results

Comprehensive comparative studies of the linear viscoelastic predictions by the two basic models has been reported in Refs 104, and 19–21. Several idealized dam cross-sections, representative of a broad range of earth-fill and rockfill dams, were used in these studies. In the finite-element models the element shear modulus G_s was invariably taken to be proportional to the square-root of the confining pressure. Inhomogeneous shear-beam models consistent with such a variation of modulus were then derived, as explained in the following section of this paper. The comparisons involved free-vibration characteristics as well as seismic histories of response to the four historic records mentioned previously. Following are the main conclusions that may be drawn from these studies.

- Regarding free-vibration characteristics:

1. The two models yield very similar fundamental natural frequencies (f_1) and fundamental mode displacements. Specifically, the shear beam invariably overestimates f_1 by about only 5%, in most cases. Among the exceptions: rockfill dams with a very soft core, for which the shear beam may overestimate f_1 by 10%–15%. This spurious 'stiffening' is mainly attributed to the suppression by the shear beam model of the vertical degree of freedom which the actual dam and its finite-element model enjoy. On the other hand, the shear beam correctly predicts an attenuation of mode displacements with depth which lies between the two extreme finite-element-computed distributions, along the inclined surfaces and along the axis of the dam.
2. The higher significant *lateral* modes computed with finite elements exhibit an increasingly stronger component of vertical deformation. The shear beam neglects this component and thereby leads to higher natural frequencies – the discrepancy generally increases with the mode number n, but remains within 10%–25% for the first three significant modes. In practice, this may still be a rather negligible difference in view of the unavoidable uncertainties in soil properties and the comparable error involved in assuming a plane rather than a 3-D geometry. Indeed, as it will be seen later (Fig. 22), the presence of even a very wide canyon (say, with aspect ration of 5 or 6) would increase the natural frequency by not less than 10%–15% over the value computed with a plane-strain analysis. On the other hand, the distributions of mode displacements predicted by the shear beam lie in most cases between the

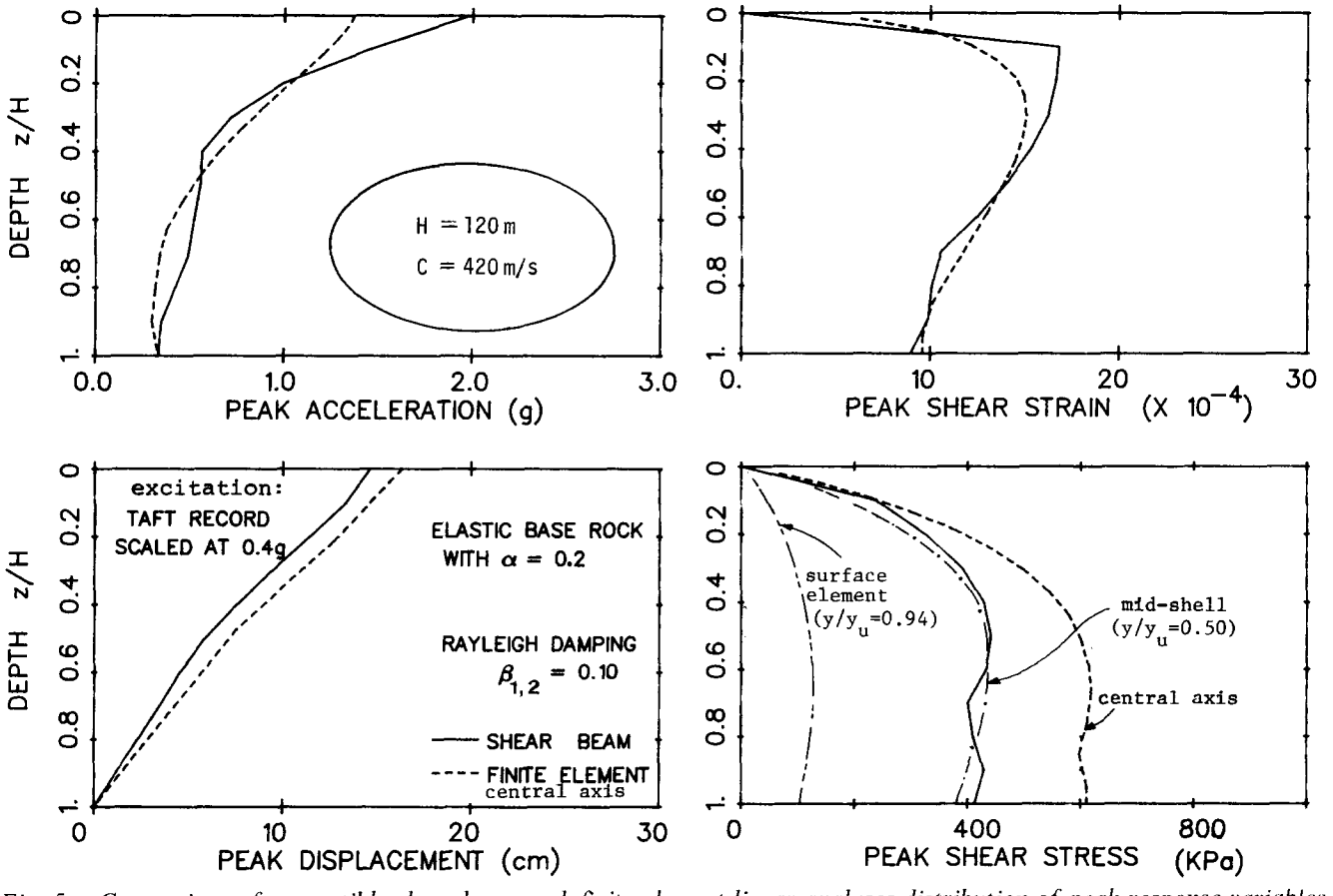

Fig. 5. Comparison of compatible shear-beam and finite-element linear analyses distribution of peak response variables with depth ('elastic' rock with rigidity-contrast ratio $\alpha = \rho C/\rho_r C_r = 0.20$)

corresponding two-extreme distributions of the finite element model.

3. The second natural mode from finite-element analysis corresponds to the fundamental shear-beam mode in purely *vertical* oscillations[104,35]. The corresponding natural frequencies and vertical mode displacements are in good accord, although the shear beam overestimates the frequency by about 10%, and ignores the accompanying horizontal component of deformation. Furthermore, the finite-element model predicts several (usually secondary) natural modes which can not be possibly reproduced with a shear beam formulation.

- Regarding seismic response (Figs 5–10):

4. Peak values and time histories of horizontal relative *displacements* computed with the two models are in very close agreement, the discrepancies being within 10% for all dams and all seismic excitations studied. In most cases the shear-beam-computed attenuation of each peak displacements along the depth lies in between the finite-element distribution of peak values along the surface and along the central vertical axis of the dam. Moreover, as illustrated in Fig. 6, the

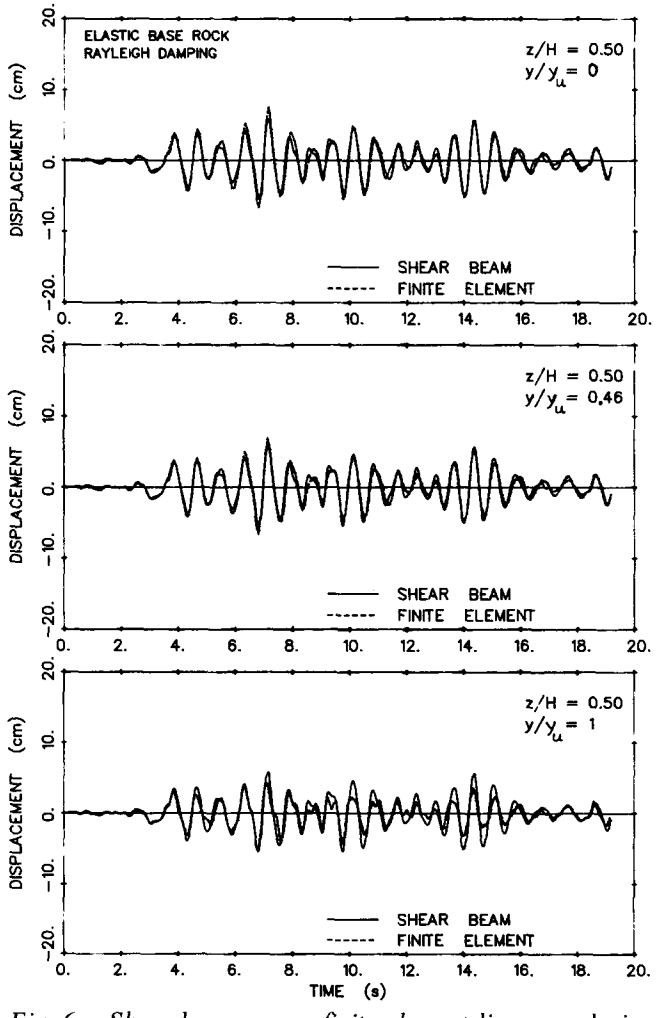

Fig. 6. Shear-beam versus finite-element linear analysis: relative displacement histories at three points across the mid-height (dam and excitation as in Fig. 5)

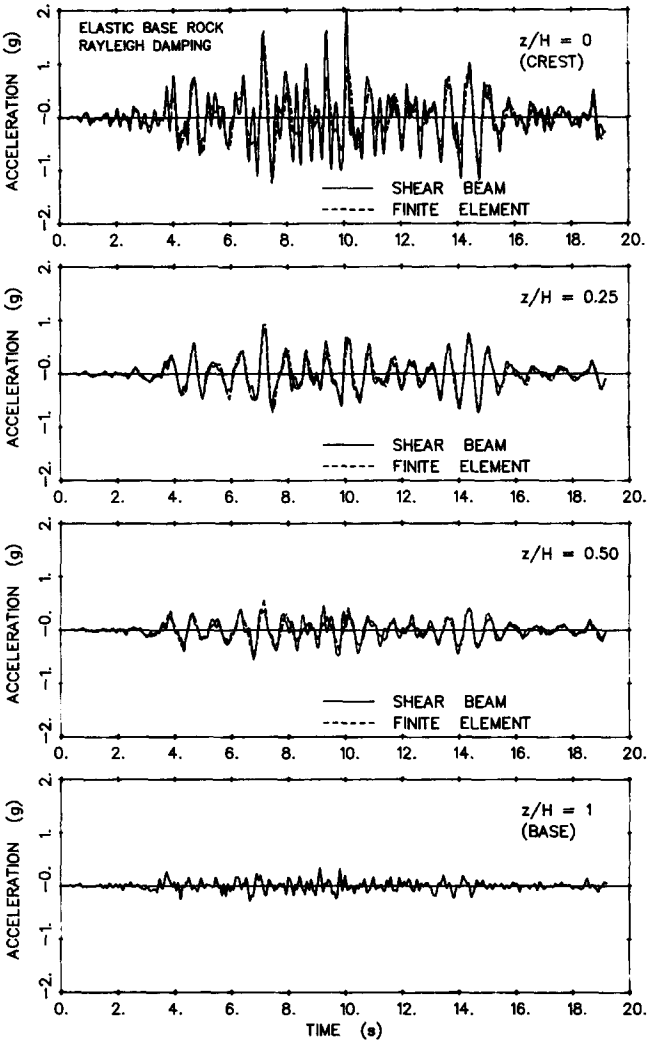

Fig. 7. Shear-beam versus finite-element linear analysis: absolute acceleration histories (dam and excitation as in Fig. 5)

displacement histories of three points ($y/y_u = 0$, 0.46, and 1) across the midheight ($z/H = 0.50$) of the 120 m-dam not only exhibit very similar peak values (at about 7 seconds), but they also are in phase with each other and in excellent agreement with *the single* shear-beam computed displacement history.

5. The most significant disagreement of the two models involves absolute accelerations of relatively flexible dams, for which the shear-beam frequently overestimates the crest peak acceleration by as much as 50% (Fig. 5). A hint at the cause of such a discrepancy may be provided by a comparison of the two time histories in Fig. 7: the shear-beam motion is much richer in very strong high-frequency components. Although one may partly blame the finite-element model for filtering out components with very small wavelengths, it seems that the error lies mostly with the shear beam; by neglecting the accompanying vertical component of deformation, the latter overestimates the relative importance of higher resonant frequencies. By contrast, plane-strain formulations predict a far greater number of closely-spaced natural

frequencies, with vertical and rocking-type deformations becoming significant at higher modes. Such modes 'attract' smaller amounts of seismic energy than the few well-separated and one-dimensional higher modes of the shear beam, which are apparently responsible for the 'whiplash' effect seen in Figs 5 and 7. Notice, however, that this discrepancy between the two models largely dissappears with relatively stiff dams which respond primarily in their fundamental mode. An example: the response of the 40 m-high dam portrayed in Figs 9–10. One semi-empirical way of improving the acceleration performance of the shear beam model is by introducing Rayleigh damping with, say, $\beta_2 = 1.50\beta_1$. However, this would hardly be necessary in most practical cases, since the unavoidable restriction provided by the boundaries of even a wide canyon has a similar increasing effect on the near-crest accelerations[22,57,65]. Since the 3-Dimensional effects are frequently ignored in practical applications, use of a shear-beam model (which overpredicts both the fundamental frequency and the crest acceleration) may be preferable in certain cases. Furthermore, nonlinearities in soil response during strong shaking would greatly reduce these spurious high-frequency high-amplitude components of acceleration, as it will be demonstrated in a later section herein.

6. Generally, the shear beam also tends to overestimate slightly the largest peak values of strain, which usually occur within the upper third of the dam. On the other hand, shear stresses are in very good accord; the shear beam predictions are approximately equal to the average-across-the-width shear stress computed with finite-elements (Fig. 8).

Overall, the performance of the shear beam is very satisfactory. In view of the substantial savings in manhours and computer costs that this model affords, its use as the basis of new developments is well justified.

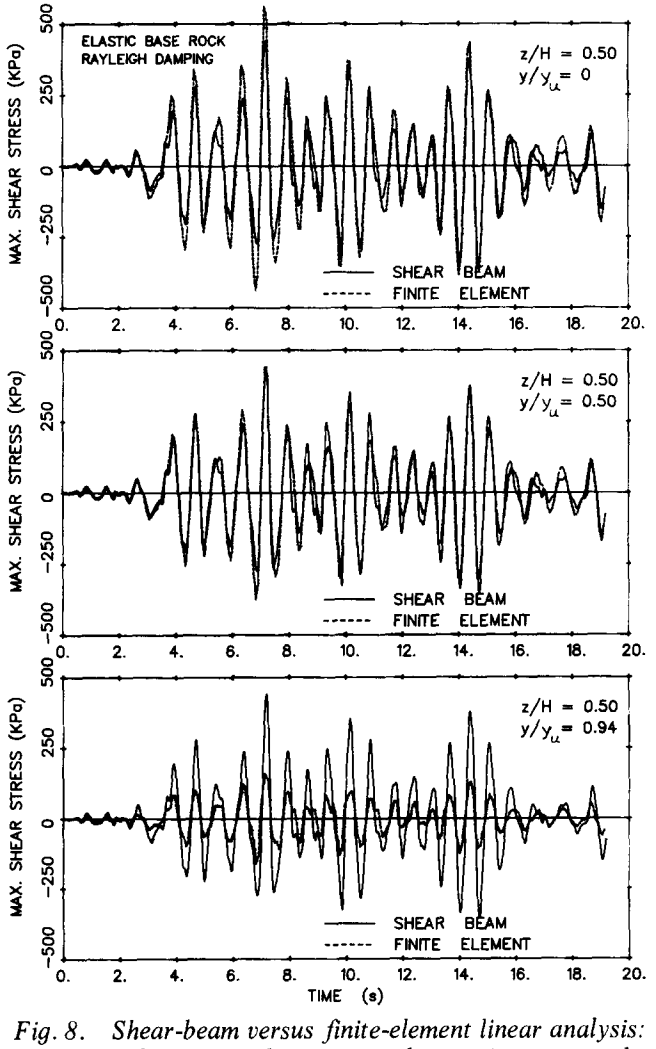

Fig. 8. Shear-beam versus finite-element linear analysis: maximum shear stress histories at three points across the midheight (dam and excitation as in Fig. 5)

5. INHOMOGENEITY DUE TO DEPENDENCE OF SOIL STIFFNESS ON CONFINING PRESSURE

5.1 Prelude

Considering uniform soil properties throughout the dam was one of the most sweeping assumptions of the classical shear beam model. Laboratory measurements of soil stiffness in the last 15–20 years [e.g. Ref. 39] have established the dependence of soil shear modulus on the confining pressure, σ_0, which in an earth dam varies from point to point, increasing with distance from crest and from the two inclined surfaces. Indeed, several geophysical and other indirect field measurements have confirmed that the average shear modulus G across the dam (defined by equation (4)) increases with depth z from the origin (Fig. 11a)[38].

Using published distributions of static confining stresses in an idealized dam section, along with the assumption that element soil modulus G_s increases in proportion to $\sigma^{1/2}$, Gazetas[32,33] recommended that G be taken as being proportional to $z^{2/3}$ – an idealization in full accord with the field data of Fig. 11a, obtained from 12 actual earth dams. The shear beam model was then readily extended to account for such a variation of modulus with depth[33] and analytical closed-form expressions were derived for free and force-vibration characteristic response parameters. Table 3 lists the most significant of these expressions.

An important first contribution of the developed *'Inhomogeneous Shear Beam'* model was to conclusively explain the primary cause of the aforementioned sharp attenutation with depth of the fundamental mode displacements recorded in Sannokai and Bouquet dams. As Okamoto had suspected, *stiffness inhomogeneity* was indeed responsible for the failure of the homogeneous shear-beam and finite-element analyses to anticipate the observed trends. On the other hand, as can be seen in Fig. 13 and in Table 4, inhomogeneity does *not* affect in any significant degree the fundamental natural period of a dam – hence the coincidental satisfactory predictions of frequencies by the various homogeneous models.

In addition, results from full-scale seismic and man-induced vibration tests on 12 actual earth dams from all over the world exhibit, in an amazingly consistent way, a sharp attenuation with depth of fundamental mode displacements, as that predicted for the Inhomogeneous

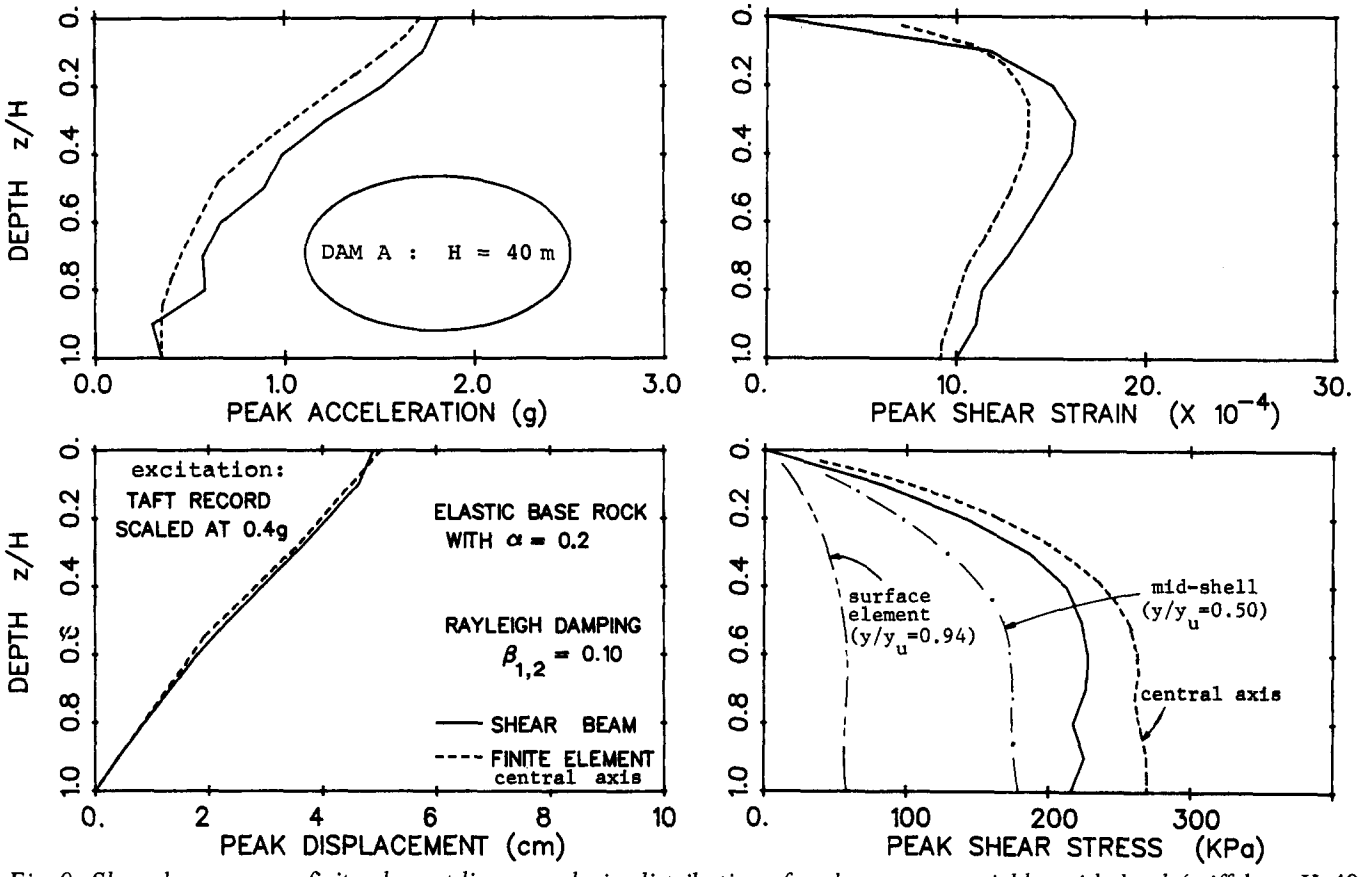

Fig. 9. Shear-beam versus finite-element linear analysis: distribution of peak response variables with depth (stiff dam: H-40 m)

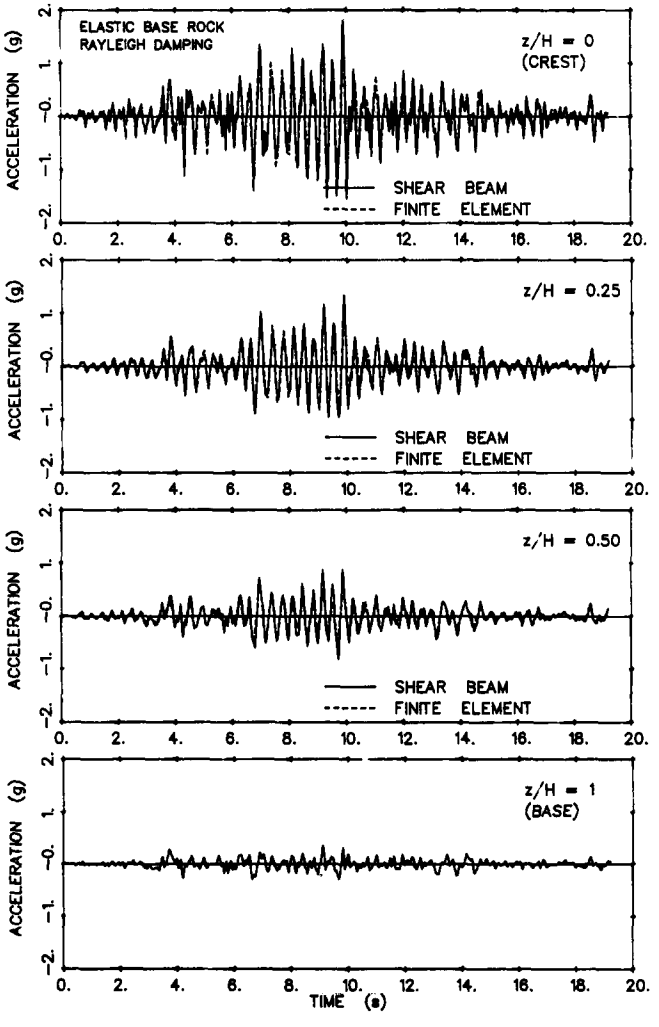

Fig. 10. Shear-beam versus finite-element linear analysis: absolute acceleration histories (dam and excitation as in Fig. 9)

Shear Beam. Fig. 11 portrays this comparison and lists the 12 related dams.

5.2 Factors influencing the variation of G with depth

A more comprehensive study, aimed at establishing bounds in the form of variation of G with depth, has been recently reported in Refs 20 and 21. The presentation herein draws mainly from these publications. $G(z)$ depends primarily on three factors

- the dependence on confining pressure of the element shear modulus G_s for each constituent material;
- the size and the relative overall stiffness of the impermeable cohesive core;
- the inclination of the two surfaces.

The shear modulus of a particular soil element at small levels of shear strain can be cast in the form:

$$G_s = F(e, OCR) \cdot \sigma_0^{\mu} \tag{6}$$

where: σ_0 = the effective normal octahedral stress (confining pressure), while e and OCR denote, respectively, the void ratio and apparent over-consolidation ratio of the particular element. The function F varies from soil to soil, monotonically increasing with decreasing e and increasing OCR. The dimensionless coefficient μ has been known to be about 0.50 for many laboratory tested soils, primarily clean sands and pure clays[86]. In the last decade, however,

(a)

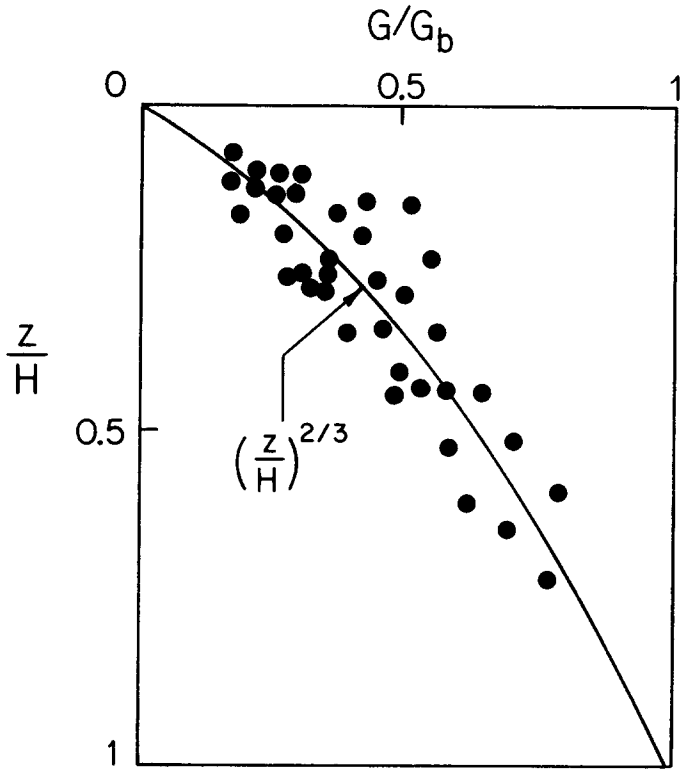

No.	Name	Country	Height (m)	Type of Recorded Vibrations	Reference
1	Santa Felicia*	USA	83	seismic, ambient, forced, hydrodynamic	Abdel-Ghaffar et al (1978, 1980)
2	Brea*	USA	27	seismic	Abdel-Ghaffar et al (1978, 1980)
3	Carbon Canyon*	USA	33	seismic	Abdel-Ghaffar et al (1978, 1980)
4	Bouquet*	USA	60	forced	Keightly (1966)
5	Mavrovo*	Yugoslavia	56	forced	Petrovski et al (1972)
6	Kisenyama†	Japan	95	seismic, ambient forced	Okamoto (1973) Takahashi et al (1977)
7	Shimokotori†	Japan	119	seismic, ambient forced	Takahashi et al (1977)
8	Nikappu†	Japan	103	seismic, ambient forced	Takahashi et al (1977)
9	Talaragi†	Japan	65	seismic, ambient forced	Takahashi et al (1977)
10	Sannokai*	Japan	37	seismic	Okamoto (1973)
11	Ainono*	Japan	41	seismic	Mori et al (1975)
12	Ushino†	Japan	21	seismic	Mori et al (1975)

*Earth-fill Dam †Rock-fill Dam

(b)

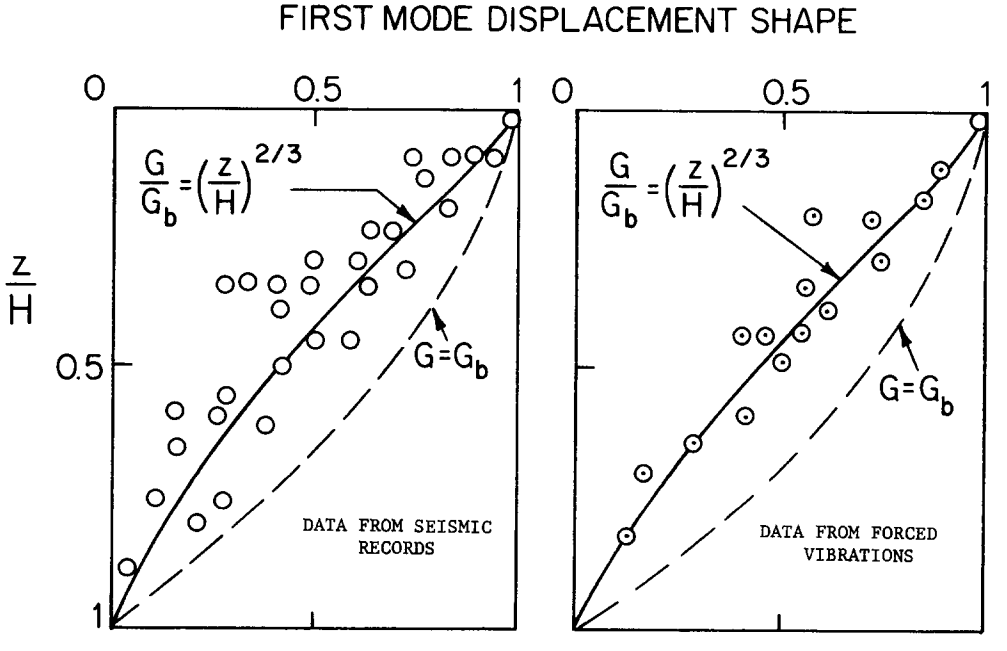

Fig. 11. Variation of shear beam modulus G in proportion to $z^{2/3}$ is consistent with geophysical and indirect field measurements in 12 listed actual dams (a), and can explain the repeatedly recorded sharp attenuation of fundamental mode displacements with depth (b)

Table 3. Some analytical expressions for inhomogeneous shear-beam models[19-21]

Inhomogeneous shear beam	Fundamental period $T_1\bar{C}/H$	Ratio of natural periods T_1/T_2	nth Natural circular frequency $\omega_n H/\bar{C}$	nth Modal displacement $U_n(x=0,z)$	nth Mode participation factor P_n	Steady-state midcrest/base transfer ('amplification') function AF $=[\ddot{u}(z=0)+\ddot{u}_g]/\ddot{u}_g$	
						I. 'Rigid-rock' amplification	II. 'Elastic-rock' amplification
$G=G_b\zeta^m$ $0\leqslant m\leqslant 1$	$\dfrac{16\pi}{(4+m)(2-m)\beta_1}$	$\dfrac{\beta_2}{\beta_1}$	$\dfrac{\beta_n}{8}(4+m)(2-m)$	$\zeta^{-m/2}J_q[\beta_n\zeta^{1-m/2}]$	$\dfrac{2}{\beta_n}\dfrac{1}{J_{q+1}[\beta_n]}$	$\dfrac{(a_0/2)^q}{\Gamma(q+1)J_q(a_0)}$	$\dfrac{(a_0/2)^q}{\Gamma(q+1)}\cdot\dfrac{1}{J_q(a_0)+i\alpha J_{q+1}(a_0)}$
$G=G_b\zeta^{2/3}$	2.57	2	$\dfrac{7}{9}n\pi$	$\zeta^{-2/3}\sin[n\pi(1-\zeta^{2/3})]$	$\dfrac{2}{n\pi}$	$\dfrac{a_0}{\sin a_0}$	$\dfrac{a_0}{\sin a_0+i\alpha\left(\dfrac{\sin a_0}{a_0}-\cos a_0\right)}$

Notation:

- $\bar{C}$ = average shear wave velocity in the dam
- $a_0=\omega H/\bar{C}$; $\zeta=z/H$; $\Gamma(\ )$ denotes the gamma function; $q=m/(2-m)$
- α = rigidity contrast ratio $=\rho C/\rho_r C_r$ where r refers to the properties of the supporting base; $i=\sqrt{-1}$
- $\beta_n=\beta_n(\mathrm{m})$ is the nth root of the 'period' relation [20], tabulated below for the first five modes ($n=1-5$) and five values of the parameters m (0, 1/2, 4/7, 2/3 and 1)

β_n

	mode n				
m	1	2	3	4	5
0	2.405	5.520	8.654	11.792	14.931
1/2	2.903	6.033	9.171	12.310	15.451
4/7	2.999	6.133	9.273	12.413	15.554
2/3	3.142	6.283	9.525	12.566	15.708
1	3.832	7.106	10.174	13.324	16.471

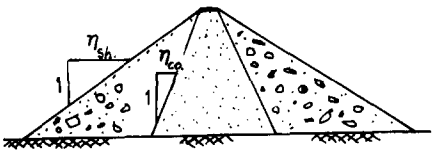

soil element moduli

core: $G_{s,co.} = F_{co.}\ \sigma_o^{\mu}$ shell: $G_{s,sh.} = F_{sh.}\ \sigma_o^{\mu}$

modulus for the shear beam

$$G = G_b \cdot (z/H)^m$$

$$m \simeq \mu + d$$

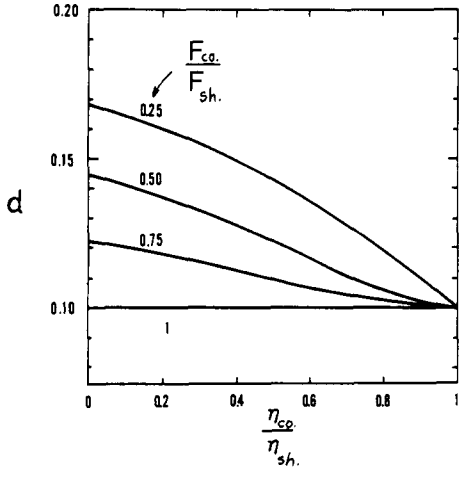

LIST OF TYPICAL μ VALUES FOR SOILS: $G_s = F \cdot \sigma_o^{\mu}$

Type of Material	Type of Test	μ	Reference
angular and round grained sands	resonant column	0.40-0.50	40,86
normally consolidated clays	resonant column; improved triaxial	0.50-0.60	53,86
compacted coarse gravel (D_{50}=45mm)	special resonant column apparatus	0.38	83
silty sand (D_{50}=0.07mm, 55% fines)	resonant column	0.60-0.90	24,105
silty sand (D_{50}=0.02mm, 80% fines)	resonant column	0.77	70
core, Kuzuryu dam	resonant column	0.69	72

Fig. 12. Dependence of modulus inhomogeneity parameter m *on material and geometric characteristics of the dam*

evidence accumulated from laboratory testing of a wide variety of real-life soils suggests that μ may take values anywhere between 0.35 and 0.90. A thorough literature survey produced an abundance of data, some of which is summarized in the Table attached to Fig. 12. This information can be utilized to make reasonably good estimates of μ for most materials to be used in the construction of dams and embankments.

Having established the likely range of μ values, parametric static finite-element analyses were conducted to determine the distribution of 'initial' gravity-induced stresses in typical dam cross-sections. Numerous linear but also a few nonlinear analyses, assuming both 'single-lift and 'multi-lift' construction, were performed. Most of the studied sections were idealized and made up of only one or two different zones, but some actual earth dam sections with known (published) material properties were also investigated. It was concluded that the average-across-the-dam modulus G, to be used in shear beam models, can in practically all cases, be expressed in the form:

$$G = G_b(z/H)^m \tag{7}$$

where G_b = the average shear modulus at the base. The coefficient m depends mainly on the material coefficient μ (equation (6)), and the geometry and relative stiffness of the core. Engineering accuracy is provided by the expression

$$m \simeq \mu + d \tag{8}$$

where $d \simeq d(F_c/F_s, \eta_c/\eta_s)$ is plotted in Fig. 12. Evidently d ranges between 0.05 and 0.20, with few exceptions. Therefore, in view of the range of μ values depicted in the list accompanying this figure, m is likely to attain values anywhere between 0.30 to 0.80. Notice also that the 2/3-power modulus variation of the aforementioned earlier studies is, indeed, most representative of the variation expected in practice.

5.3 Linear solution and results for the inhomogeneous shear beam

Analytical closed-form expressions have been derived in Refs 19 and 20 for natural frequencies and modal shapes, steady-state transfer ('amplification') functions, and seismic participation factors for a dam modelled as a triangular inhomogeneous shear beam, for an arbitrary value of the inhomogeneity factor m. Table 3 lists these expressions, along with those for the special case of $m = 2/3$, for easy reference.

Parametric results illustrating the effect of the degree of inhomogeneity (reflected in the parameter m) are shown: in Fig. 13 for natural periods, and modal displacement

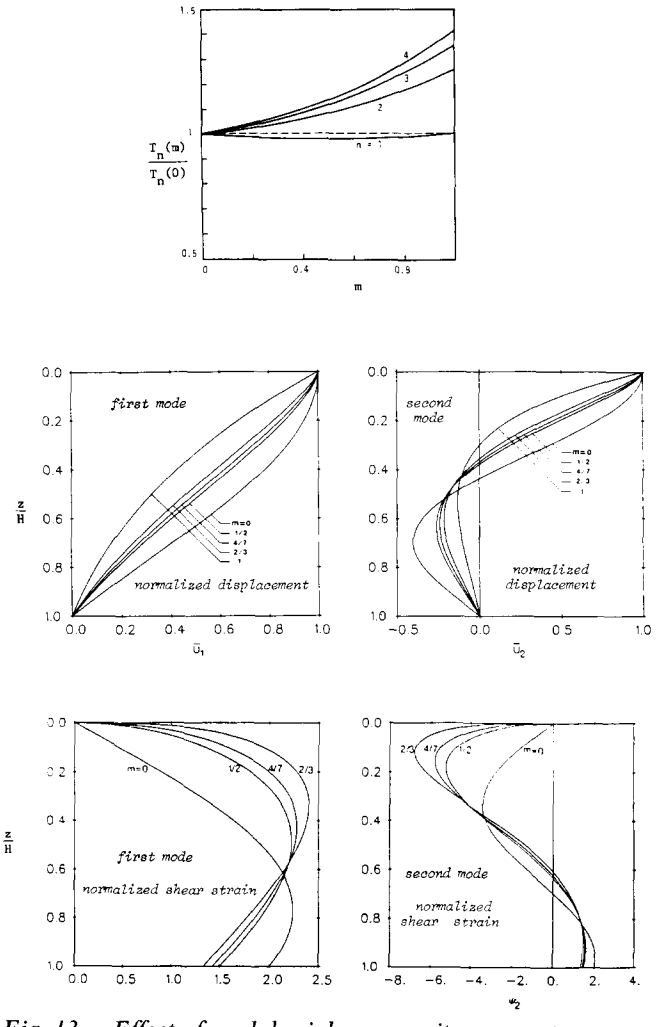

Fig. 13. Effect of modulus inhomogeneity parameter m *on natural periods, modal displacements and modal strain participation factors* [*Refs* 20–21]

and shear-strain shapes, and Fig. 14 for rigid-base crest amplification functions. It should be noticed that *increasing m leads to:* (i) sharper attenuation of mode displacements with depth; (ii) almost identical fundamental frequency; (iii) closer-spaced higher natural frequencies; (iv) higher displacement and acceleration amplification values at all resonances; (v) greater relative importance of the higher modes; and (vi) occurrence of maximum values of shear-strain modal shapes closer to the crest.

The effect of inhomogeneity on the linear seismic response of the afore-studied 120 m *tall and flexible* uniform dam is illustrated in Fig. 15–16. Subjected to the Taft 1952 NE component of recorded motion and modelled as a shear beam, the dam experiencies peak values of absolute acceleration which depend on the assumed value of m. Fig. 15 plots the distribution of peaks with depth for three values of m: 0 (homogeneous), 1/3, and 2/3. Several trends are worthy of note.

First, at the top quarter of the dam, peak acceleration and, to a less extent, peak displacements are sensitive to m. There is an about 60% difference in crest accelerations experienced by the homogeneous and the 2/3-inhomogeneous dam, while the corresponding crest displacements differ by only 25%. The response of the $m=1/3$-dam, on the other hand, only slightly exceeds the response computed for the homogeneous model. The difference among the three models practically disappear at the lower three quarters of the dam.

To get a better feeling on the nature of the crest response and its dependence on inhomogeneity, Fig. 16 compares the respective crest acceleration and displacement histories for $m=0$ (homogeneous) and $m=2/3$. It is evident that the higher natural frequencies play a significant role for accelerations only. Hence, since the relative importance of the higher modes (compared to that of the fundamental mode) increases with increasing inhomogeneity, as evidenced in the comparison of amplification functions in Fig. 14, higher m tends to lead to higher accelerations.

Second interesting observation is that shear *stresses* are hardly influenced by m. As a result, shear *strains*, being at all times inversely proportional to $G(z)$, are strongly affected by inhomogeneity. Notice in Fig. 15 that the location of the largest peak moves very close to the crest as m increases towards 2/3.

It is pointed out, however, that the foregoing conclusions based on Figs 15–16, are quantitatively appropriate only for *very flexible* earth structures and *linear* analysis. With stiffer dams the differences due to different m values may significantly decrease, since the higher modes play a less important role in the response.

Moreover, *nonlinear inelastic* soil behaviour during stong ground shaking may even reverse some of the trends observed in Figs 15–16, as discussed below.

5.4 Inelastic response of inhomogeneous shear beams

The very high amplification of near-crest accelerations computed for many inhomogeneous earth dams (with $m=0.60$–0.75) has prompted the question of whether such a behaviour is realistic. While it is true that substantial field evidence supports the inhomogeneous shear beam concept, most of the related field data involve the response of dams either to very weak seismic ground shaking, or to man-induced vibrations. Both types of loading induce very small shear strains and the constituent materials behave in a quasi-linear elastic manner. Such was the case, for instance, with aforementioned 12 dams listed in Fig. 11. The successful evaluation of the 2/3-model through another case study reported in Ref. 74 and outlined in the following section of this paper, also involved small-amplitude forced vibration tests and, thereby, quasi-linear behaviour. But *what about nonlinear inelastic response* to strong ground excitation?

Methods of analysing the inelastic response of earth dams are presented in detail in a subsequent section of this paper. Using one of these methods, the 'Layered Inelastic Shear Beam'[101], results have been obtained for the nonlinear-inelastic response of a 120 m tall dam having *stiffness characteristics compatible* with those of the 120 m dam studied in Figs 15–16. Again three different values of the modulus inhomogeneity parameter, $m=0$, 1/3, and 2/3, were considered. However, the average stress-average strain relationship for each layer superelement (Fig. 2) was assumed to be hyperbolic:

$$\tau=\tau(z,\gamma)=G(z)\frac{\gamma}{1+\gamma/\gamma_r} \tag{9}$$

with $G(z)$ = the low-strain elastic modulus $=G_b(z/H)^m$;

Table 4. Analytical expressions for some 2-D and 3-D earth dams models

Earth dam model	Fundamental period T_1	Ratio of natural periods T_1/T_2	nth Natural circular frequency ω_n	nth Modal displacement $U_n(x=0,z)$	nth Mode participation factor $\lvert P_n\rvert$	Steady-state midcrest/base transfer ('amplification') function $AF=[\ddot{u}(z=0)+\ddot{u}_g]/\ddot{u}_g$	
						I. 'Rigid-rock' amplification	II. 'Elastic-rock' amplification
Homogeneous 1-D shear-beam [42, 7]	$2.61\frac{H}{C}$	2.3	$\beta_n\frac{C}{H}$	$J_0(\beta_n\zeta)$	$\frac{2}{\beta_n J_1(\beta_n)}$	$\frac{1}{J_0(a_0)}$	$\frac{1}{J_0(a_0)+i\alpha J_1(a_0)}$
Inhomogeneous 1-D shear-beam $G\sim z^{2/3}$	$2.57\frac{H}{C}$	2	$\frac{7}{9}n\pi\frac{C}{H}$	$\zeta^{-2/3}\cdot\sin[n\pi(1-\zeta^{2/3})]$	$\frac{2}{n\pi}$	$\frac{a_0}{\sin a_0}$	$\frac{a_0}{\sin a_0+i\alpha\left(\frac{\sin a_0}{a_0}-\cos a_0\right)}$
Homogeneous shear-beam in semi-cyclindrical valley [22]	$2\frac{H}{C}$	2	$n\pi\frac{H}{C}$	$\frac{\sin(n\pi\zeta)}{n\pi\zeta}$	2	$\frac{a_0}{\sin a_0}$	$\frac{a_0}{\sin a_0+i\alpha\left(\frac{\sin a_0}{a_0}-\cos a_0\right)}$
Homogeneous shear-beam in rectangular valley with $L/H=2$	$2.19\frac{H}{C}$	2	$\left(\beta_n^2+\frac{\pi^2}{4}r^2\right)^{1/2}\frac{C}{H}$	$J_0(\beta_n\zeta)\cdot\sin(r\pi\zeta/2)$	$\frac{8}{\pi\beta_n J_1(\beta_n)}$	*	*
Approx. 3-D model of homogeneous dam in rectangular valley with $L/H=2$ [61]							
(i) steep slope $B/H=1.5$	$2.37\frac{H}{C}$	1.80	$\left(\delta_n^2+\frac{\pi^2}{4}r^2\right)^{1/2}\frac{C}{H}$	*	*	*	*
(ii) flat slope $B/H=3.0$	$2.51\frac{H}{C}$	1.82					

Notation:

- $\beta_n=n$th root of $J_0(\beta)=0$; for example: $\beta_1=2.40$, $\beta_2=5.52$, $\beta_3=8.65$ and so on
- $\delta_n=n$th eigenvalue of the 2-D plane-strain problem, $\delta_n=$function of slope B/H; $\delta_n\leqslant\beta_n$; for example: $\delta_1\approx 2.15$ for $B/H=1.5$
- $a_0=\omega H/C$; $\zeta=z/H$
- $C=$average shear wave velocity of the inhomogeneous dam
- $\alpha=$rigidity contrast ratio $=\rho C/\rho_r C_r$, where r refers to the properties of the supporting base; $i=\sqrt{-1}$

* no closed-form solution available

and γ_r = the reference strain = $\tau_{max}(z)/G(z)$. Two different *constant* values of γ_r were considered for simplicity: $\gamma_r = 0.003$ and $\gamma_r = 0.0013$; the resulting average two $\tau-\gamma$ curves for all three dams are plotted in Fig. 17, chosen so that the dam experiences mildly and strongly inelastic response, respectively, when subjected to the NE Taft record scaled to 0.40 g. It is pointed out that use of such semi-realistic nonlinear dam models in this study does not necessarily imply their endorsement for general use; it has rather been motivated by the fact that they can be defined with only three parameters: the average value of low-strain modulus G, the inhomogeneity parameter m, and the reference strain γ_r.

Figure 18 contrasts the distributions of peak values of absolute acceleration and shear strain from the compatible linear, moderately nonlinear ($\gamma_r = 0.003$) and strongly nonlinear ($\gamma_r = 0.0013$) analyses.

Several trends are worthy of note:

1. For all types of inhomogeneity ($m = 0, 1/3, 2/3$) strong nonlinear action leads to substantially reduced amplification. Peak crest accelerations decrease on the average from about 1.50 g during linear oscillations to barely 0.50 g during strongly inelastic shaking.

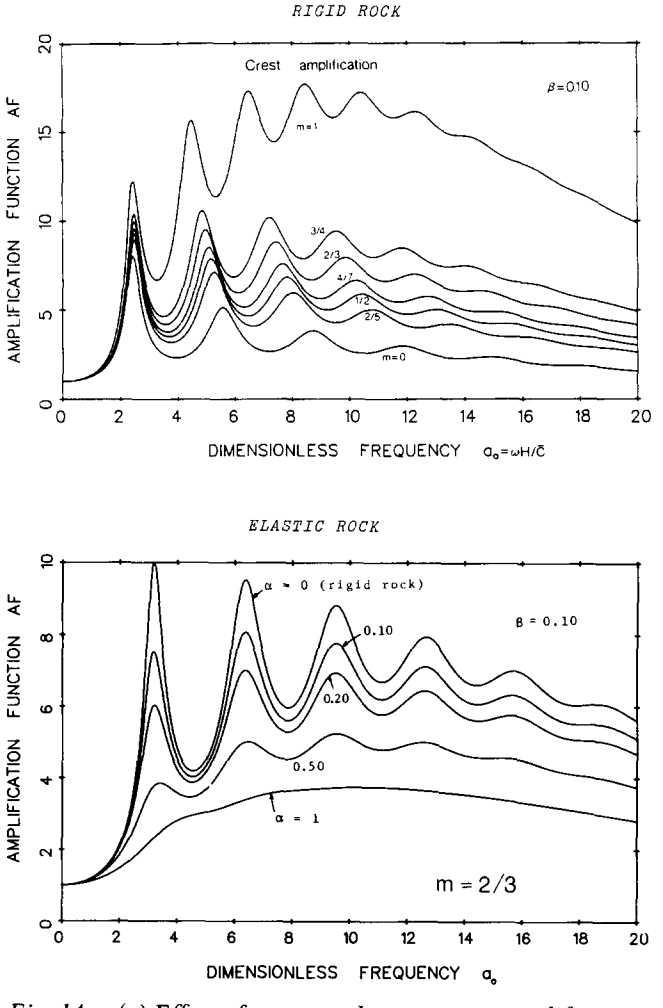

Fig. 14. (a) Effect of m *on steady-state crest amplification function: 'rigid rock' case. (b) Effect of rigidity contrast ratio* $\alpha = \rho C/\rho_r C_r$ *on crest amplification for* m = 2/3*: 'elastic rock' case*

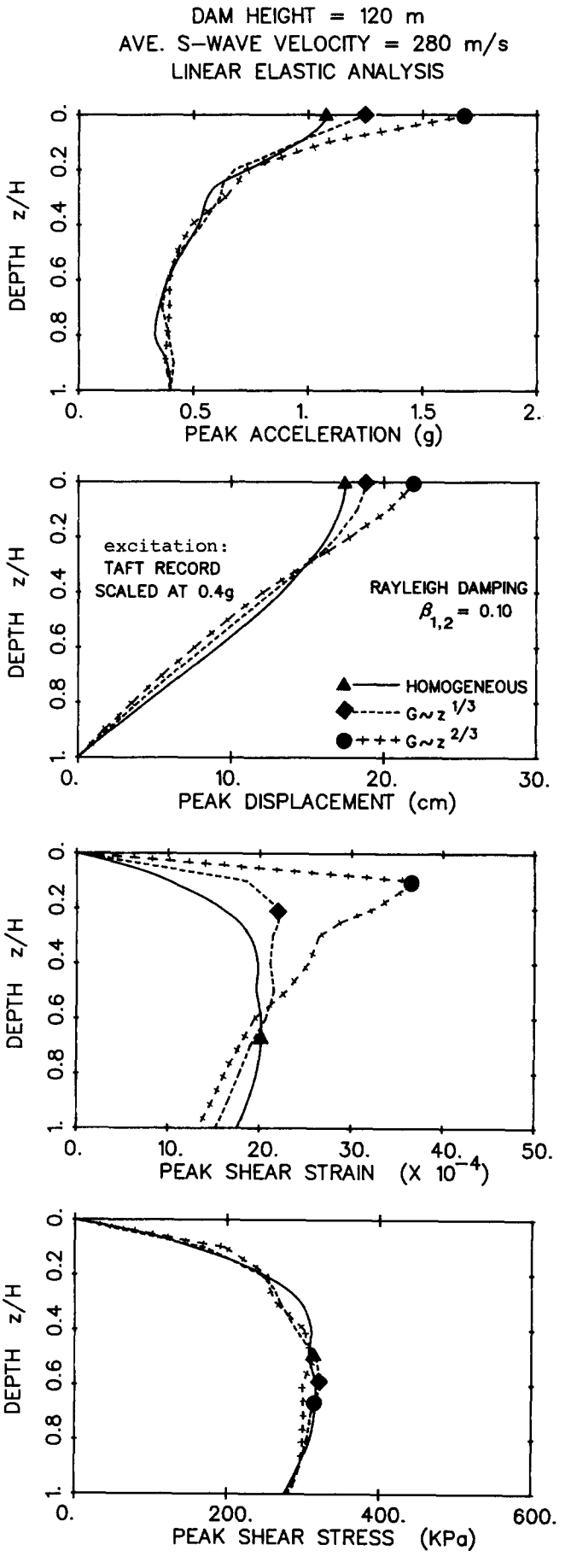

Fig. 15. Effect of degree of inhomogeneity on distribution with depth of peak seismic response variables. Notice substantial difference in crest acceleration

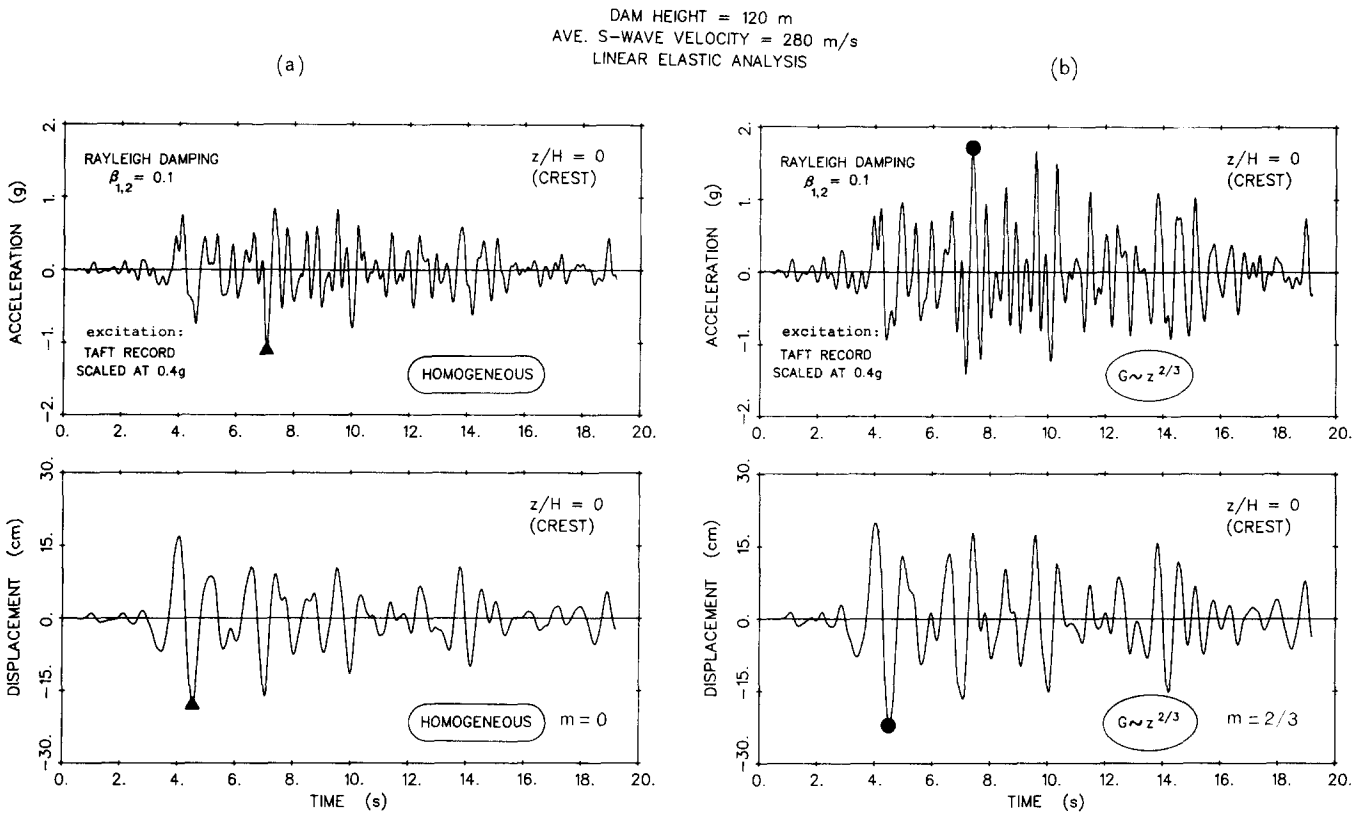

Fig. 16. Effect of inhomogeneity on crest acceleration and displacement histories (dam and excitation as in Fig. 15)

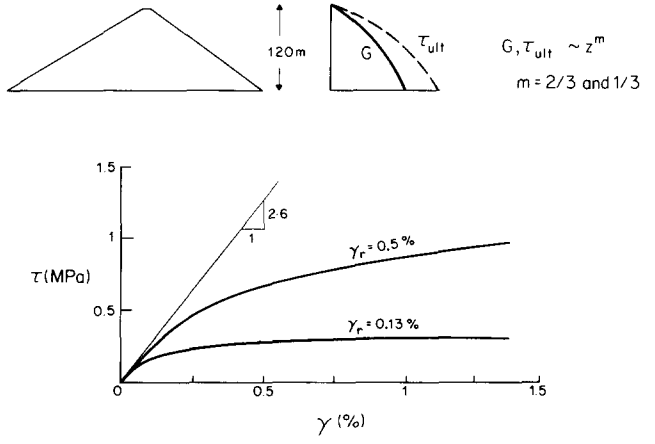

Fig. 17. Average hyperbolic layer shear stress-strain relations used in the study of inhomogeneity versus nonlinearity

2. The '$m = 2/3$-model' seems to be particularly sensitive to nonlinearities. Thus, for $\gamma_r = 0.0013$ this model predicts a peak crest acceleration which is smaller than the one computed with the '$m = 1/3$-model' – a rather dramatic reversal of the trend noted previously in the linear results. Notice also in Fig. 19 the substantial changes in the frequency content of the crest acceleration history of the '$m = 2/3$-model'.
3. Despite the inelastic action during the two nonlinear analyses (or perhaps because of it), the distributions of peak shear strains essentially retain their linear-elastic shape. The only noticeable difference is the increased concentration by crest of the peak strains induced in the '$m = 2/3$-model'. The differences between relative-displacement peaks (not shown here) further increase with increasing magnitude of nonlinearities.

In conclusion, inelastic behaviour plays a essential role in the seismic response of earth dams: it may cause a reversal of some of the linear effects of stiffness inhomogeneity, and a reinforcement of others. The magnitude of such changes, however, depends on the stiffness and strength characteristics of the dam, and the intensity, frequency characteristics, and details of the excitation.

6. 3-D EFFECTS OF CANYON GEOMETRY

The assumption of plane-strain conditions is exactly valid only for infinitely long dams subjected to synchronous lateral base motion. For dams built in narrow valleys, as is frequently the case in mountainous regions, the presence of relatively rigid abutments creates a 3-D stiffening effect, whereby natural frequencies increase and modal displacement shapes tend to become sharper as the canyon becomes narrower. These 3-D effects were first qualitatively studied about 30 years ago, when Hatanaka[42] and Ambraseys[8] extended the shear-wedge model to account for a rigid rectangular canyon. These early studies were only isolated attempts to address the issue of the effects of the shape and dimensions of the supporting canyon. It is only the last 6 years that satisfactory solutions to this complicated 3-D problem have been published.

These 3-D developments are listed in Tables 1 and 2 depending on whether they are based on the shear-beam

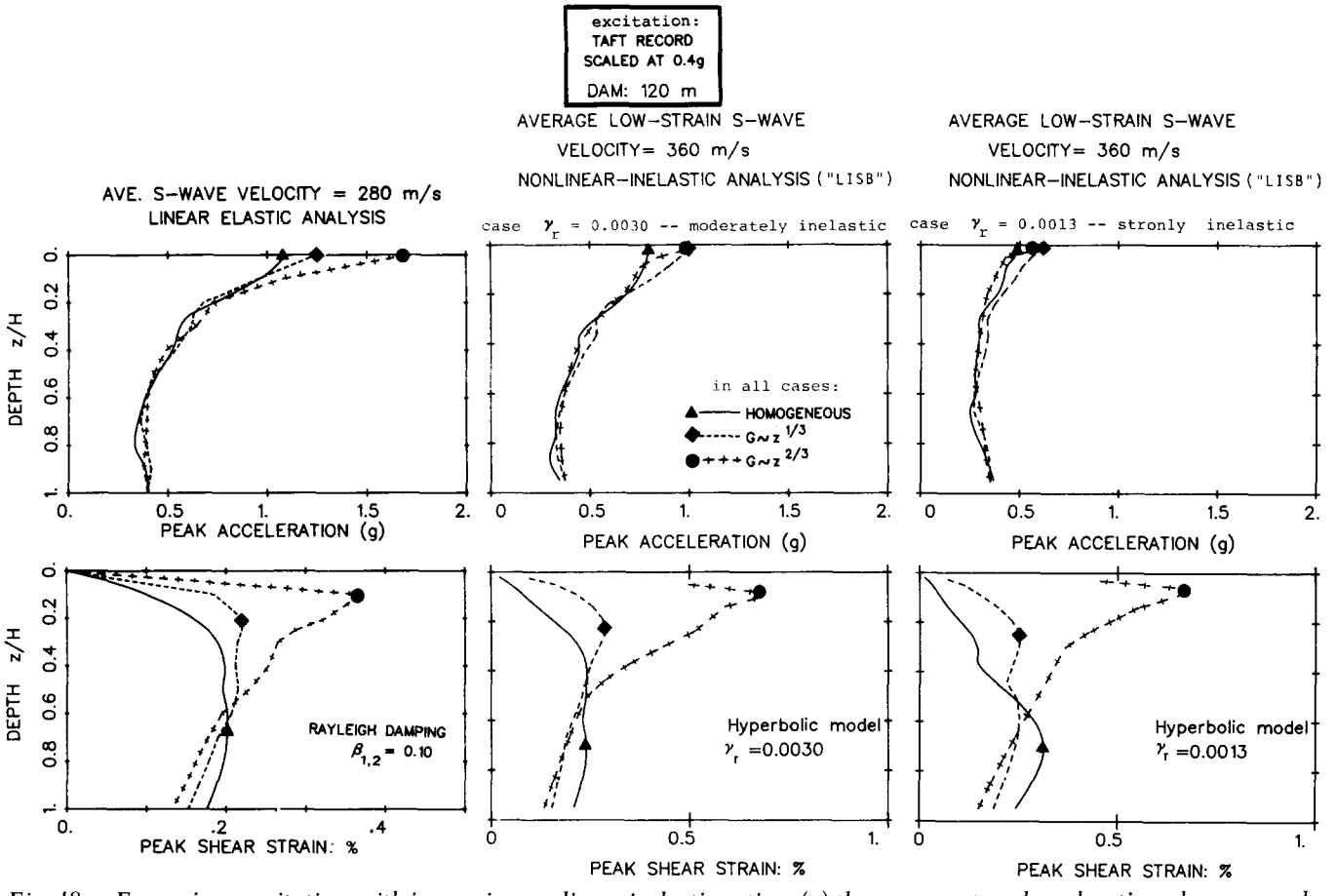

Fig. 18. For a given excitation, with increasing nonlinear inelastic action: (a) the near-crest peak acclerations decrease and the effects of inhomogeneity tend to diminish; but (b) the peak shear strain distributions remain nearly unchanged, both in magnitude and shape

concept[6,73,22] or make use of a finite-element discretization[61,57,64,27]. (The formulation of Ref. 6 being of a semi-analytical nature is listed in Table 1, although it is not restricted to shearing deformations.) Fig. 20 sketches the canyon profiles for which numerical results have been published.

6.1 Outline of methods of analysis

For earth dams having a plane of symmetry perpendicular to the longitudinal axis, Martinez and Bielak[61] have developed a numerical procedure which overcomes the expense of 3-D finite-element analyses. To this end, they neglect the (indeed secondary) longitudinal deformation and discretize in finite elements only the dam midsection, which coincides with the plane of symmetry. Displacements and inertia forces are expanded in Fourier series (of m terms) in the logitudinal direction and the problem is reduced to solving m uncoupled 2-D finite element problems:

$$[M]\{\ddot{v}\}_j+[K+K_{0j}]\{v\}_j=\{f\}_j \qquad (10)$$
$$j=1, 2, \ldots, m$$

where only a small number m of longitudinal modes needs to considered. $[M]$ and $[K]$ in equation (10) are the 2-D mass and stiffness matrices of the finite-element discretized midsection. The effect of the third dimension is reflected in the 'added' stiffness matrix $[K_{0j}]$ and the effective excitation vector $\{f\}_j$. Note that K_{0j} is proportional to $(j/L)^2$ implying that the stiffening effect of the canyon will be especially important in very narrow valleys and for very high modes in the logitudinal direction. The presented parametric results bear out these canyon effects on natural frequencies, natural modal shapes and distribution of seismic stresses; substantial differences are noted between dams in narrow triangular and rectangular canyons (both of aspect ratio $L/H=1$), as it will be later on.

A different approximate formulation based on the shear-beam concept has been presented by Ohmachi[73,74]. Both longitudinal and vertical displacements are ignored, but no symmetry is required. The dam is divided into super-elements through vertical, closely-spaced transverse planes, as sketched in Fig. 21a. Each super-element has the shape of a truncated pyramid the bases of which are two neighbouring cross-sections and which is assumed to behave as a triangular shear beam whose geometry and properties are from the middle section of that element. The law of distribution of displacements within each element is obtained from the shear-beam modal shapes. This implies that the distribution of mode-shape displacements along the depth is not affected by the presence of the canyon; this is not correct, especially for the higher modes, but for the first two or three modes it may be a good approximation as discussed later. A linear interpolation function is used to express the displacement shape in the longitudinal direction and, by enforcing compatibility of deformation between the super-elements,

the solution is obtained in the form of natural frequencies and modal shapes. Ohmachi's results for rectangular, trapezoidal and triangular canyons confirm the significance of canyon geometry found by Martinez and Bielak, although some quantitative differences exist between the natural frequencies reported in the two studies for dams in triangular canyons. Of particular interest in Ref. 74 is the successful use of this approximate 3-D shear-beam model, in conjunction with an average-across-the-width shear modulus proportional to $z^{2/3}$, to reproduce the previously mentioned results of full-scale forced-vibration tests on Bouquet Dam[51] (see Fig. 47).

Abdel-Ghaffar and Koh[6] have presented a more rigorous although computationally quite efficient 3-D semi-analytical solution for dams built in canyons of any shape but having a plane of symmetry. This solution is based on the Rayleigh-Ritz method with the shear-beam modal shapes or even simple sinusoids as 'basis functions', and involves an appropriate transformation of the dam geometry into a cuboid. Results have been presented for natural frequencies and mode shapes of an inhomogeneous dam in a trapezoidal canyon, and an attempt has been made to reproduce the recorded seismic response of the Santa Felicia Dam during the 1971 San

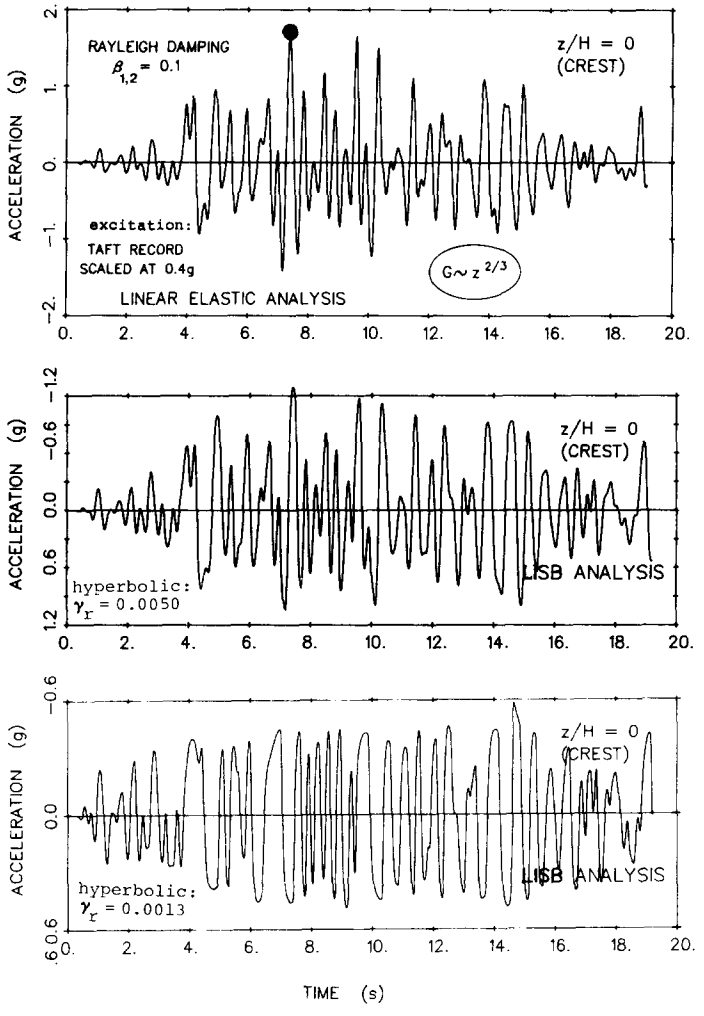

Fig. 19. Inhomogeneity versus nonlinearity: linear, moderately nonlinear ($\gamma_r = 0.005$) and strongly nonlinear ($\gamma_r = 0.0013$) response crest acceleration histories in an inhomogeneous dam with m = 2/3. *The frequency content of the motion changes as dramatically as its intensity*

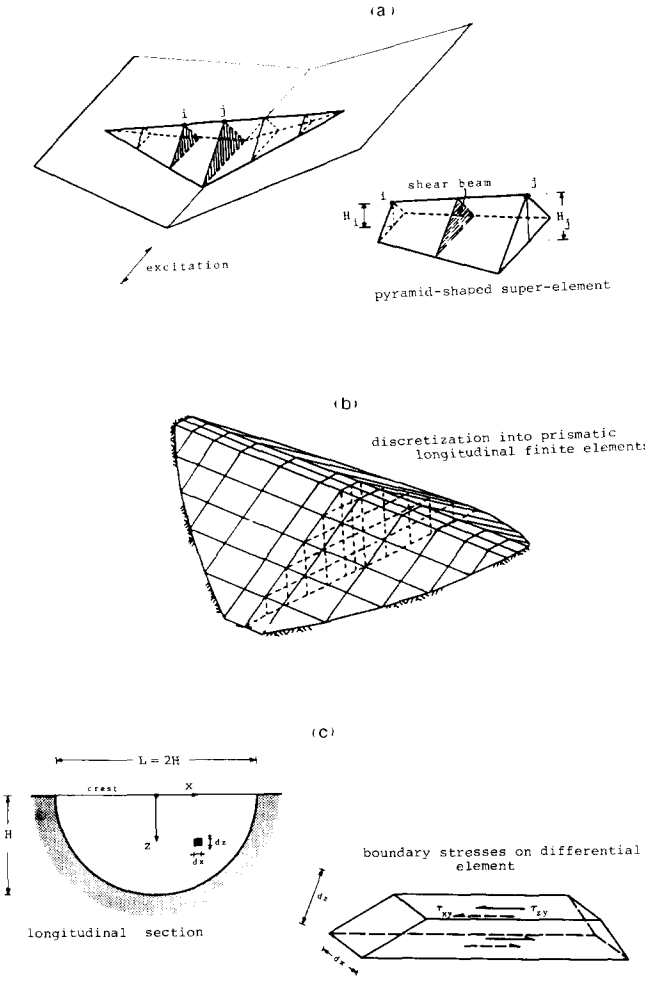

Fig. 21. Sketches of some models for dams in 3-D canyons: (a) approximate combination of shear beam with finite element method[73,74]; (b) 3-D finite-element method[57,64,65]; (c) semi-cylindrical shear beam[19,22]

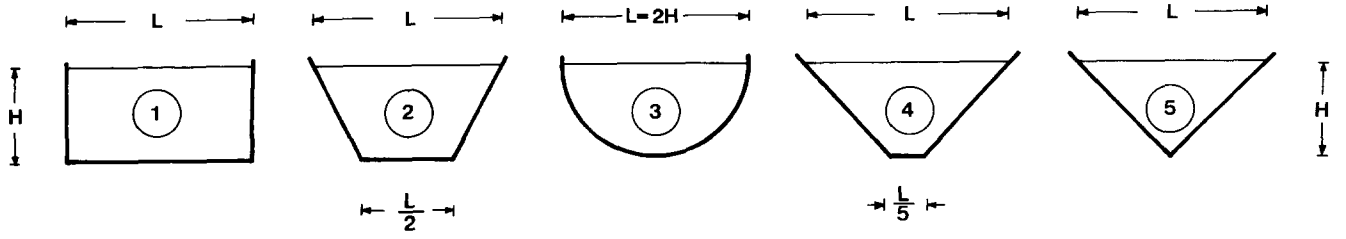

Fig. 20. Canyon geometries which have been studied in the literature (1: rectangular; 2: wide trapezoidal; 3: semi-cylindrical; 4: narrow trapezoidal; 5: triangular)

Fernando Earthquake. Of particular significance is the versatility of the method which has been recently extended[27] to formulate a realistic approximate solution for the nonlinear inelastic response of dams in nonrectangular canyons. This unique development will be addressed later herein.

Relatively efficient 3-D finite-element formulations have been developed at Berkeley. Makdisi *et al.*[57] outline such a formulation which is derived by replacing the 2-D plane-strain isoparametric elements of the computer code LUSH with prismatic logitudinal elements having six faces and eight nodal points (Fig. 21b). To reduce computer storage and time requirements, they ignore the secondary longitudinal displacements and assume that only shear waves can propagate vertically and horizontally in the embankment. Using this model, results are obtained for steady-state and transient response of homogeneous dams in triangular canyons. Subsequent work at Berkeley[64,65] has avoided the aforementioned simplifying restriction on longitudinal deformations and presented results for seismic accelerations and shear stresses in dams with idealized, as well as actual, cross-sectional geometries. These studies show that the presence of the rigid triangular boundary increases the fundamental frequencies, and seems to substantially increase the seismic acceleration while decreasing the seismic shear strains. In addition, the method of Ref. 64 has been used to backfigure the dynamic stiffness characteristics of the Oroville Dam using its recorded response to the August 1975 Oroville Earthquakes; the obtained values are in reasonable agreement with laboratory test results on material from the shell of the dam.

All the foregoing 3-D formulations resort, one way or another, to numerical computations which in most of the cases require substantial computer storage, and data-preparation and execution times. It may be questioned whether such methods are justified for use in preliminary design calculations, especially in view of the fact that they ignore several other important phenomena: non-synchronous excitation by vertical and oblique seismic waves, nonlinear-inelastic soil behaviour, radiation of energy into the supporting valley.

Thus, it is of particular interest that a very simple analytical closed-form solution has been derived by Dakoulas and Gazetas[22] for the dynamic lateral response of a homogeneous earth dam built in a *semi-cylindrical* valley. The solution is based on a generalization of the shear-beam concept. Only lateral displacements and shear deformations are allowed, and they are assumed to be uniformly distributed across the dam, i.e., independent of y (Fig. 21c). With these assumptions, the solution is exact; no other approximation is introduced such as, for example, the assumption of independent vertical and horizontal distributions of mode shapes in the aforementioned Ohmachi[73] formulation. The results are presented in the form of surprisingly simple algebraic expressions for natural periods, modal shapes, steady:state transfer functions for harmonic base motion, and participation factors for transient seismic excitation. Table 4 depicts these expressions and compares them with those for a (homogeneous) 1-D shear beam[7] and a homogeneous 2-D shear beam in a rectangular canyon. Also given in this Table for direct comparison are (i) the formulae corresponding to an inhomogeneous 1-D shear beam with modulus proportional to $z^{2/3}$ [Refs 32 and 33]; and (ii) approximate formulae for the 3-D natural frequencies of a homogeneous dam in a rectangular canyon[61] obtained without neglecting vertical displacements and normal stresses and strains. Further discussion of Table 4 is deferred to the following subsections.

It is worthy of note that although the choice of a semi-cylindrical canyon has been primarily motivated by the ensuing mathematical convenience, such a shape does in fact constitute a reasonable idealization of many actual cases. For example, the valleys of the Kisenyama and Makio rockfill dams in Japan[77], of El Infiernillo dam in Mexico[90], of Rama earth dam in Yugoslavia[81], of Long Valley dam in California[99] and of Polyphytos dam in Greece, just to name a few, may be idealized with good accuracy as semi-cylindrical.

6.2 Characteristic results of linear analysis

a. *Natural periods and mode shapes.* The stiffening effect of a narrow canyon on the fundamental natural period, $T_1 = T_1(L/H)$, of a dam is demonstrated in Fig. 22a for the five different canyon shapes sketched in Fig. 20 (see also Table 4). Both shear-beam and finite-element based

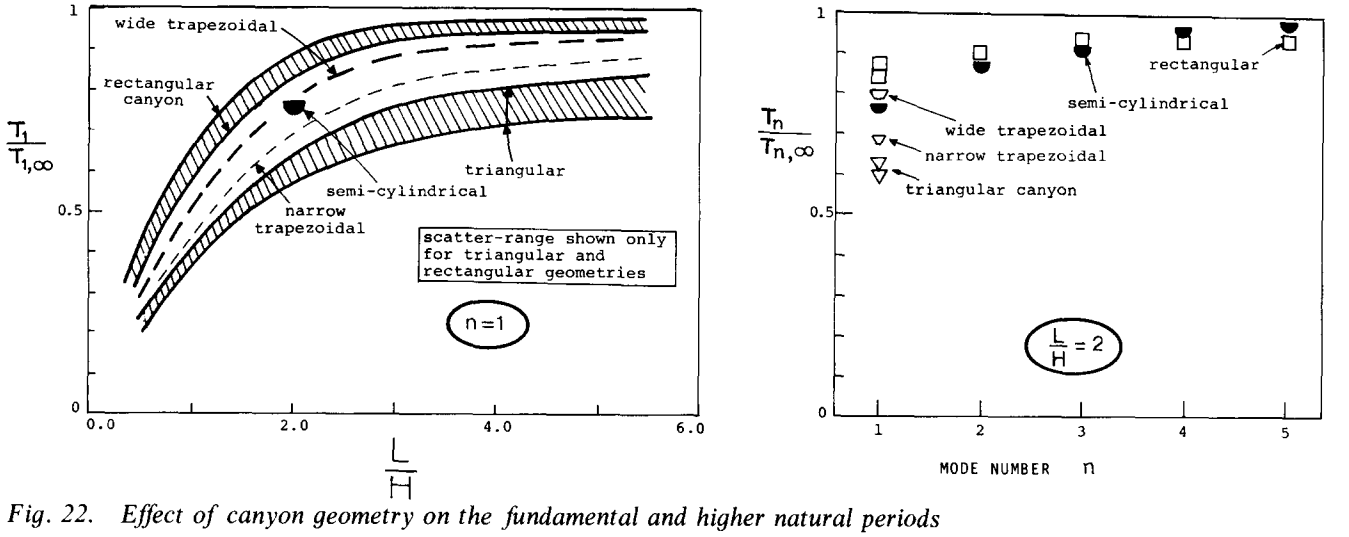

Fig. 22. Effect of canyon geometry on the fundamental and higher natural periods

results are shown in this figure. $T_{1,\infty}$ represents the natural period of an infinitely long dam under plane deformation, and L/H is the aspect ratio. Only results for homogeneous dams have been used for this figure; however, for a given aspect ratio and canyon shape, the ratio $T_1/T_{1,\infty}$ is hardly influenced by inhomogeneity and hence Fig. 22a may be used for estimating the canyon effects with any type of dam.

Another interesting observation is that the ratio $T_1/T_{1,\infty}$ is essentially the same for both shear-beam and finite-element type idealizations. In other words, while shear-beam formulations usually underestimate $T_{1,\infty}$ by about 5%–10%, they also tend to underestimate $T_1(L/H)$ by approximately the same amount. Two other factors, namely the presence of a relatively soft clay core and the flattening of the slopes, also tend to increase T_1 and $T_{1,\infty}$ by roughly proportional amounts and hence, again, the ratio $T_1/T_{1,\infty}$ may be estimated from Fig. 22a.

The higher natural periods T_n, $n=2-5$, of dams in valleys with $L/H=2$ are compared with the respective periods $T_{n,\infty}$, of the infinitely long shear wedge in Fig. 22b. Results are only available for semi-cylindrical and rectangular canyons. Perhaps suprisingly, the differences among the three sets of periods wither away as n increases, and for $n\geqslant 3$ it appears that T_n is practically independent of canyon geometry. However, this near-coincidence of higher natural periods is rather circumstantial and is due to the fact that the ratio T_1/T_n for both of these canyons is lower than the corresponding $T_{1,\infty}/T_{n,\infty}$ ratio, as evidenced in Table 4. For instance, for a dam in a semi-cylindrical canyon $T_1/T_3=3$, from which $T_3=(0.67)\,H/C$; by contrast, the shear beam solution gives $T_{1,\infty}/T_{3,\infty}\approx 8.65/2.40\approx 3.60$ from which $T_{3,\infty}\approx(0.72)\,H/C$. Therefore, $T_{3,\infty}$ is only 9% greater than the 3-D value of T_3, compared with the 24% discrepancy in the

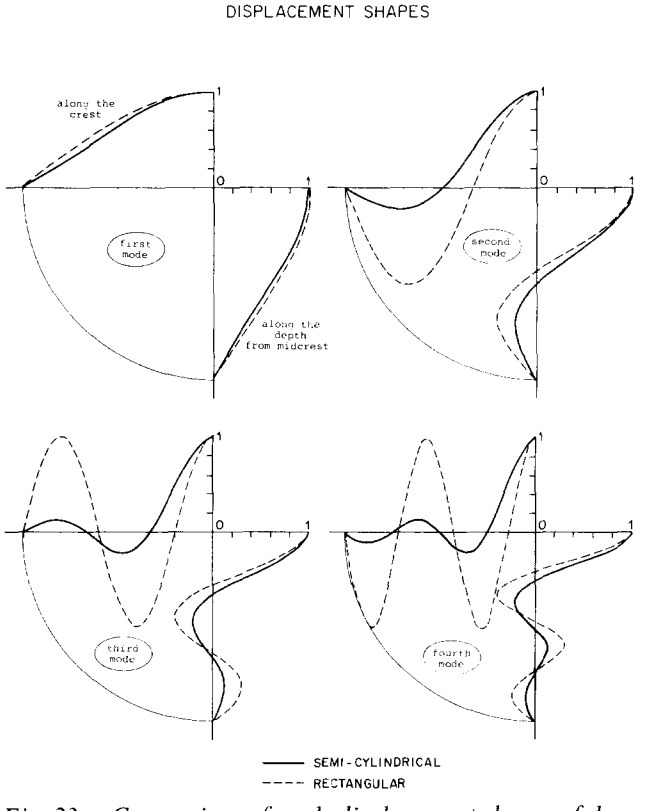

Fig. 23. Comparison of mode displacement shapes of dam in semi-cylindrical and in rectangular valley, with L/H = *2*

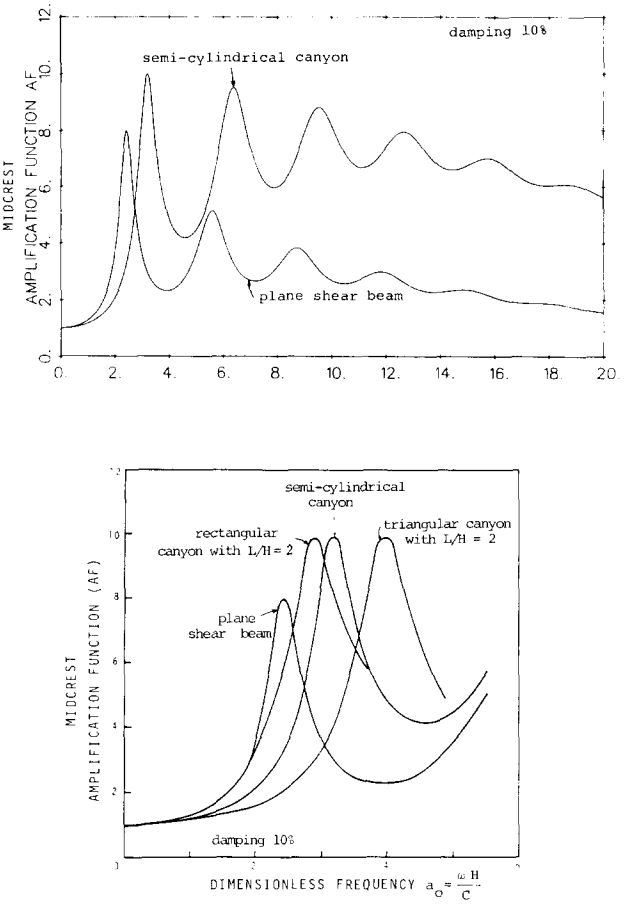

Fig. 24. Steady-state response to harmonic base excitation: (a) mid-crest amplification function for semi-cylindrical dam determined from 3-dimensional and from plane shear-beam analysis; (b) effect of canyon shape on midcrest amplification function

respective fundamental periods $T_{1,\infty}$ and T_1. Note, however, that the modal displacement shapes at these higher natural periods are more sensitive than the fundamental shape is to variations in canyon geometry.

The comparison of four natural mode shapes in Fig. 23 also pertains to dam in a circular and a rectangular canyon (both with $L/H=2$) modelled as shear beams. (Few published results are available for the mode shapes of dams in canyons of other geometries.) Shown are the distributions along the crest, and along the depth from midcrest. Notice that the cylindrical canyon leads to a slightly sharper attenuation of displacements with depth.

However, the effects of a narrow canyon on the higher mode shapes may be significantly more important when the vertical and horizontal displacement components are *not* neglected. For instance Martinez and Bielak[61] found that only the fundamental (lateral) mode resembles a pure shear distortion; significant vertical displacements are present in the second symmetric (lateral) mode which, consequently, shows little resemblance with a shear type mode. Abdel-Ghaffar and Koh[6] found that even logitudinal displacements are not insignificant during this second mode in dams built in narrow valley.

b. *Steady-state harmonic response.* The effect of a narrow-canyon geometry on the steady-state response of a dam to a harmonic rigid base excitation $\ddot{u}_g\exp(i\omega t)$ is portrayed in Fig. 24. Analytical expressions for the crest amplification functions (AF) are shown in Table 4 for a

semi-cylindrical canyon, and for a rectangular canyon with $L/H=2$.

Figure 24a, compares the midcrest 'rigid-rock' AF for a dam in a semicylindrical canyon to that obtained from a 1-D shear-beam analysis for the midsection of the dam. It is evident that, in addition to predicting lower natural frequencies, the plane shear model underpredicts both the amplification at first resonance and the relative importance of higher resonances.

The effect of different canyon shapes on AF are illustrated through the comparison of Fig. 24b. All dams have an aspect ratio $L/H=2$. Results for triangular canyon[57] are available only for values of the frequency factor a_0 up to about 5, and thus the comparison is limited to a frequency range encompassing only the fundamental of the natural frequencies of the studied dams. The curve for the rectangular canyon is based on the classical 2-D shear-beam solution[42,7]. The plots in Fig. 24 exhibit a consistent trend and reveal that the value of AF at first resonance, AF_{max}, is practically independent of the exact canyon shape; for the considered value of the hysteretic damping ratio, $\beta=0.10$, $AF_{max}\approx 10$. Moreover, additional results in Ref. 57 show that, in triangular valleys, $AF_{max}\approx 10$ for all values of the aspect ratio L/H – a somewhat paradoxical result which has yet to be fully understood.

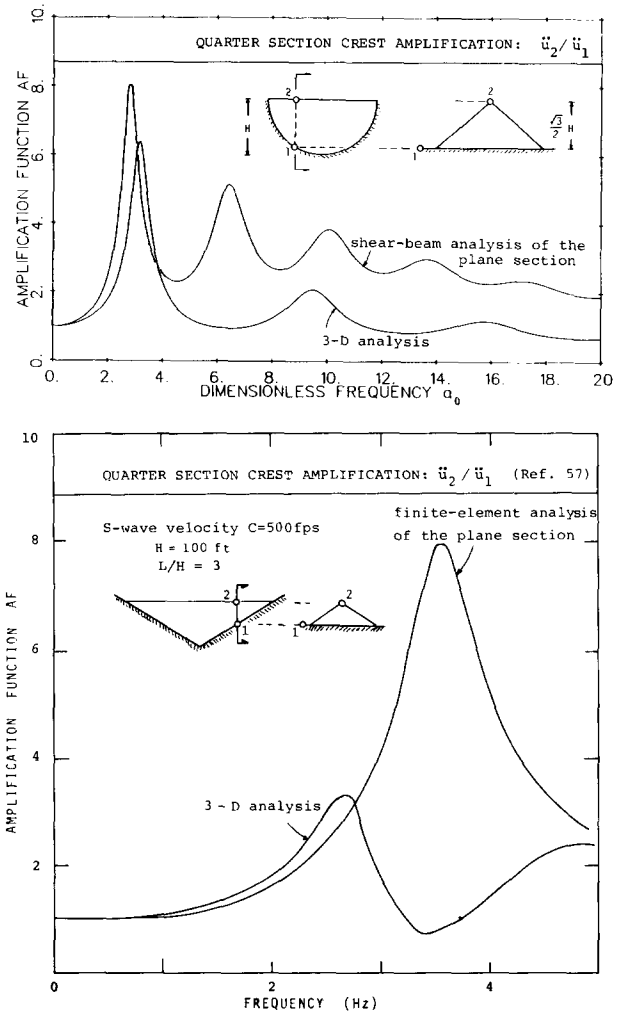

Fig. 25. Crest amplification functions at the quarter section of (a) semi-cylindrical dam and (b) triangular-canyon dam: 3-Dimensional versus plane analysis

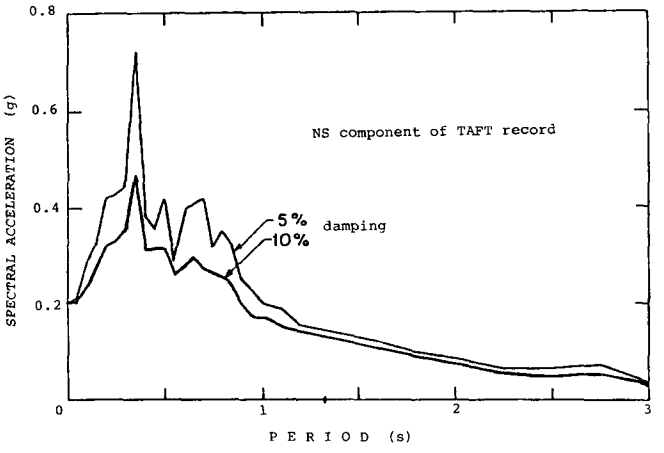

Fig. 26. Absolute acceleration spectrum of scaled Taft record

Frequently in practical seismic analyses of dams built in narrow valleys, various cross-sections in addition to the midsection are studied using plane formulations. To investigate the validity of such a procedure, Fig. 25a compares two 'rigid-rock' amplification functions (AF) for the crest of the quarter-section ($x/L=0.25$) of a dam in a cylindrical valley: one AF obtained from a plane shear-beam model having a height equal to $\sqrt{3H/2}$, and the other from the previously discussed cylindrical canyon shear model for $x/L=0.25$. Notice that, in this case, the plane fundamental resonant peak exceeds the respective cylindrical resonant response by about 30%. The discrepancies at higher frequencies are even greater, with the plane solution always exceeding the approximate 3-D response. Similar trends are evident in Fig. 25b for a triangular canyon with $L/H=3$[57].

Results for steady-state shear strains and stresses, not presented here, exhibit a rather different trend: the plane solution often overestimates the resonant strains at midcrest and tends to underestimate them at the quarter section. See Refs 22 and 65 for more details.

c. *Seismic response.* Earthquake ground excitation differs from a harmonic motion in that it contains a fairly broad spectrum of frequencies, and it is of a random and transient nature. Hence seismic response is transient and the effect of each contributing frequency is not necessarily the same as when it acts alone, under steady-state conditions.

As an example, the response of an idealized 120 m high dam in a U-shaped canyon is subjected to the NE component of the ground acceleration recorded at Taft during the 1952 Kern County earthquake, scaled to a peak acceleration value of 0.20 g. The pseudo-acceleration response spectrum (5% and 10% damping) is presented in Fig. 26. For this type of ground excitation, the dynamic uniform properties of the dam are taken: $C=280$ m/s and $\beta=10\%$.

The '3-D' acceleration, displacement and shear-strain response histories computed with the semi-cylindrical shear-beam model for several points in the dam, are compared in Figs 28–29 with the respective histories computed for the dam midsection from a plane shear beam. The distributions with depth from the crest of the corresponding three sets of peak values are compared in

Fig. 27. The following trends may be noted:

1. The largest discrepancy between semi-cylindrical ('3-D') and plane ('2-D') shear beam results involves absolute accelerations; the '2-D' peak accelerations at the upper third of the dam are only about one-half of the '3-D' values. This is consistent with the findings of Makdisi *et al.*[57] which are summarized in Fig. 30, and may be explained by noticing that: (i) the 10% damped spectral acceleration of the input motion at the fundamental period $T_1 = 2 \times 120/280 \simeq 0.86$ s of the '3-D' dam equals about 0.22 g, compared to only 0.14 g that corresponds to the $T_1 = T_{1,sb} \simeq 2.16 \times 120/180 \simeq 1.12$ s of the '2-D' dam and (ii) the contribution of the higher modes to the near-crest accelerations is much more important for the '3-D' dam, as evidenced in the comparison of Fig. 24, and, also, by recalling that while the participation factor $|P_n|$ of the nth mode remains constant for the '3-D' dam (Table 4), in the '2-D' case $|P_n|$ decreases monotonically with n ($|P_1| \approx 1.61$, $|P_2| \approx 1.07$, $|P_3| \approx 0.85$, $|P_4| \approx 0.73$, and so on).

2. The differences between the corresponding relative displacements, as well as between shear strains (both time histories and peak values) are not so dramatic. This may be explained in view of: (i) the nearly equal values (about 1.4 inches) of spectral relative displacement of the input motion at the two fundamental periods; and (ii) the comparatively secondary importance of higher modes on displacements and strains. This becomes evident by comparing acceleration *versus* displacement histories: oscillations of both '3-D' and '2-D' displacements occur at essentially the fundamental natural periods of each system (0.86 and 1.12 s, respectively), with smaller participation of higher modes. In fact, repeating the analyses with *only* the first mode participating in the response, yields similar displacement histories, with peak values within 30% of the 'exact' ones. Notice also the different frequency contents of displacement and acceleration histories; the latter exhibit vividly the substantial contribution by the higher modes – in accord with the remarks of the preceeding paragraph. On the other hand, shear strains show an intermediate behaviour with some participation of higher harmonics.

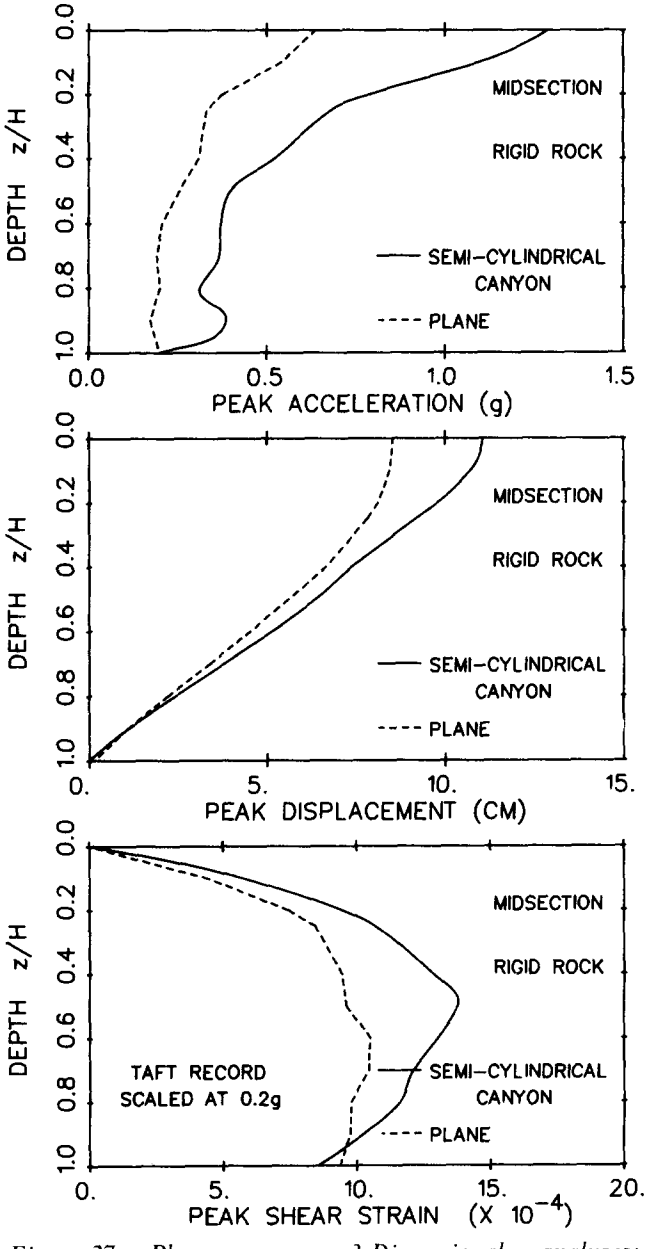

Fig. 27. Plane versus 3-Dimensional analyses: distribution with depth of peak response variables (dam: H = 120 m, C = 280 m/s, β = 0.10; excitation: Fig. 26). Notice substantial differences in accelerations

The above trends seem to be qualitatively valid for different input motions. For instance, Ref. 22 compares '3-D' and '2-D' distributions of peak accelerations, displacements and strains in the same 120 m dam subjected to NS component of the 1901 Avenue of Stars record in the 1971 San Fernando earthquake, also scaled to 0.2 g. Again, '3-D' acceleration are about two times the corresponding '2-D' values. Displacements and strains from the two models are about equal. In fact, the 'plane' displacements exceed by about 10% the corresponding 'semi-cylindrical' values – not an unexpected result in view of the somewhat different shape of relative displacement spectrum for this record.

d. *Effects of 'Elastic Canyon' and 'Strong' Rayleigh damping.* A question of practical interest is whether the very high absolute crest accelerations computed for dams in semi-cylindrical and triangular valleys are realistic. Indeed, each of the following three phenomena, although ignored in all the foregoing studies, may play a role in keeping crest accelerations substantially lower than predicted with linear 3-D solutions:

- transmission of wave energy into the supporting resilient canyon or canyon-alluvium system ('elastic canyon' effect)
- presence of logitudinal and vertical, in addition to lateral, components of motion at higher frequencies
- nonlinear inelastic soil behaviour during strong ground shaking

An approximate way has been previously outlined to account for the dissipation of part of the input seismic energy through waves spreading outward into the supporting valley. To this end, following the technique of Roesset[88], the input seismic motion is considered as the motion at the free-field *rock outcrop* rather than at the base of the dam. As shown in Table 4 the resulting crest amplification is reduced by an amount which depends on the 'rigidity contrast ratio', $\alpha = \rho C / \rho_r C_r$.

By suppressing the logitudinal and, in the case of shear-beam type solutions, the vertical components of motion

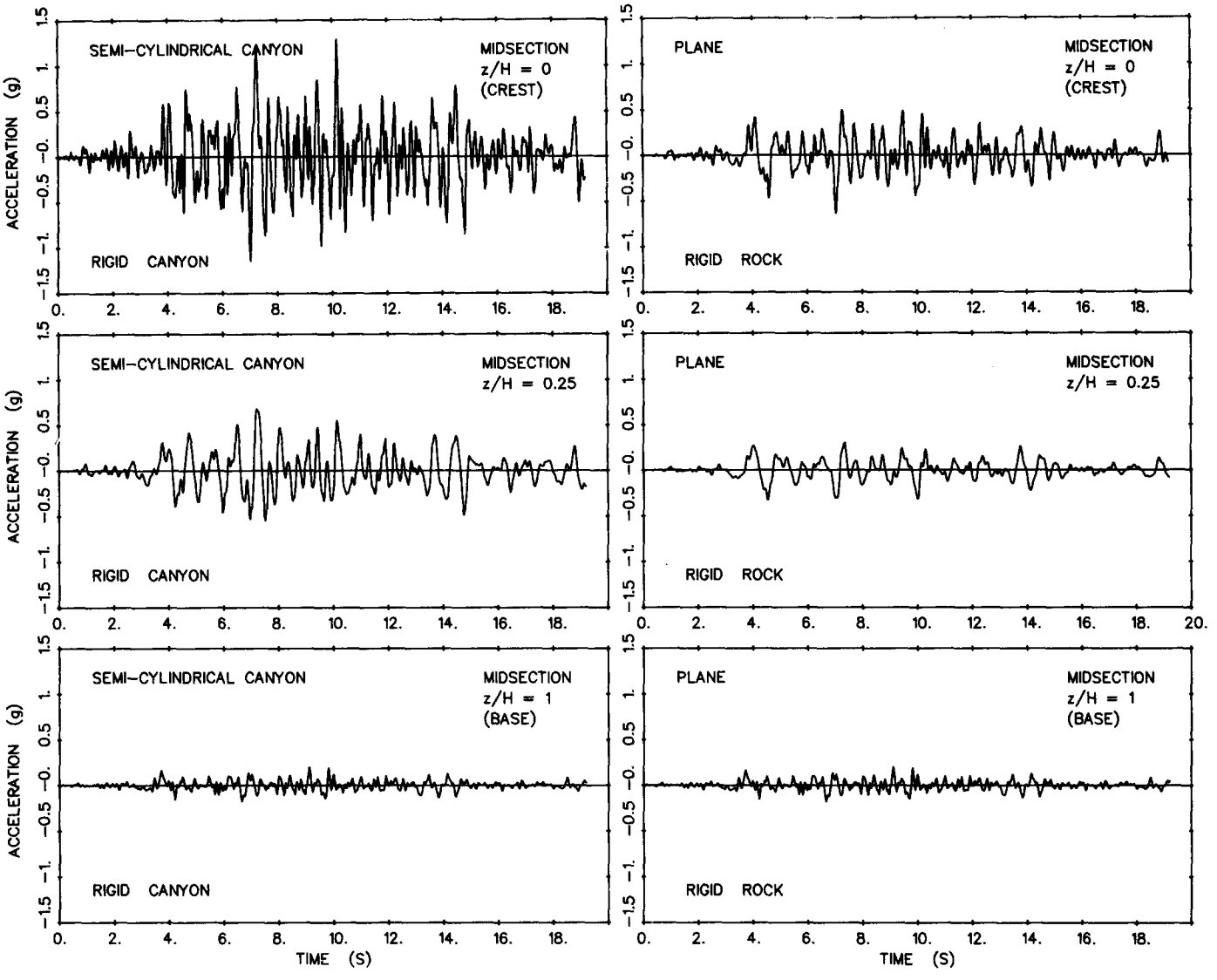

Fig. 28. Plane versus 3-Dimensional analyses acceleration histories at various depths (dam and excitation as in Fig. 27). Notice difference in frequency content of crest motion

the participation of the higher natural modes of oscillation in the response is undoubtedly exaggerated. This has already been discussed when plane shear-beam and finite-element solutions were compared in a preceding section. It seems that every time important degrees of freedom are artificially constrained the system appears as stiffer and more sensitive to resonances than in 'reality.' Rigorous solutions[6,61] strongly indicate that dams in narrow canyons oscillating in their third and higher natural modes undergo very substantial vertical and logitudinal deformations, accompanied by normal stresses and strains. Hence the artificially large high-frequency resonant peaks, which contribute to the computed high crest acceleration.

To get a *rough feeling* for the effect of such, perhaps spurious high-frequency components, an empirical 'correction' is applied herein: 'strong' Rayleigh damping is assumed instead of constant modal damping. Damping ratios start with $\beta_1 = 10\%$ and increase linearly with mode number – a rather bold assumption aimed solely at unveiling the effects of an extreme, but distinct, possibility when nonlinear inelastic soil behaviour is expected.

The combined application of the elastic-canyon and the Rayleigh-damping 'corrections' leads to the results plotted in Fig. 31 for the aforesaid 120 m dam. Now the Taft record is applied to the rock outcrop and the resulting effective base motion is shown at the bottom of Fig. 31. The rigidity contrast ratio: $\alpha = 0.20$.

It is evident from these figures that: (i) the response of both dams decreases considerably; (ii) the decrease of the near-crest accelerations in the semi-cylindrical dam is spectacular; (iii) the effect of the 'corrections' on the plane shear-beam predictions is smaller than on the semi-cylindrical results, and thus the discrepancies in the two sets of solutions tends to diminish. It has also been found (but is not shown here) that each of the applied two 'corrections' shares almost equally the responsibility for the above changes.

6.3 Effect of inelastic action on 3-D response

Generally speaking, soil nonlinearity tends to reduce peak accelerations. Two of the primary causes: increased hysteretic dissipation of wave energy, and destruction of any potential resonances. We have already seen in the

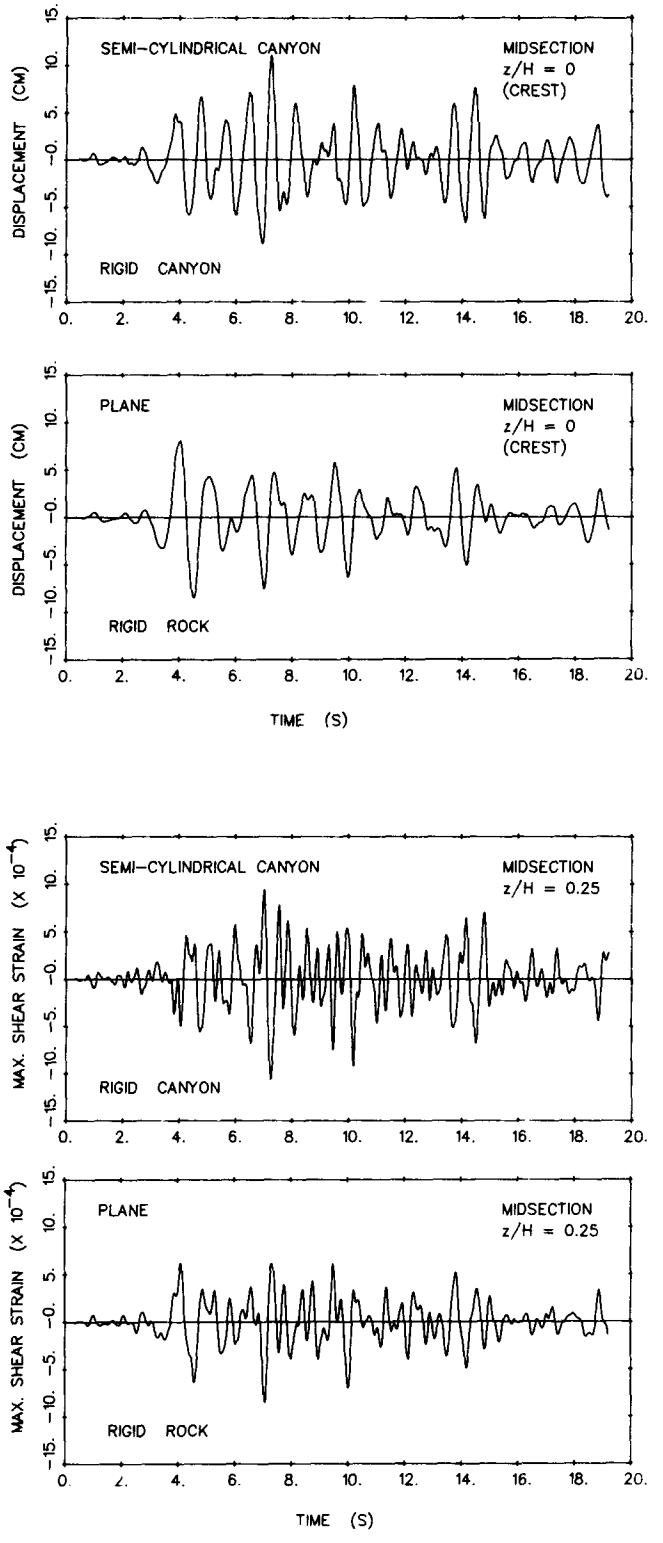

Fig. 29. Plane versus 3-Dimensional analyses: displacement and shear strain histories (dam and excitation as in Fig. 27)

section on inhomogeneity that strong inelastic action may have a dramatic effect on near crest accelerations. Particularly vulnerable have been the high-frequency high-amplitude acceleration components which tend to generate in inhomogeneous dams (e.g., recall Figs 18–19). Hence, it is reasonable to expect that the similar high-frequency high-amplitude near-crest acceleration components experienced by dams built in narrow canyons (Fig. 27 and Fig. 46) would be similarly depressed during strong inelastic action.

A first piece of tentative analytical evidence that this is indeed the case has been recently provided by Prevost *et al.*[85]. Using a 3-D finite-element method which performs rigorous nonlinear inelastic analysis based on a multisurface kinematic plasticity theory, they computed (with the help of an admittedly rather coarse 3-D mesh) the crest accelerations of the Santa Felicia dam, subjected to two excitations: (i) the lateral motion recorded near the outlet works of the same dam during the 1971 San Fernando Earthquake[1] (duration: 35 sec, peak acceleration: 0.22 g); and (ii) the Pacoima Dam record shown in Fig. 42 (duration used: 15 sec, peak acceleration: 1.20 g): Table 5 compares the peak crest accelerations computed for a compatible 2-D model of the mid-cross-section and from the 3-D analyses. The latter predict lower values, in both cases, with the discrepancy increasing considerably with the intensity of excitation. Although it is likely that some high-frequency (low wavelength) components are artificially filtered out by the coarse mesh, these results are qualitatively consistent with the trends noted in Figs 18–19. Hence, it is more that a mere suspicion that soil nonlinearity may considerably reduce the adverse effects of narrow canyon geometries on mid-crest accelerations.

7. NONLINEAR AND INELASTIC SEISMIC RESPONSE

7.1 Background: The 'equivalent linear' approximation

Rigorous nonlinear and inelastic analyses of earth dams would require prohibitively expensive step-by-step numerical integration with use of realistic cyclic constitutive models for the constituent materials of the dam. With today's standards such analyses are not practical, except perhaps in major critical projects.

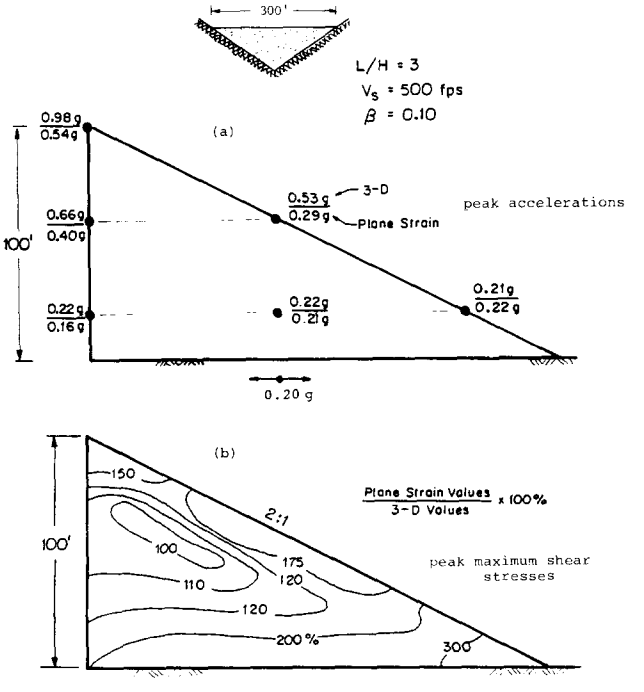

Fig. 30. Plane versus 3-Dimensional analyses for dam in triangular canyon: peak accelerations and peak maximum shear stresses in the midsection[57]

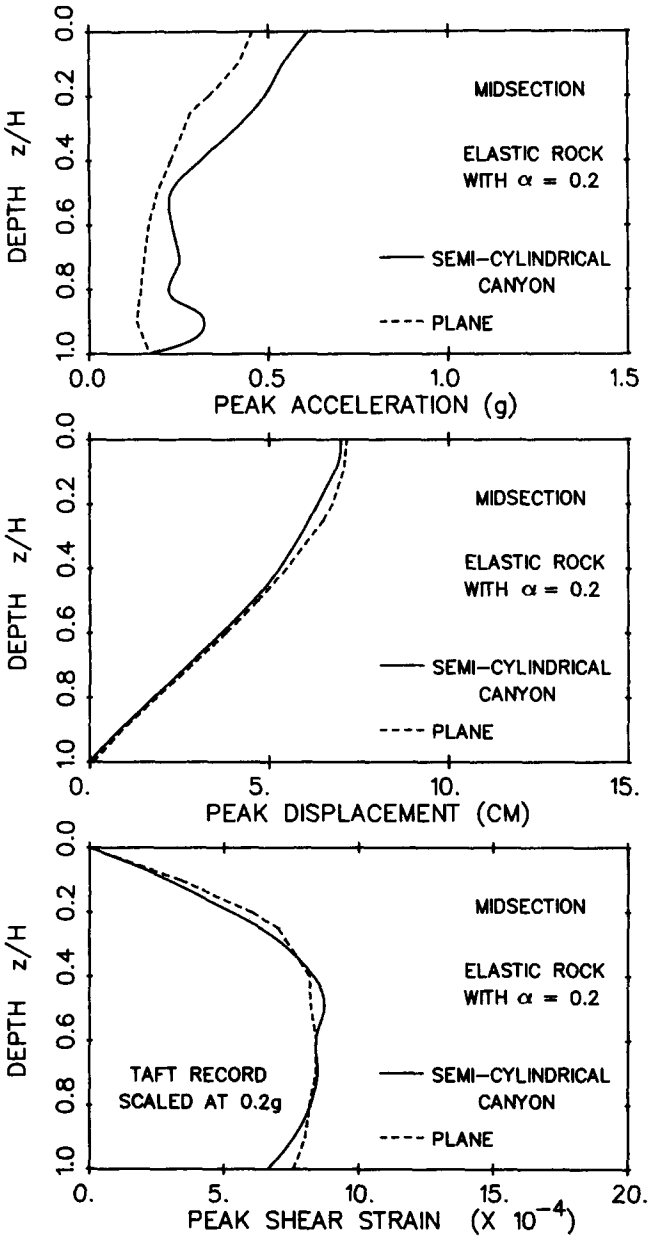

Fig. 31. Plane versus 3-Dimensional analyses: combined effect of 'elastic rock' and of 'strong Rayleigh' damping

Indeed, the nonlinear – hysteretic cyclic soil behaviour is only crudely reflected into currently established methods of response analysis through the well known 'equivalent linear' iterative scheme[46].

The basic premise of this scheme is that an approximate solution can be obtained by a linear viscoelastic analysis, provided the soil stiffness and damping used are compatible with the level of induced shearing strains. The method utilizes results of laboratory tests in the form of shear modulus and damping ratio *versus* sinusoidal shear-strain amplitudes. A set of moduli and damping values is initially assumed for each soil element and the system is analyzed linearly. The solution provides the time-history of the shear strain at each element from which an 'equivalent' effective strain amplitude γ_e is estimated and checked against the strain that is compatible with the values of shear modulus and damping used in the analysis. If they are not compatible, a new analysis is performed using soil properties corresponding to γ_e, and the process is repeated until convergence has occurred (usually within five iterations). The response of the last iteration is taken as an approximation to the nonlinear response.

The method is empirical and its convergence to the 'correct' answer can not be proved theoretically. Its advantages and limitations have been extensively debated during the last decade in connection with the problem of 1-dimensional 'soil amplification'[16,18,29,48,49,87,89]. It is now clear that reasonable estimates of peak response values may be obtained only for moderate levels of shaking intensity; the response to strong excitation may be over or underestimated depending on the geometry of the deposit and on the frequency characteristics and details of the motion. The following potential limitations of the method are worth keeping in mind:

1. A crucial step in the analysis is to deduce the amplitude γ_e of a sinusoidal strain history 'equivalent' to the erratic time-history of the computed strain. To this end, a strain reduction factors, often taken as 2/3, is applied to the peak shear strain amplitude. Clearly the arbitrary selection of this factor is a major drawback of the method. Peak strain amplitudes, important as they may be, often bear very little relation to the overall level of deformation; they are just spikes occurring instantaneously while during the rest of the motion deformation amplitudes may or may not be of a comparable magnitude. Therefore, it is quite possible for this method to lead to an artificially over-damped and over-softened system; or vice-versa, in case of relatively uniform motion to underestimate both damping and softening. Consequently, even if the predicted peak response values are good, the method may not be appropriate for reproducing the detailed history of the response and hence assessing *number and amplitude of cycles* – important information in liquefaction and fatigue-type studies.
2. Since the method is linear there is a tendency for *spurious resonances* to develop and thereby to exaggerate the response[29]. This tendency has been confirmed in several comparative studies using 1-D models and may be explained by the fact that the final analysis is carried out with a single set of 'compatible' linear soil parameters, for the entire duration of the earthquake shaking. Hence, it is quite possible that one of the predominant periods of the input motion may coincide with one of the natural periods of the earth structure corresponding to this final set of 'compatible' properties. In nonlinear reality such a tendency for pseudo-resonance will not develop, thanks to the constantly changing stiffness properties.
3. The method can not possibly provide information on permanent displacements and deformations, since it is essentially an elastic method. Hence the need for the developed separate procedures for assessing residual and sliding displacement, e.g., by using the aforementioned 'Newmark' concept[71,55] or the concept of 'strain

Table 5. Inelastic 2-D versus 3-D peak crest acceleration for Santa Felicia Dam[85]

Excitation record	Inelastic 2-D prediction	Inelastic 3-D prediction
Santa Felicia, 1971	0.26 g	0.22 g
Pacoima, 1971	0.86 g	0.58 g

potential' of Seed and coworkers[96]. The procedures related to these two concepts are intuitive semi-empirical approximations that can not enforce compatibility of deformations induced in the dam [see Ref. 29 for additional discussion of this point].

4. Application of the equivalent linear approximation to earth dams which are 2-D or 3-D structures introduces a new uncertainty because of the need to define the variation with shear-strain amplitude of a second soil parameter, in addition to shear modulus. In some formulations it is assumed that Poisson's ratio remains constant, independent of strain, while Young's modulus decreases with increasing strain and remains proportional to the shear modulus. This implies that the bulk modulus of the material would decrease upon intense shearing – a questionable assumption for undrained loading conditions[89]. In other formulations, however, it is the bulk modulus which is kept constant while Poisson's ratio varies with strain level. A further uncertainty in 2-D formulations arises from the need to define which shear strain sould be considered. The usual practice is to take *a fraction* ($\approx 2/3$) *of the peak maximum shear-strain* as the 'equivalent' strain amplitude. Although the orientation of maximum strain changes continuously in space and time, the above assumption is fairly reasonable for earth dams responding primarily in shear, since maximum and horizontal shear strains are nearly equal in such cases.

A final note: the present-day incorporation of the equivalent linear technique into 2-D finite-element codes [e.g., 46] entails not insignificant computer storage and time requirements, making it perhaps prohibitively costly for preliminary parametric studies. Conceptual simplicity and computational efficiency have been important objectives in developing the three nonlinear methods that are described in the sequel.

7.2 Three new procedures for nonlinear response

a. *'Simplified nonlinear' analysis*[19,23]. This is an approximate nonlinear (but essentially elastic) procedure that attempts to overcome to a large extent and in a simple way the first two limitations of the 'equivalent linear' method addressed in the preceding subsection. The basic premise of the method is that soil moduli and damping ratios can be updated at various time intervals so as to be consistent with the root-mean-squared (rms) values of the shear strain during the same interval. In other words, updating of the soil parameters is enforced at several points along the time axis, in contrast with the single, after-the-analysis updating of the 'equivalent linear' scheme.

The numerical analysis is performed in two consecutive phases. The first phase aims at obtaining an estimate of the time history of the rms shear strain, $\gamma_{\text{rms}}(t)$; the second phase computes the dam response through piece-wise linear analysis in small time steps. The specific details of each phase are as follows:

Phase 1. The duration of shaking is divided into M intervals (t_i, t_{i+1}), $i=1,2,\ldots,M$. The length $\Delta T = t_{i+1} - t_i$ of each interval is taken to be slightly greater than the fundamental period T_1 of the dam, i.e., $\Delta T \approx 2.5\, H/\bar{C} =$ the average S-wave velocity. Such a restriction ensures that ΔT is sufficiently large for a meaningful computation of γ_{rms} within each interval, and sufficiently small to describe in reasonable detail the time-variation of soil stiffness and damping.

For each and every time interval i, (t_i, t_{i+1}), a series of linear analyses is performed, each using moduli and damping factors consistent with the rms strain $\gamma_{\text{rms},i}$ of the previous analysis for that same interval:

$$\gamma^2_{\text{rms},i} = \frac{1}{\Delta T}\int_{t_i}^{t_{i+1}} \gamma^2(t)\,\mathrm{d}t \tag{11}$$

The equivalent sinusoidal shear strain amplitude γ_e, corresponding to $\gamma_{\text{rms},i}$ is found by equating *shear strain energies* of the actual with a sinusoidal motion:

$$\gamma_{e,i} = \sqrt{2}\gamma_{\text{rms},i} \tag{12}$$

This value of $\gamma_{e,i}$ is used to read consistent G_i and β_i for the next iteration. Convergence is usually achieved within three iterations, and then $\gamma(t)$, $t_i \leqslant t \leqslant t_{i+1}$, in equation (11) is computed by modal superposition for each element under consideration. A typical output of Phase I, $\gamma^{\text{I}}_{\text{rms}}(t)$, is plotted in Fig. 32.

Phase II. Since the time intervals of phase I are of fairly large duration $\Delta T \simeq T_1$, the computed $\gamma^{\text{I}}_{\text{rms}}(t)$ exhibits large and rather spurious fluctuations, as evidenced in Fig. 32. Phase II starts with a simple empirical correction: the smoothing by linear interpolation of the rms strain. An example of the resulting $\gamma^{\text{II}}_{\text{rms}}(t)$ is also shown in Fig. 32. Thereby, a continuous smooth variation with time of the effective modulus and damping ratio can be constructed from the available experimental graphs.

The duration of shaking is then divided into considerably shorter time intervals, e.g., of duration $\Delta t \approx 0.1\text{ s} \ll \Delta T$. The time integration analysis proceeds step by step. Linear analysis is performed in each time interval with soil properties G and β compatible with γ_0 at the beginning of the interval. No iteration is necessary in view of the small size of Δt; parameter studies have in fact shown that the influence of the exact value of Δt is insignificant, in agreement with earlier related studies[37]. The outcome of this phase is an approximation to the exact inelastic response.

Notice that the size of ΔT should be large enough ($> T_1$) to contain more or less a full response cycle. Indeed, a sensitivity study on the effect of the size of ΔT

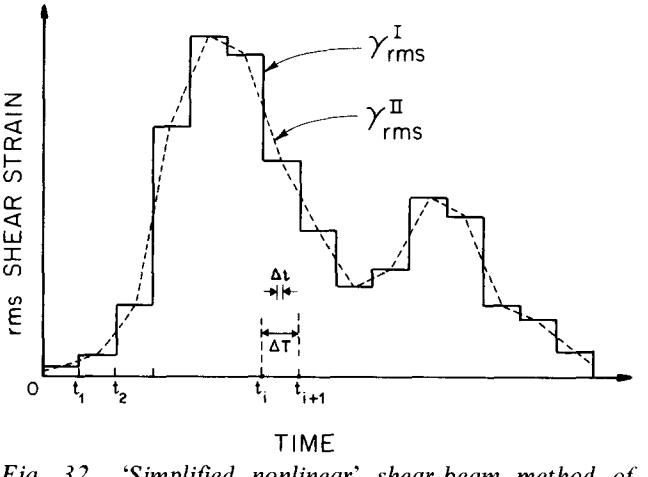

Fig. 32. 'Simplified nonlinear' shear-beam method of analysis[23]*: variation of rms shear strain computed in phases I and II*

showed that for $\Delta T \geq T_1$ convergence in phase I is stable and rapid (usually 3 or 4 iterations). For $\Delta T < T_1$, however, the process may converge to a wrong value since γ_{rms} may be obtained either near a peak response or near its zero crossing portion. In all cases, the maximum deviation from the results with $\Delta T = T_1$ is within about 10% for displacements, 15% for shear strains and 20% for accelerations.

The method has so far been implemented in conjunction with a general 1-D inhomogeneous shear-beam model. A single value of shear strain, namely the average shear strain along the height of the dam, is considered as representative of the whole state of deformation in the dam – a reasonable approximation in many cases.

The 'simplified nonlinear' (inhomogeneous) shear-beam formulation has been compared in Refs 19 and 23 with the 'equivalent linear' finite-element analysis using the computer code QUAD-4[46]. As an example, for the aforementioned 120 m dam, with soil element moduli proportional to $\sqrt{\sigma_0}$, Fig. 33 plots displacement, acceleration and shear strain histories due to excitation by the Taft NS component of motion scaled to 0.4 g peak acceleration and applied at the rock outcrop. 'Elastic rock' amplification was considered with rigidity-contrast ratio $\alpha = 0.20$. Therefore, this is a case of a fairly flexible dam subjected to a moderately-strong shaking. Several trends are worthy of note:

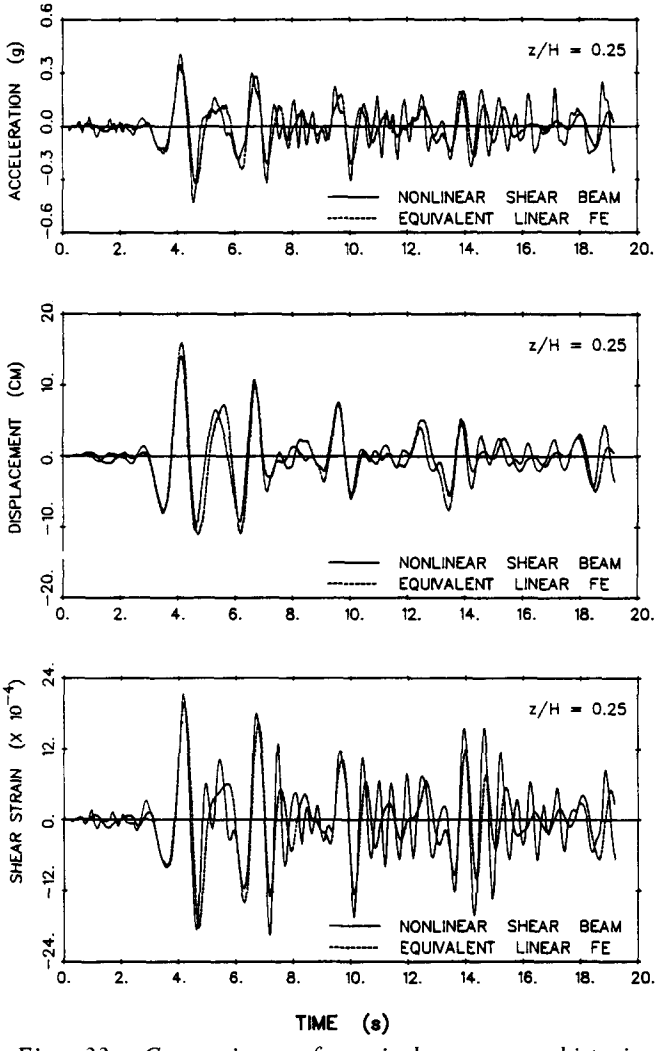

Fig. 33. Comparison of typical response histories computed from 'simplified nonlinear' shear beam and from 'equivalent linear' finite-element methods. (dam: H = 120 m, C̄ = 280 m/s; excitation: scaled Taft record)

(i) There is a good overall agreement, especially among the corresponding displacement and shear strain histories. (Note, however, that this is not always true. In fact, the response to the strong ground motion of a stiffer dam, shown later, reveals considerable disagreement between the two methods.)

(ii) The equivalent linear solution filters out some of the high frequency components of motion which are preserved by the simplified nonlinear formulation. The presence of such high frequency components has also been noted in more rigorous inelastic solutions, as discussed later.

(iii) The overall cost of the developed procedure is lower by more than two orders of magnitude.

b. *'Nonlinear hysteretic Galerkin' formulation*[27,84]. A more rigorous (but still simplified) method for determining the non-linear *inelastic* response of earth dams has been recently developed at Princeton University. The method is based on a Galerkin formulation of the equations of motion in which the solution is expanded using *basis functions* defined over the whole dam. 1-D, 2-D and 3-D geometries can be handled with the method. Calling in general $u_i = u_i\,(x,y,z;t)$ the three components ($i = x,\ y\ and\ z$) of the displacement vector relative to the base, a Galerkin approximation is written as:

$$u_i(x,y,z;t) \approx \hat{u}_i(x,y,z;t) = \sum_{n=1,2\ldots}^{N} \phi_{ni}(x,y,z) q_n(t) \tag{13}$$

in which ϕ_n denote the basis functions ($n = 1, \ldots, N$) and $q_n(t)$ are the unkonwn time-dependent generalized (modal) displacements. Substituting the above equation into the general equation of motion leads to

$$[M]\{\ddot{q}\} + \{s\} = \{p\} \tag{14}$$

where $[M]$ ($N \times N$) is the mass matrix; $\{q\}$ ($N \times 1$) is the vector of unknown displacements; $\{s\}$ ($N \times 1$) is the vector of internal nonlinear forces; and $\{p\}$ ($N \times 1$) is the vector of applied external forces. For example, the elements in $\{M\}$ and $\{s\}$ are given by:

$$M_{nm} = \sum_{i=1}^{NSD} \int_v m \phi_{ni} \phi_{mi}\, dv \tag{15a}$$

$$s_n = \sum_{i,j=1}^{NSD} \int_v \sigma_{ij} \phi_{ni,j}\, dv \tag{15b}$$

where NSD = number of spatial dimensions (= 1, 2 or 3). By selecting the (orthogonal) normal eigenmodes of the corresponding linearized problem as the set of basis functions ϕ_n, the mass matrix is diagonalized. However, due to the presence of the nonlinear internal stress terms, the equations remain coupled. Solution is obtained by time-integration of the resulting semi-discrete equations using Newmark's finite-difference time-stepping algorithm. The term $\{s\}$ is evaluated at any time by

dividing the dam into a number of elements and using Gaussian quadrature for integrating over each element.

The hysteretic cyclic stress-strain behaviour of each soil element is modelled by using elasto-plastic constitutive equations based on multi-surface kinematic plasticity theory. The procedure allows fitting of the soil model to any given 'backbone' curve, and generates cyclic hysteresis curves of the extended Massing type.

Numerical results have already been presented for homogeneous dams in plane as well as 3-D environments, excited by sinusoidal as well as recorded seismic ground motions of different intensities and frequency characteristics. As an example, Fig. 34 portrays the Fourier Amplitude Spectra of the test accelerations experienced by a homogeneous plane model of the Santa Felicia Dam subjected to three motions. Each motion was derived by scaling (up or down) the Array-No. 7 record of the 1979 Imperial Valley earthquake, so as to achieve peak input accelerations of about 0.10 g, 0.50 g and 1.50 g respectively. The following conclusions may be drawn from this figure:

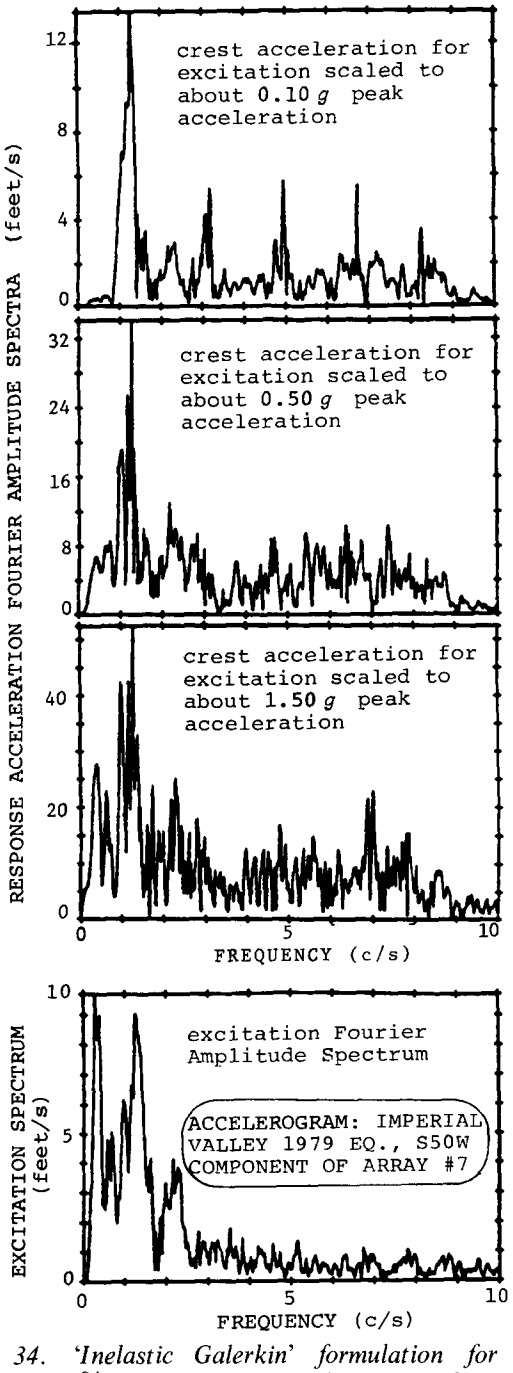

Fig. 34. 'Inelastic Galerkin' formulation for Santa Felicia dam[84]: Fourier Spectra of crest acceleration for input motion scaled to different intensities

(i) For small-amplitude excitation (0.10 g) there are distinct and well-defined resonant peaks at essentially the linear natural frequencies of the dam.

(ii) As the excitation intensity increases, additional peaks at frequencies different from the modal frequencies appear; this is due to the yielding behaviour: with increasing amplitude of the input motion the effective linear moduli of the soil elements decrease and so do the effective natural frequencies of vibration of the dam. Hence, earthquake-input energy is absorbed at frequencies lower than the linear natural frequencies. It is important to point out that no 'equivalent linear' method can predict this phenomenon since the effective natural frequencies do not change with time.

(iii) Comparing the overall amplitudes of the three Spectra, it is evident that the greatest amplification relative to each input motion is associated with the weakest excitation, during which quasi-linear elastic behaviour prevails; the smallest amplification is observed with the strongest excitation during which nonlinear hysteretic action is substantial.

The foregoing observations suggest that one must be particularly careful when using recorded crest/base 'amplification spectra' to obtain natural dynamic characteristics of earth dams. Unless a quasi-linear behaviour is ensured, some of the observed peaks will be a by-product of the yielding response of the dam and will correspond neither to linear natural frequencies nor to dominant input frequencies.

It is instructive to compare the results of various formulations which assume linear, equivalent linear, nonlinear, and inelastic constitutive laws to model soil response, despite the fact that it is not always straightforward to ensure the compatibility of the soil models to be used in such an endeavor[29].

The comparative study refers to the Santa Felicia Dam cross-section shown in Fig. 35, modelled as a 72 m-high homogeneous plane section with low-strain S-wave velocity $C = 263$ m/s. The basic shear stress-strain relationship is taken as hyperbolic with

$$\tau_{ult} = 3900 \text{ psf}$$

$$\gamma_r = 0.0013$$

$$G_0 = 3000 \text{ ksf}$$

from which the $G(\gamma)$ and $\beta(\gamma)$ curves are derived. The excitation consists of the SE component of the Pacoima Dam record triggered in the 1971 San Fernando earthquake. Shown in Fig. 35, this very strong motion has a peak acceleration of about 1.20 g and is expected to result in strongly nonlinear plastic response.

Five different formulations are used in this comparison: (a) linear homogeneous shear beam; (b) 'equivalent linear' homogeneous shear beam[19,23]; (c) 'simplified nonlinear' homogeneous shear beam[19,23]; (d) 'nonlinear hysteretic Galerkin' formulations with basis

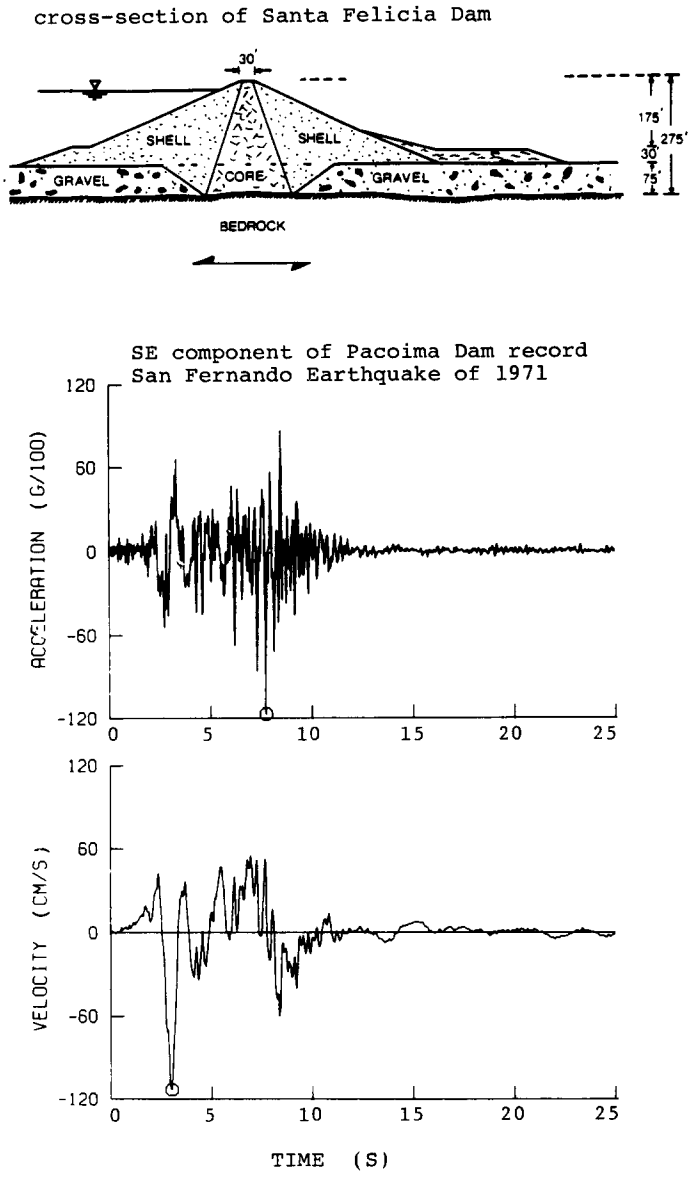

Fig. 35. Geometry of Santa Felicia dam mid-section and utilized component of Pacoima dam 1971 record

functions the eigenfunctions of the linear homogeneous shear beam[27,84]; and (e) elastic-plastic finite-element method[85]. For models (b) and (c) updating of the soil properties was based on the average-along-the-height shear strain. Model (d) used a five mode expansion. Model (e), while being in principle rigorous, involved a rather crude mesh (element thickness ≈ 20 m) to avoid prohibitive computer storage and time requirements.

Figure 36a compares the shear-strain histories computed with the more rigorous models (c), (d) and (e) for a depth $z = 0.75$ H along the centreline of the dam. There is an overall agreement in the three predictions. Especially encouraging is the performance of the 'simplified nonlinear' shear-beam [model (c)] which not only closely predicts the maximum peak strain ($\gamma \approx 1\%$), but it also reproduces reasonably well the frequency content of the motion. Of course, being essentially an elastic procedure, the proposed method cannot possibly reproduce the permanent set predicted by the two inelastic solutions [models (d) and (e)] after 4 seconds of shaking.

By contrast, the equivalent-linear shear-beam solution, plotted in Fig. 36b, fails to predict well the response near the peak, while it spuriously filters out some of the high frequency components. Fig. 36b compares the simplified nonlinear prediction with the one obtained from a linear analysis with stiffness and damping corresponding to an expected average shear strain of 7×10^{-3}. This shear strain is indeed very similar to the computed peak value and thus the linear analysis predicts reasonably well the peak response. It fails, however, to predict the response history at time $t > 5$ s.

Another interesting remark in Fig. 36 relates to the effect of peak ground acceleration and frequency content on the response of a dam. Notice that the peak of about 1.20 g occurring at time $t = 7.8$ s has a negligible effect on the response of the dam compared to the effect of the smaller in amplitude (about 0.65 g) but larger in duration acceleration pulse occurring between the second and fourth seconds of the shaking. Indeed this later pulse is associated with a very substantial *velocity increment* of about 150 cm/s (Fig. 35); such velocity increments known to control the behaviour of flexible inelastic sttuctures. On the other hand, in Fig. 37 a typical 40 m-high stiff dam subjected to the same Pacoima record experiences its peak response at $t = 8$ s, immediately following the high-frequency peak of the ground acceleration. Moreover the peak crest acceleration in this 'stiff' (not shown here) dam is about 60% higher than that in the 'flexible' Santa Felicia dam. It is apparent that while the 'flexible' dam filters out the high frequency components of the excitation, the 'stiff' dam amplifies them, as illustrated through the Fourier amplitude spectra of the crest acceleration plotted in Fig. 38 for each of the two dams.

c. '*Layered Inelastic Shear Beam*' (LISB)[101]. This recently developed dynamic procedure attempts to combine the simplicity and efficiency of the 1-D shear-beam types of analyses with the versatility of plane-strain finite-elements in handling zones of different materials and nonlinear element behaviour. To this end, the procedure is divided into two separate stages as schematically explained in Fig. 39. The first stage performs *static* incremental nonlinear finite-element analyses and aims at deriving monotinic constitutive relations for a number of horizontal layers (superelements) on which the dam section is divided. In the second stage, a *dynamic* 1-Dimensional analysis is performed with the dam modelled as a layered shear beam and with each layer having a cyclic stress-strain behaviour which is estimated from the monotonic inelastic superelement constitutive relations of the first stage, in combination with the extended Massing criterion. It is noted that a somewhat similar dynamic analysis using the method of characteristics was implemented in Ref. 80, but with arbitrarily chosen layer stress-strain relations.

The first stage starts with estimating the gravity-induced initial state of stress by means of finite-element analyses in which the (experimentally determined) nonlinear soil behaviour and the (anticipated) construction sequence are properly simulated. With the initial stresses known, the stiffness and strength characteristics of each soil element are determined. Then an *incremental static nonlinear finite-element* analysis is

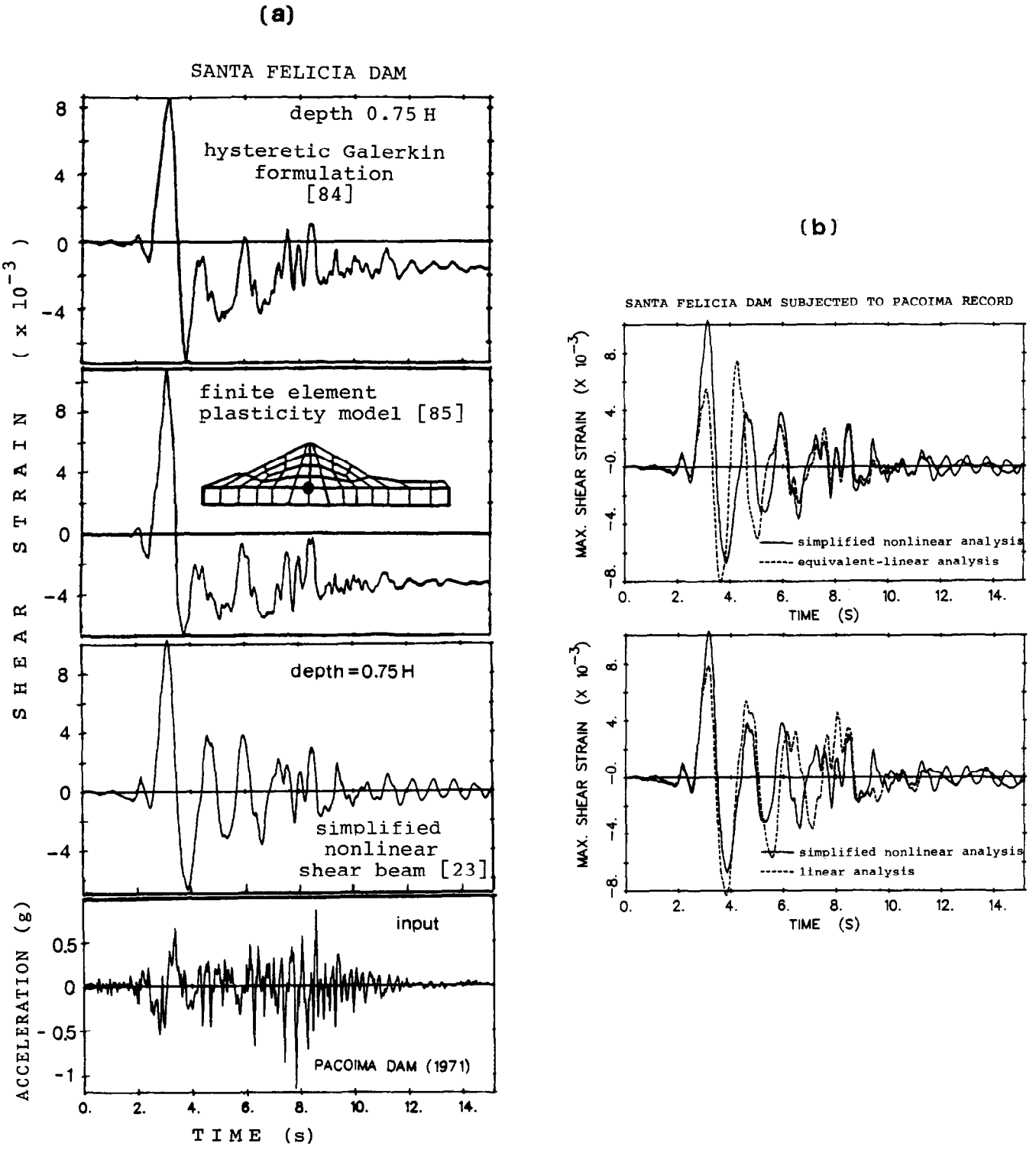

Fig. 36. Shear strain history at a point in Santa Felicia Dam computed by five different linear and nonlinear formulations

performed. Horizontal inertia-like loading is applied on each and every finite-element in incremental steps. In each step the intensity of the lateral 'inertia' loads is uniform across the width but nonuniform along the height of the dam. A triangular distribution is a first natural choice for the assumed distribution of intensity along the height; such a distribution is consistent with the fundamental mode shape of the dam. However, other studied distributions resulted in reasonably similar superelement stress-strain curves. During the incremental analysis this 'inertia' load distribution remains unchanged, while the dam is progressively subjected to total lateral forces of increasing magnitude and the various soil elements respond by exhibiting progressively larger nonlinearities. For each of the horizontal layers to be considered in the subsequent dynamic study, the incremental static analysis provides a relation between total horizontal shear force and average horizontal layer distortion, on the basis of which the 'backbone' 'layer $\tau_i - \gamma_i$' curve is constructed. These layer backbone curves

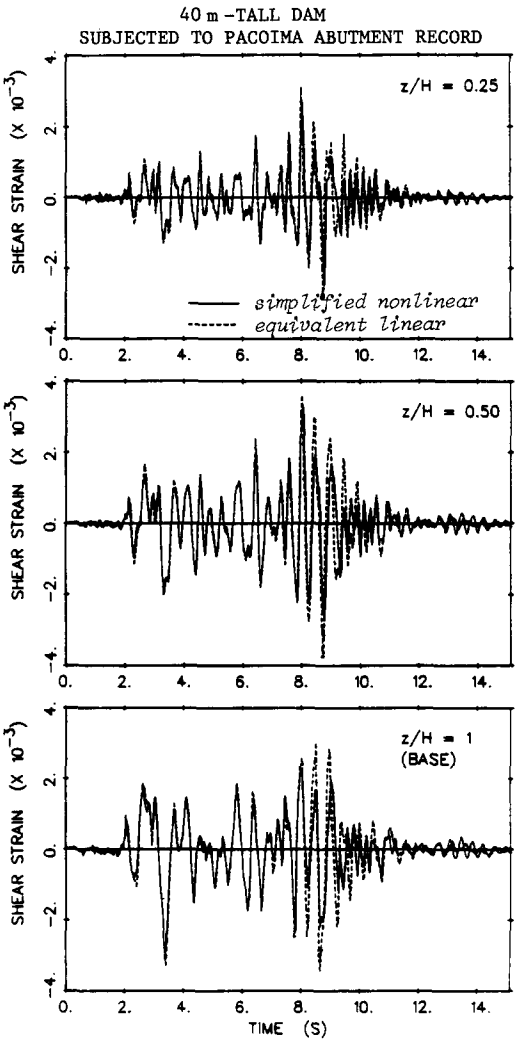

Fig. 37. Shear strain history at various depths in 40 m tall dam computed from two shear-beam based formulations

are idealized as hyperbolic, Ramberg-Osgood, or Iwan-type, and along with the 'extended Massing' criterion provide the complete hysteretic cyclic constitutive relationship of the layered shear beam. Fig. 40 portrays such superelement monotonic relations (plotted as data points) and fitted with a hyperbola (plotted as a line). These plots were derived (a) for a model of the Santa Felicia Dam, and (b) for a model of the lower San Fernando Dam. Note that a *hyperbolic* backbone curve had been originally assumed for each soil element, in both cases.

The layer distortions that are obtained from the dynamic analysis translate directly only into average layer shear strains across the respective horizontal plane, as is always the case with shear beam models. A realistic approximate estimation of the more meaningful *local (element) values of shear strains* is made by urilizing these average values and the corresponding element strains of the incremental static analysis. To this end, it is assumed that the ratio 'local element shear strain'/'average layer shear strain' remains the same in the two (static and dynamic) analyses – an intuitive engineering approximation which is expected to work quite adequately especially when dams respond primarily in their fundamental mode. Substantial evidence supporting this approximation is provided in Ref. 101.

As an example, Fig. 41 portrays the evolution of the ratios 'element shear stress (strain)'/'layer shear stress (strain)' *versus* increasing layer stress (strain), for a depth $z \simeq 0.76\,H$ in a 120 m high dam. Notice that an element near the surface, enjoying only a small confining pressure, develops stronger nonlinearities as the incremental loading progresses than an element near the centre. Hence, its 'local/average' *strain* ratio increases, while the 'local/average' *stress* ratio decreases as the softening element transfers increasing portion of its load to the stronger neighbours. The reverse is true for a well-confined element near the centre.

From the foregoing discussion it is evident that although the dynamic shear beam model is one-dimensional, its stress-strain characteristics reflect the two-dimensional interactions among all the elements of a cross-section. It is of interest to note that similar inelastic shear beam models have been found very successful in predicting plastic deformation of multistory building frames.

The accuracy of the method has been successfully tested in Ref. 101 through comparisons with the plasticity-based finite-element analysis of Prevost *et al.*[85] and with the recorded response of several actual dams. Some indirect evidence supporting the method is presented in the next section of this paper.

Results of seismic response computed with the 'Layered Inelastic Shear Beam' (LISB) have already been presented in Figs 18–19, in which the effects of stiffness inhomogeneity have been studied under linear-elastic and nonlinear-inelastic soil behaviour.

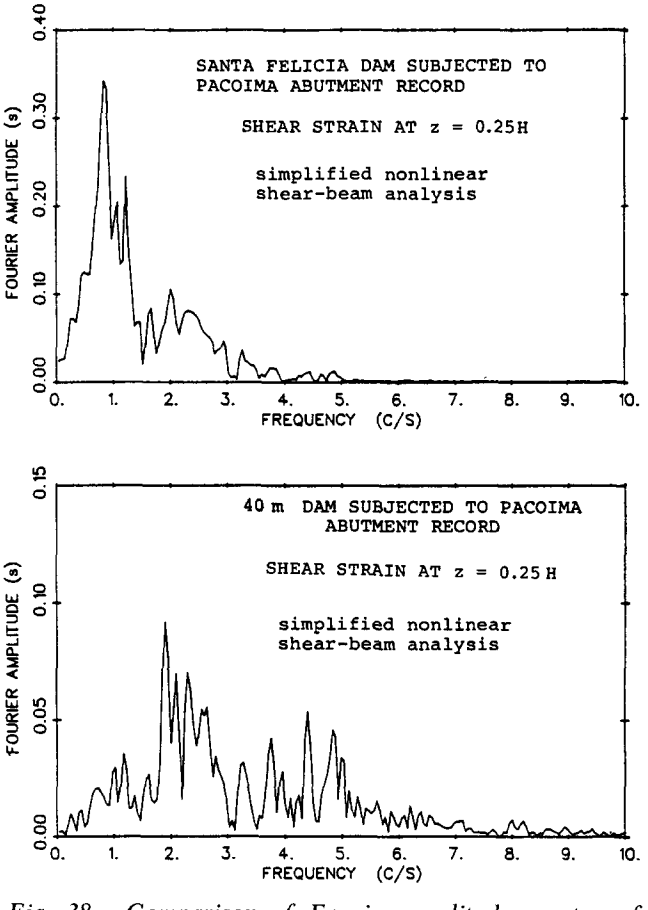

Fig. 38. Comparison of Fourier amplitude spectra of shear strain at a point near crest in Santa Felicia and in 40 m-high dam, both subjected to Pacoima dam 1971 record

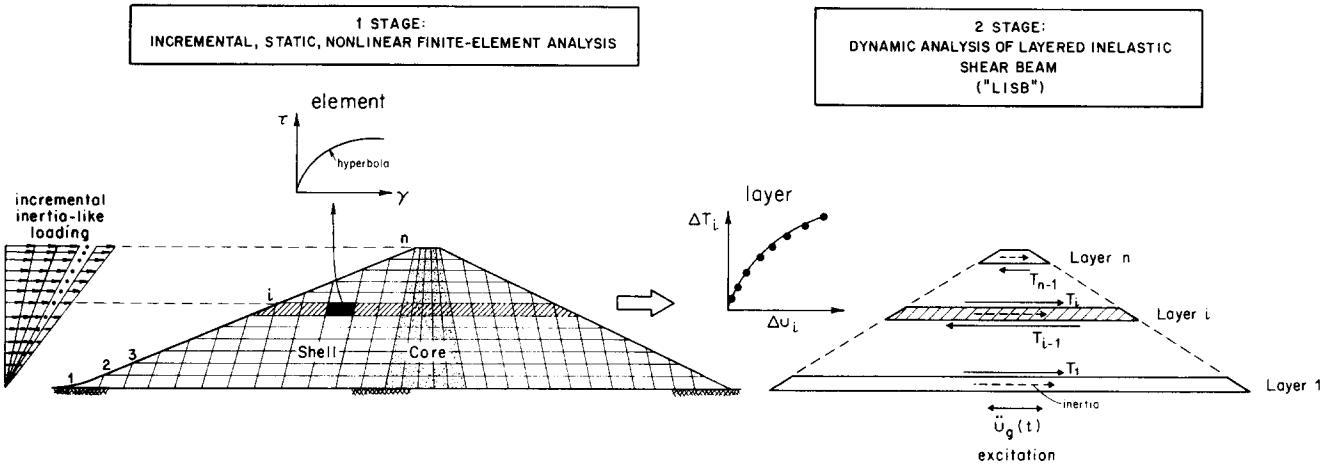

Fig. 39. Illustration of two stages of 'Layered Inelastic Shear Beam' (LISB) method for response analysis of earth dams during strong shaking[101]

Another set of typical results computed with LISB are given in Figs 42–43. A 40 m high earthfill dam, with properties corresponding to a stiff silty-clay material of an actual modern earth dam[101], is subjected to five historic recorded motions, all scaled to three different peak accelerations: 0.2 g (moderate), 0.4 g (strong) and 0.7 g (very strong). Plotted in Fig. 42 are the distributions with depth of the peak values of absolute accelerations and layer shear strains. Notice the diminishing amplification of peak crest accelerations from about 2.1 to 1.6 and finally to 1.0, as the peak ground acceleration increases from 0.2 g and 0.4 g to 0.7 g. At the same time the largest value of peak layer shear strains increases from 0.055% to 0.13% and to 0.23%, i.e., roughly in proportion with the peak ground acceleration.

Figure 43 plots the time histories of mid-height layer-shear strain and of the crest acceleration computed with the 'moderate' (0.2 g) and 'very strong' (0.7 g) Pacoima records as excitation. It is worth noticing the changes in frequency content (as well as amplitude) of the crest acceleration. Also, in addition to larger peak amplitude, layer-shear strains exhibit a progressively increasing permanent set, as previously discussed in relation to Fig. 36.

The 'Layered Inelastic Shear Beam' (LISB) seems a promising cost-effective dynamic procedure, which can capture qualitatively and quantitatively the inelastic phenomena associated with the response of earth dams to very strong earthquake shaking. Two case histories at the end of the next section provide further evidence on the potential of the method.

8. SOME CASE HISTORIES

One can hardly overstate the unique value of well documented case histories in gaining confidence in the advantages of analytical tools, and in developing an improved insight and understanding of the role of the many factors influencing the response. In addition to some (limited) field evidence already presented in the paper (Figs 11 and 42), this section summarizes the recorded observations of the response of five dams, in Mexico, Japan and the United States. In three cases the records are compared with post-event predictions using methods of analysis described previously. Also, the first three cases involved a clearly quasi-linear elastic soil behaviour, while in the last two cases soil nonlinearities of varying degrees play some role in the response.

8.1 Case History I: Linear response of El Infiernillo dam

The geometry of this 148 m high rockfill dam, built in Mexico in the early 1960's[90], is given in Fig. 44a, through the maximum cross-section, the plan and the profile along the longitudinal axis. On April, and again on September of 1966 the dam was shaken by two seismic events. Motions were recorded in the underground powerhouse in rock not far from the base of the dam, and the mid-crest of the dam. The peak ground acceleration in the rock during both events was about 0.02 g. Fig. 44b shows the 5%-damped response spectra of these rock motions. The peak crest accelerations were about 0.075 g and 0.06 g, respectively, during the two events. The respective response spectra can be found in Ref. 90.

The ratios of the corresponding two sets of crest and powerhouse acceleration spectra (S_a) are plotted in Fig. 44c. It has been shown by Roesset[88] that such ratios of response spectra can be used to obtain estimates of steady state transfer (amplification) functions (AF) in soil deposits. Of course, since the response spectra refer to *transient* rather than *steady-state harmonic* excitation, some small differences should exist at the fundamental frequencies of the system, where the plot of the S_a ratio is somewhat flatter. Also, at high frequencies, AF$\rightarrow$0 whereas the S_a ratio tends to the ratio of the respective peak accelerations. Otherwise AF and S_a-ratios match in general fairly well, if the soil deposit is properly modelled.

For this case, modelling the canyon of El Infiernillo as semi-cylindrical, and using the stiffness characteristics reported in Ref. 80, leads to an 'elastic-rock' amplification function (AF) which is also plotted in Fig. 44c. The used value of the rigidity-contrast ratio $\alpha = 0.30$ was selected to reflect (in an admittedly simplified way) both *radiation* damping as well as damping due to *'incoherent scattering'* – the latter arising from several phenomena including geometry imperfections, inevitable material heterogeneities, and asynchronous base excitation.

Notwithstanding the several simplifications and uncertainties in the analysis, Fig. 44c provides supporting evidence favouring the semi-cylindrical canyon model.

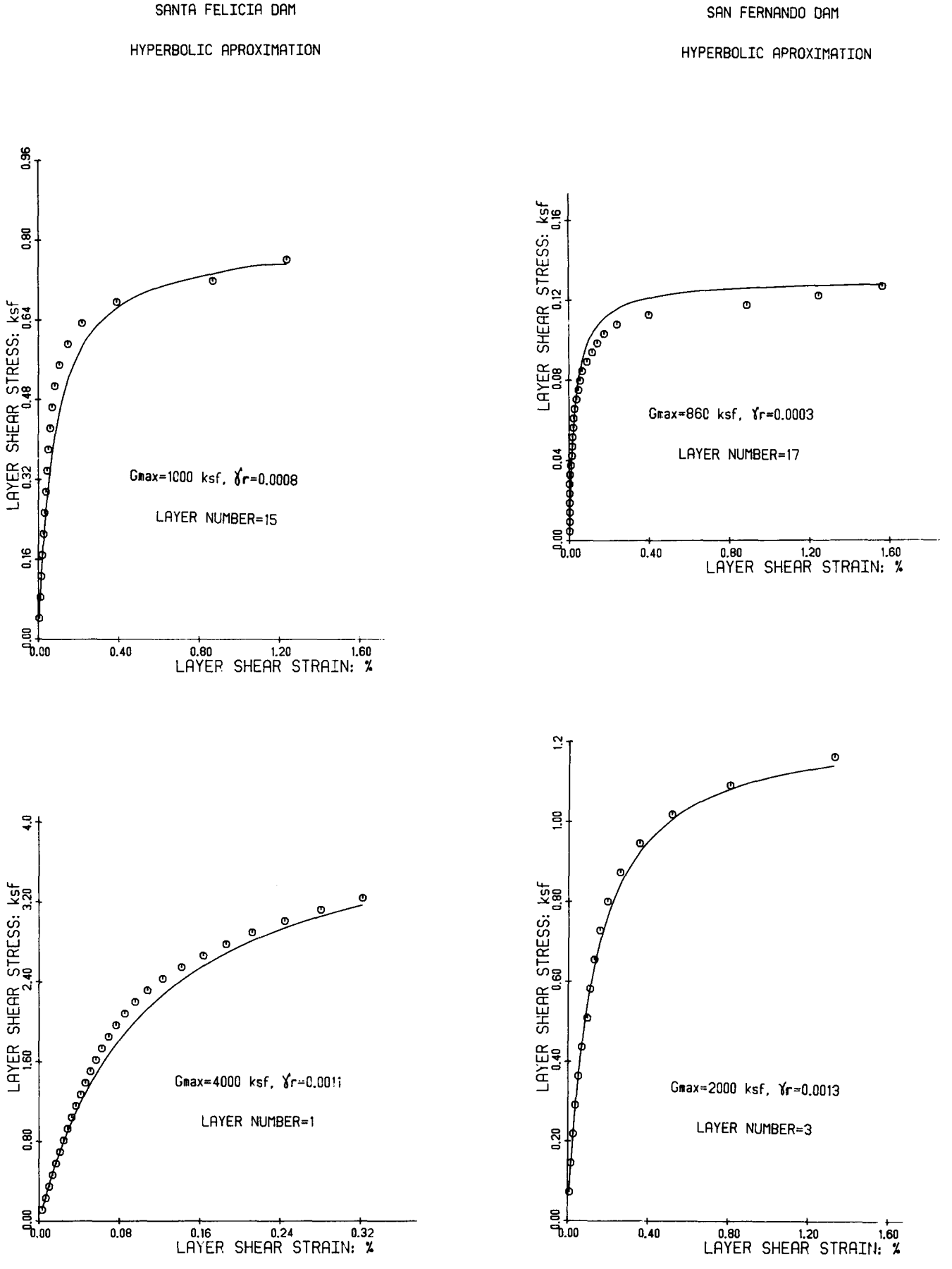

Fig. 40. Typical results of incremental static nonlinear analysis with inertia-like loading (Stage 1): layer shear stress-layer shear strain in two dams[101]

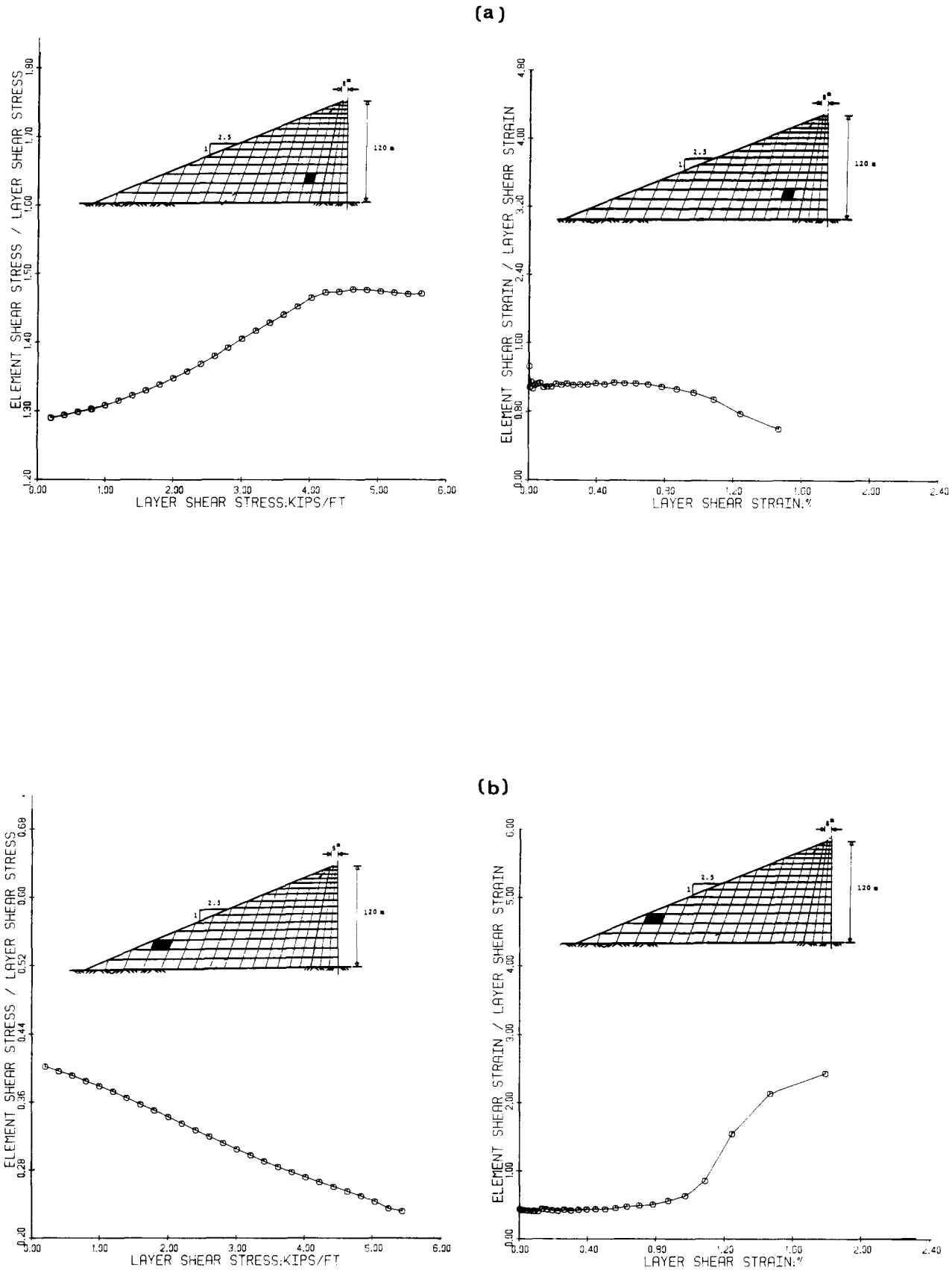

Fig. 41. Results of incremental static nonlinear analysis with inertia-like loading (Stage 1): evolution of the ratios of local element shear strain or stress to layer (superelement) shear strain or stress; (a) element near centre, (b) element near surface[101]

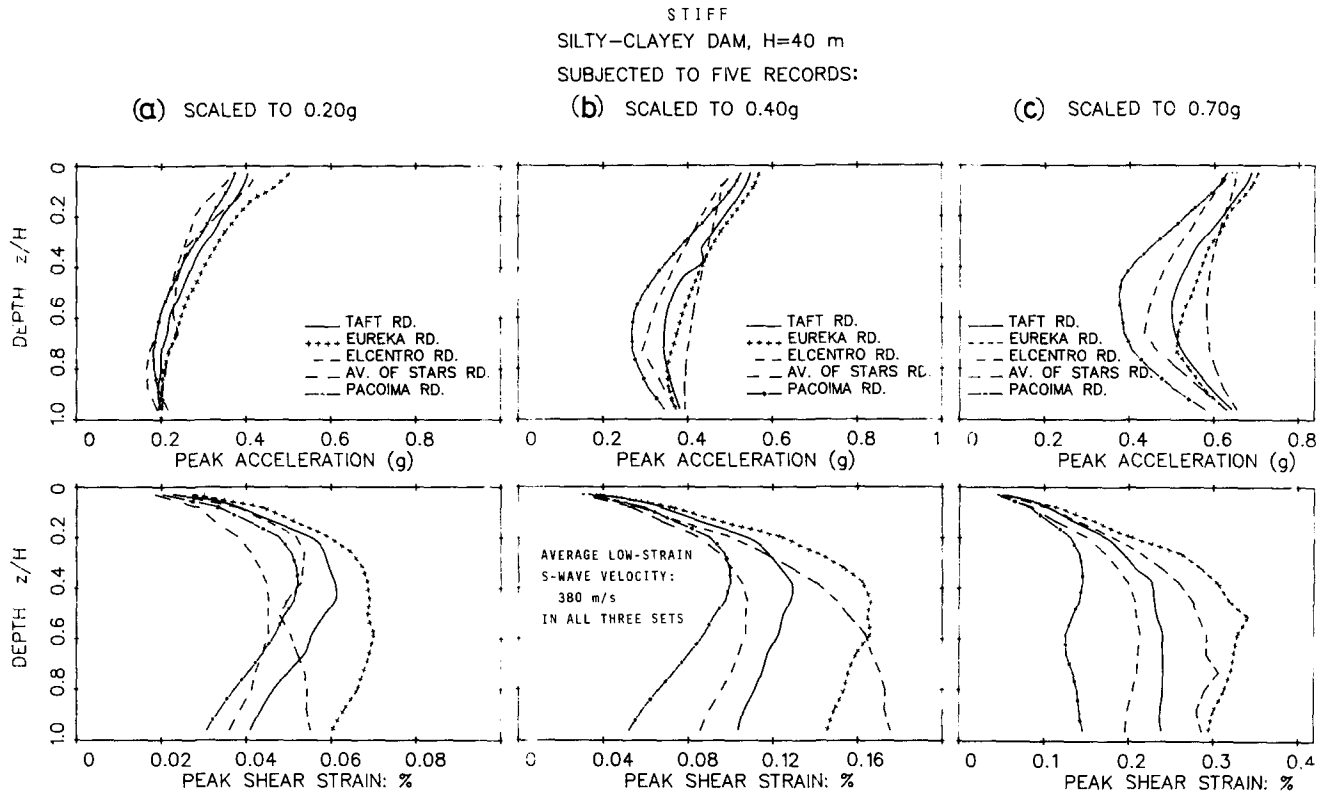

Fig. 42. Typical results of 'Layered Inelastic Shear Beam' (LISB) analysis[101] for a modern earthfill dam section: effects of frequency content, details and intensity of excitation. Notice decrease of crest amplification to about 1 when max $a_g = 0.70$ *g*

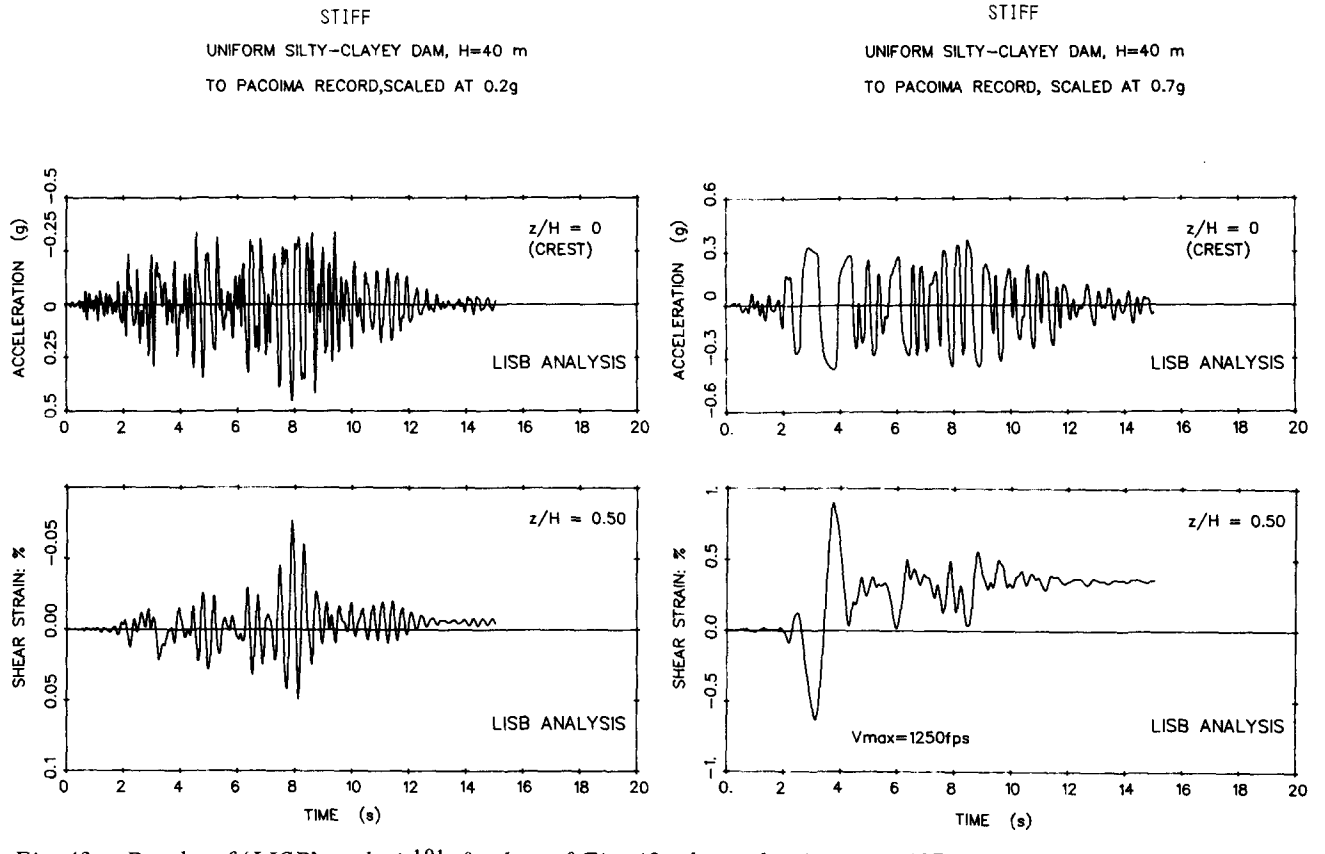

Fig. 43. Results of 'LISB' analysis[101] for dam of Fig. 42 subjected to Pacoima 1971 record scaled to moderate (left) and strong (right) intensity. Notice substantial changes in frequency characteristics and developing permanent deformations with increasing intensity

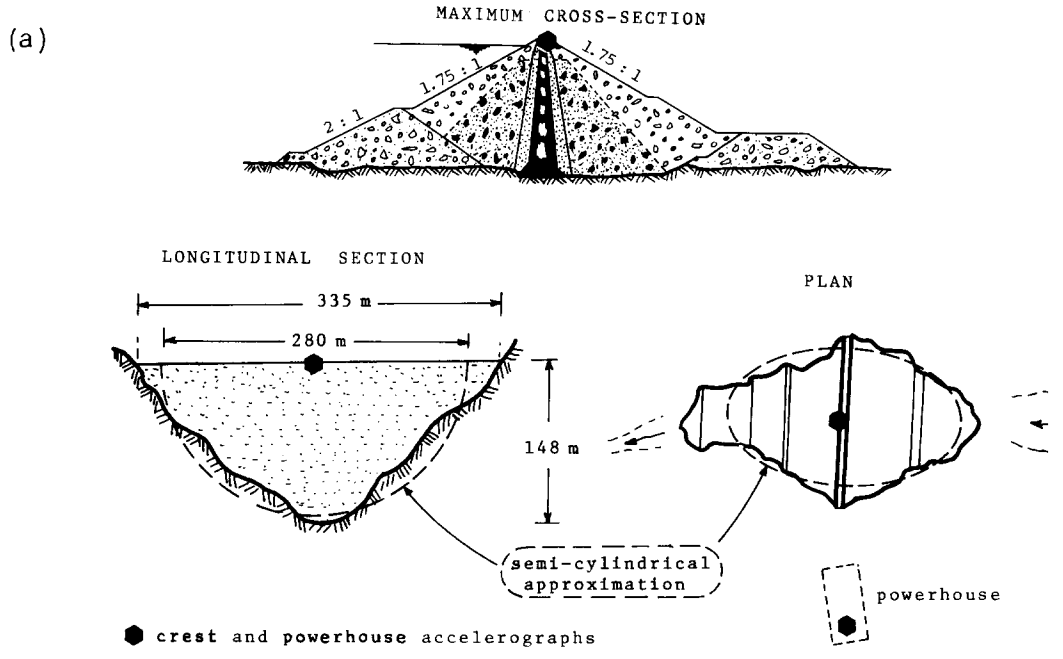

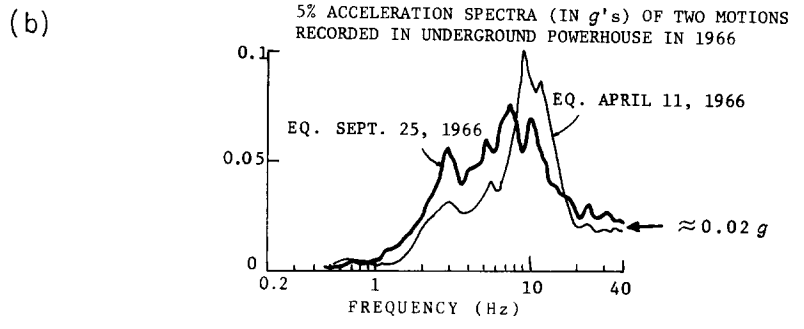

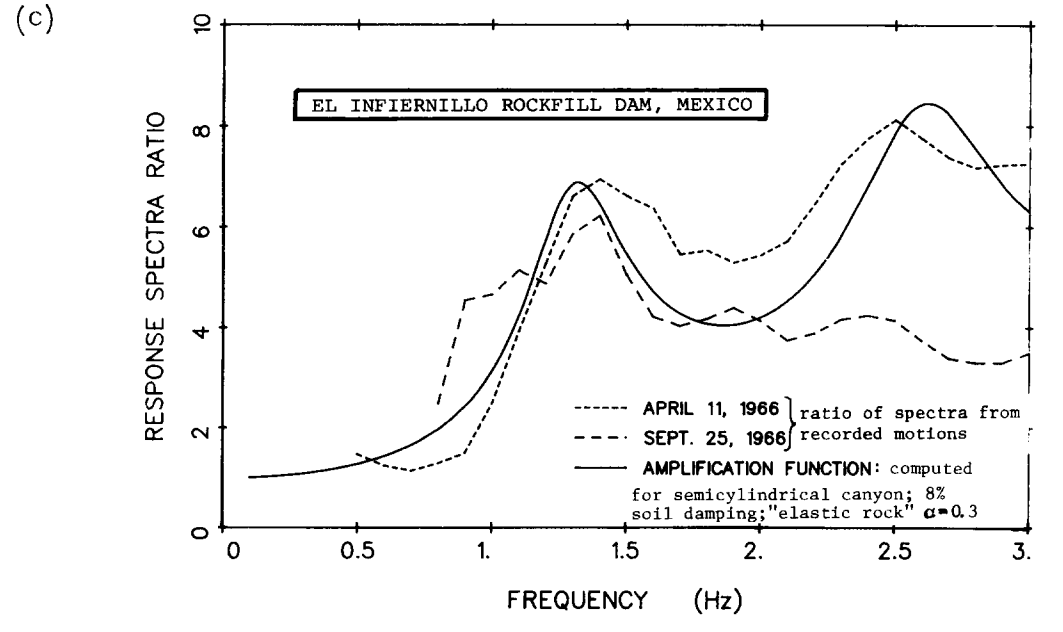

Fig. 44. Case history I: El Infiernillo rockfill dam in Mexico subjected to two weak seismic motions

8.2 Case History II: Linear response of Kisenyama dam

The geometry of this 95 m clayey-core rockfill dam, built i n 1969, is sketched in Fig. 45. The dam is located in a narrow valley and founded on rock (slate)[77]. On September 1969, shortly after completion, the dam was subjected to seismic shaking which produced the shown acceleration records at 5 seismometers installed in the dam (S_1–S_4) and at the downstream rock outcrop (S_5). No analysis was performed in this case, since the rock motion was not available in an appropriate base-line-corrected form.

Nevertheless, the substantial amplification (by a factor of about 10) of the acceleration only at the crest, and the resulting sharp attenuation of acceleration peaks with depth, are reminiscent of the distributions of peak accelerations portrayed in Fig. 27 (homogeneous dam semi-cylindrical canyon) and in Fig. 15 (plane inhomogeneous model with $G \sim z^{2/3}$). Similar trends were also observed in the respective longitudinal records of seismometers S_1–S_5.

Since these motions were too small for this modern rockfill dam ($C \approx 360$ m/s) to develop any noticeable nonlinearities, it may be concluded that it is primarily the narrow canyon and soil inhomogeneity which have caused the relatively high accelerations at the crest of the dam.

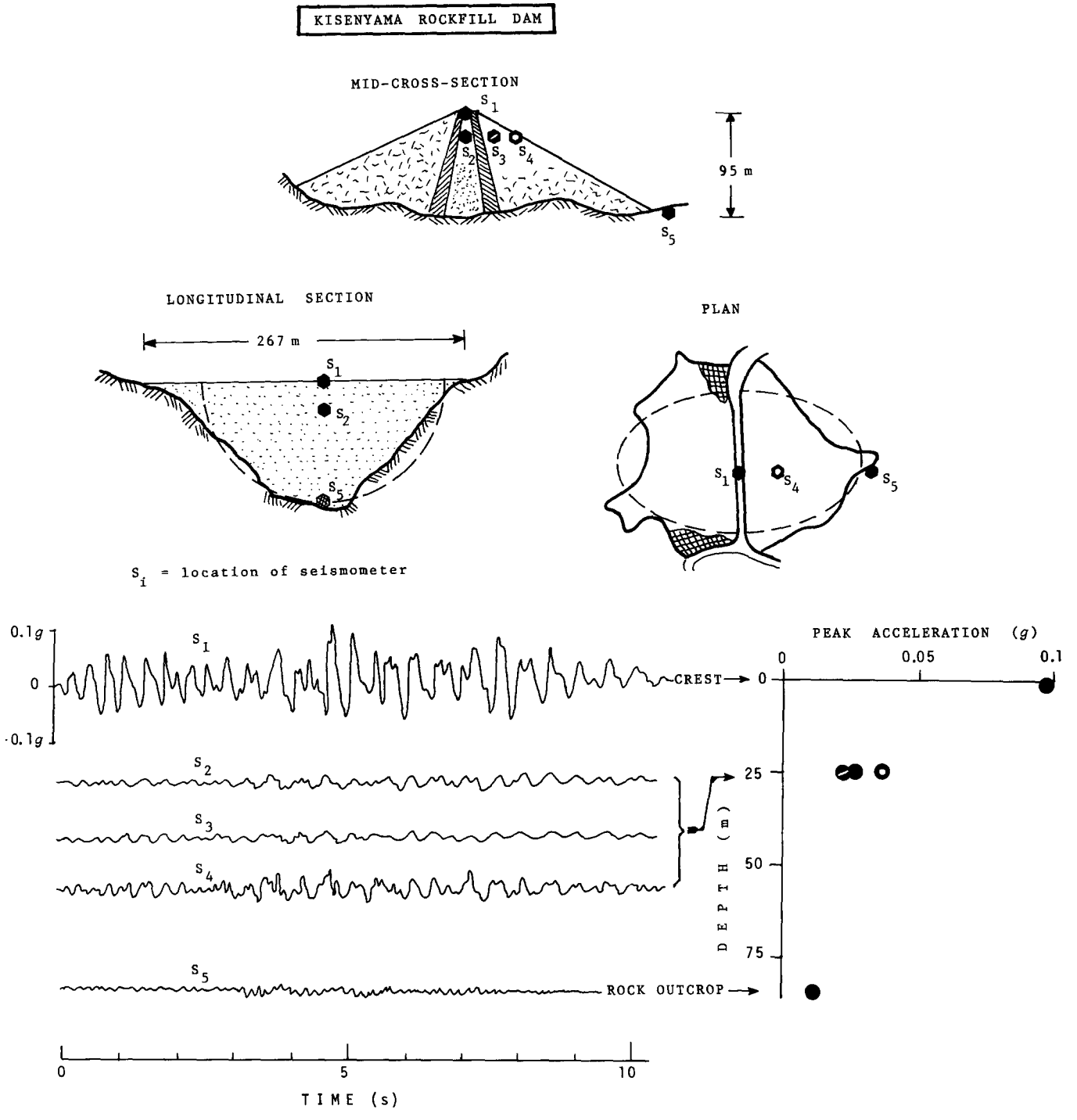

Fig. 45. Case history II: Kisenyama rockfill dam in Japan subjected to a weak seismic shaking

8.3 Case History III: Linear response of Bouquet dam

The cross-section and profile of this 60 m high earthfill dam are shown at the top of Fig. 47. It is built as a relatively wide trapezoidal-shaped valley and consists mainly of a compacted fill of sandy clay. As already mentioned in preceding sections, Keightly[50,51] performed field measurements of the steady-state response of this dam, excited by a shaking machine located at the crest (Fig. 46). He thus obtained estimates of: (i) natural frequencies; (ii) distribution of mode displacements with depth and along the crest of the dam; and (iii) steady-state displacement transfer functions.

As mentioned in conjunction with Fig. 11, a plane inhomogeneous shear-beam model with $G \sim z^{2/3}$ would anticipate not only the measured major natural frequencies of the dam, but also the sharp attenuation of fundamental and second mode displacements with depth[32,38]. By contrast, the homogeneous model failed to explain such a sharp distribution of displacements [Figs 1 and 11].

Moreover, a very good prediction of the recorded displacement transfer functions at several recording stations along the surface was afforded by the approximate 3-D shear-beam model of Ohmachi[90], assuming the 2/3-power variation of shear modulus with depth. Fig. 46 portrays the comparison of predictions with measurements for two stations near the mid-crest of the dam. Evidently, the performance of this model is quite satisfactory, despite of the fact that it does overestimate the first resonant peak.

8.4 Case History IV: Moderately nonlinear response of Long Valley dam

This dam, located in California is shown in plan and cross-section in Fig. 47. It rises about 38 m above the original streambed elevation and 60 m above the bedrock on which it rests. It is essentially a uniform dam consisting mainly of compacted fill of silty sand and gravel, having a permeability coefficient of about 10^{-5} cm/s[99]. In May of 1980 the dam was subjected to a series of moderate earthquakes, three of which had magnitudes of about 6. The dam was instrumented with 22 channels of strong motion recording devices.

Figure 47 shows the peak values of accelerations recorded during the strongest event. Notice that the peak accelerations in rock near the downstream base were about 0.17 g and 0.24 g in upstream-down-stream and longitudinal direction, respectively. They were amplified to about 0.52 g and 0.49 g, respectively, at the crest of the dam.

Some inelastic action of the constituent material during such shaking is inevitable. In fact, although the dam suffered no discernible damage, some indirect evidence of nonlinear behaviour does exist. Just beyond the toe of the

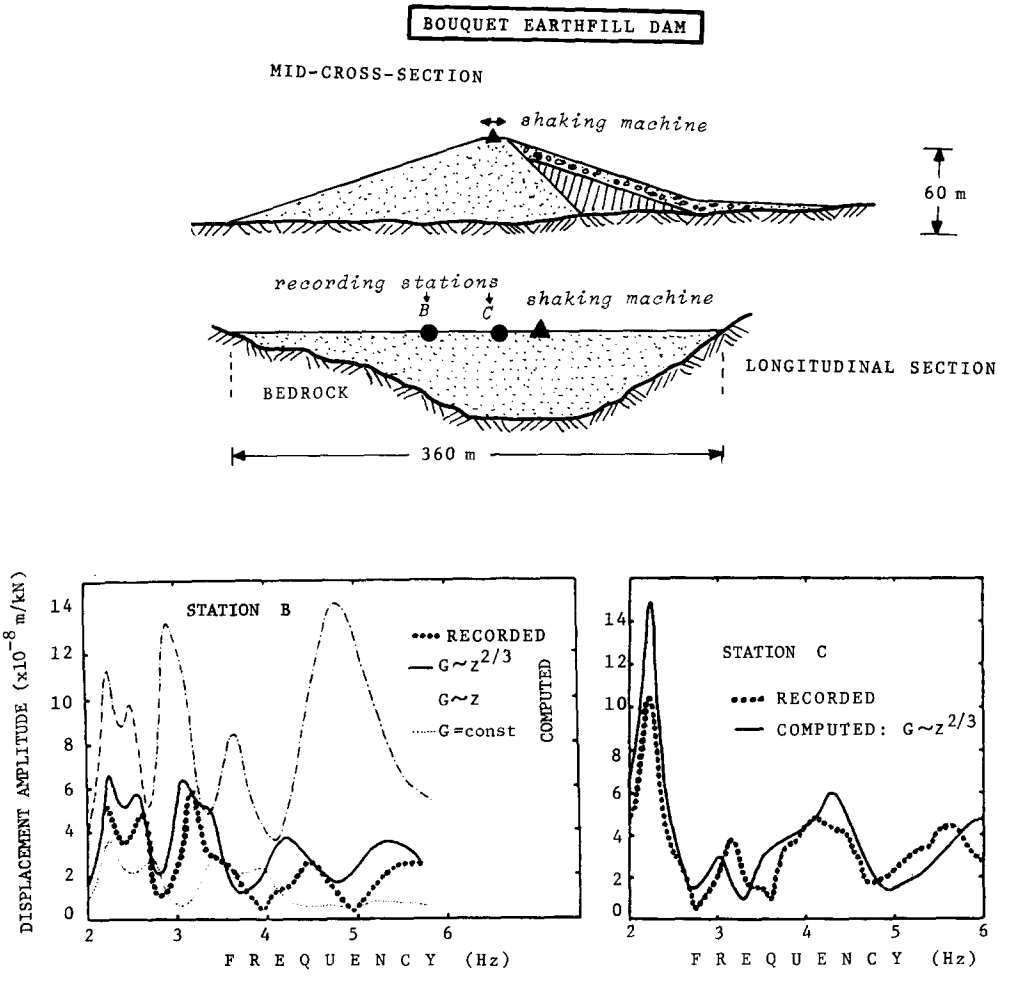

Fig. 46. Case history III: Full-scale forced vibration tests on Bouquet earthfill dam in California. Analysis results from Ref. 75

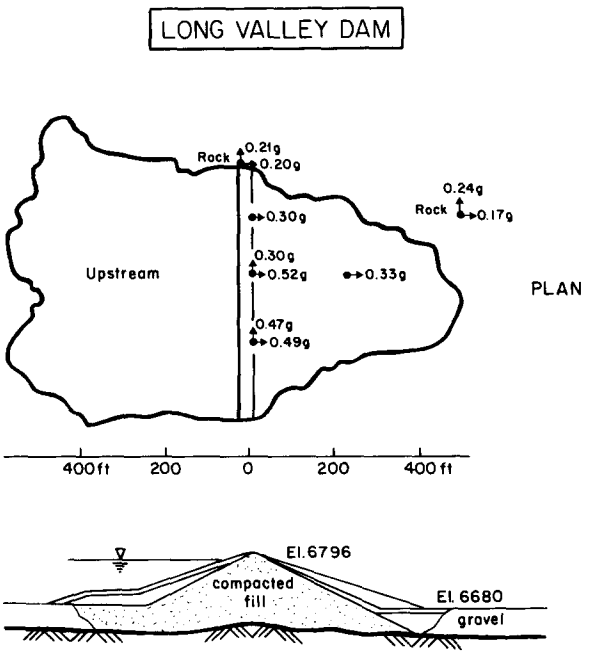

Fig. 47. Case history IV: Long Valley earthfill dam in California subjected to moderately strong seismic excitation

dam water was observed to come from the ground surface, with the flow continuing for several minutes after the earthquake – evidence of liquefaction of the loosely compacted fill in this region[99]. Moreover, a marked increase in flow occurred in the toe drains (from 200 to 460 gpm) and in the spillway tunnel drain (from 310 to 790 gpm), indicative of cracking and of loosening of the rock structure in the abutment[99].

It is worth comparing the recorded peak values of lateral accelerations with those plotted in Fig. 42a. The latter were computed with LISB[101] for a fairly similar silty-clayey 40 m-high dam, under plane conditions. Clearly, the observations are consistent with the analytical results, with the recorded crest amplification only slightly exceeding the one computed for the hypothetical 40 m-high dam subjected to the Eureka record.

However, some differences in material and geometric characteristics between the two dams are worth keeping in mind. The Long Valley Dam: (i) is built in a relatively narrow valley, the abutments of which would provide a stiffening effect that is not modelled in the plane-strain analysis yielding Fig. 42; and (ii) is underlain by an additional 20 m-thick compacted fill which would increase its overall flexibility. It appears that, for moderately-strong nonlinear response, the second effect may to a large extent compensate for the first effect; hence the good agreement measured and computed peak response values.

A more detailed analysis including the records of the other shocks is, of course, necessary.

8.5 Case History V: Nonlinear response of L. Anderson dam

Leyroy Anderson Dam was built in California in 1950. It is a 72 m-high earth and rockfill embankment with a wide central core (Fig. 48). In April 24, 1984, the dam was severely shaken during the Morgan Hill Earthquake, the epicentre of which was about 16 km from the dam. Two accelerographs, one at the crest and the other at the 'free-field' a few hundred feet downstream of the toe of the dam, gave the records shown in Fig. 48. The crest instrument recorded peak accelerations of 0.63 g (lateral), 0.39 g (longitundinal), and 0.20 g (vertical).

As a result of the shaking, the dam suffered some damage, consisting mainly of two sets of logitudinal cracks on the crest, as sketched in the plan of Fig. 48. The length of each set of cracks was about 300 m; the maximum crack opening near the middle of the crest was about 2 cm; and the maximum depth of an upstream crack (revealed through a trench) was nearly 2 metres. Only in three out of nine crack locations explored with trenches the cracks did penetrate into the core.

There should not be much doubt, therefore, that the dam experienced nonlinear inelastic deformations during this seismic shaking. The recorded peak crest-acceleration amplification, equal to about 1.50 in the upstream-downstream direction (as well in the logitudinal direction), is generally consistent with the amplification of similarly strong motions computed for hypothetical dams and shown in Fig. 42b (40 m-high model) and in Fig. 18 (120 m-high model). A more detailed analysis is currently being performed.

9. CONCLUDING REMARKS

To make a realistic prediction of the response of an earth dam to a particular earthquake shaking, careful consideration must be given to the potential effects of the following major phenonema/factors:

(a) nonlinear-inelastic soil behaviour
(b) dependence of soil stiffness on confining pressure
(c) narrow canyon geometry
(d) dam-alluvium interaction.

Depending on the particular situation, one or more of these phenomena may have an appreciable influence on the response of the dam and will thereby dictate the proper method of analysis. Comprehensive numerical procedures which could rationally simulate all of the foregoing phenomena, while in principle feasible, they may be prohibitively expensive at the present time.

Based on evidence presented in this paper, it appears that the magnitude of nonlinearities is the single major factor in deciding which phenomena to attempt to simulate in the analysis and with what degree of sophistication. Whenever nonlinearities are unimportant, as may be the case with stiff modern dams subjected to ground shaking having peak accelerations of the order of 0.20 g or less, it seems that all the other listed three factors, i.e., (b), (c) and (d), should be properly modelled. Note however, that some of the effects (b) and (c) may be counterbalanced by the effect of factor (d). Indeed, as the degree of inhomogeneity (due to dependence of stiffness on confining pressure) increases and as the canyon becomes narrower a 'whip-lash' effect tends to occur; as a result, high absolute accelerations and high shearing deformations develop at the uppermost quarter of the dam, by the crest (recall Figs 14–15, and Figs 24 and 27). On the other hand, the interaction with a relatively soft alluvial valley tends to: increase the effective damping, due to increasing radiation of wave energy; to filter some

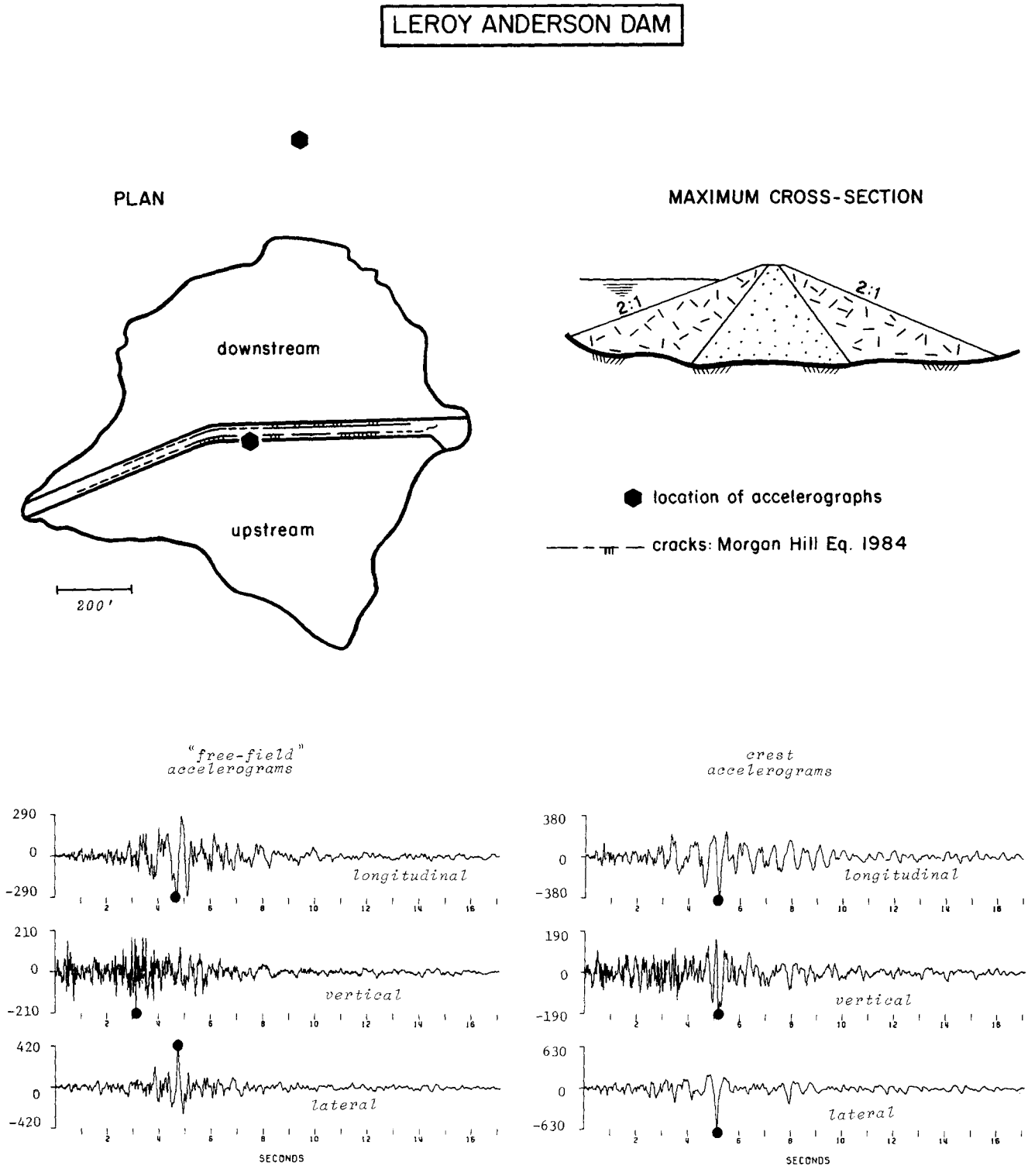

Fig. 48. Case history V: Leroy Anderson earthfill dam in California subjected to strong seismic excitation

of the high frequency components of excitation, which tend to produce the high crest accelerations; and to change the natural mode characteristics of the system, counteracting the respective changes caused by factors (b) and (c).

Thus, a preliminary assessment of the importance of each of these three factors, (b), (c) and (d), using simple analysis procedures such as some of those described in the paper, is recommended as a first step, before embarking into comprehensive sophisticated numerical computations.

For the more interesting case of designing against very strong potential shaking, during which the dam is expected to respond in a highly nonlinear – inelastic fashion, the other listed phenomena may lose some of their importance. This was evidenced: (i) in Fig. 18 – the effects of stiffness inhomogeneity on near-crest accelerations, being substantial in the linear case, withered away or even reversed during strongly inelastic oscillations; (ii) in Table 4 – the effects of 3-D canyon geometry, being again appreciable in the linear range, seem to tend to reverse with increasing inelastic action;

and (iii) in Case Histories IV and V – the amplification of crest acceleration was seemingly consistent with the relatively small amplification values anticipated on the basis of plane-strain inelastic analyses (Fig. 42).

It is emphasized, however, that the foregoing potentially very significant conclusions are based on a rather limited number of theoretical and field studies. More research is needed in the area of inelastic response, including comprehensive parameter studies using realistic material parameters and systematic evaluation of response case histories, before definitive conclusions may be safely drawn.

Finally, another topic deserving systematic attention refers to the nature of excitation assumed in the 3-D analyses of canyon effects. So far, all such studies have invariably assumed that the points at the dam-valley interface experience *identical and sychronous (in-phase) oscillations;* hence, a single accelerogram sufficed to describe the excitation. Evidently reality is more complicated. Seismic shaking is the result of a multitude of body and surface waves striking at various angles and creating reflections and diffraction phenomena. The resulting oscillation differ (in phase, amplitude and frequency characteristics) from point to point along the dam-valley interface.

The simplifying assumption of identical and sychronous excitation, advanced solely for mathematical convenience, may be reasonable only for the relatively low frequencies associated with the first one or two fundamental modes of the dam. At higher frequencies, when the wavelengths of the incident seismic waves become equal to or smaller than a characteristic dimension of the dam (e.g., its height), substantial differences are expected to arise in both magnitude and phase angle of the motions at various points of the base; such differences would render the 'in-phase' hypothesis unrealistic. Since it is precisely the higher modes which trigger the aforementioned 'whip-lash' effect in tall dams built in narrow canyons, it is reasonable to expect that assuming a more realistic excitation than rigid-body motion would tend to reduce the high crest amplifications computed by current method of analysis (beneficial effect). However, other effects that can hardly be anticipated with the presently assumed excitation (i.e., large shearing deformations and tensile strains in the logitudinal direction, potentially leading to treacherous lateral cracks) may also arise. Hence, the need for theoretical research and field studies in this area.

ACKNOWLEDGEMENTS

The research of the Author and his coworkers reported in this paper has been supported by the U.S. National Science Foundation through Grant No. CEE-8205345 and Grant No. ECE-8413472 to Rensselaer Polytechnic Institute. The help by Panos Dakoulas in obtaining many of the reported results, and the several suggestions by Ricardo Dobry are acknowledged with gratitude.

LITERATURE CITED

1 Abdel-Ghaffar, A. M. and Scott, R. F. Analysis of an earth dam response to two earthquakes, *J. Geotech. Engrg., ASCE* 1979, **105**, GT12, 1379–1404

2 Abdel-Ghaffar, A. M. and Scott, R. F. Shear moduli and damping factors of earth dams, *J. Geotech. Engrg., ASCE* 1979, **105**, 1405–1426

3 Abdel-Ghaffar, A. M., Scott, R. F. and Craig, M. M. Full-scale experimental investigation of a modern earth dam, *EERL-80-02 Report*, 1980, Caltech, Pasadena

4 Abdel-Ghaffar, A. M. and Koh, A.-S. Longitudinal vibration of non-homogeneous earth dams, *Earthq. Engrg. and Struct. Dyn.* 1981, **9**(3), 279–305

5 Abdel-Ghaffar, A. M. and Koh, A.-S. Earthquake-induced longitudinal strains and stresses in non-homogeneous earth dams, *Earthq. Engrg. and Struct. Dyn.* 1981, **9**(6), 521–541

6 Abdel-Ghaffar, A. M. and Koh, A.-S. Three-dimensional dynamic analysis of nonhomogeneous earth dams, *Soil Dyn. and Earthq. Engrg.* 1982, **1**, 136–144

7 Ambraseys, N. N. On the shear response of a two-dimensional truncated wedge subjected to an arbitrary disturbance, *Bull. Seism. Soc. Am.* 1960, **50**(1), 45–56

8 Ambraseys, N. N. The seismic stability of earth dams, Proc. 2nd World Conf. on Earthq. Engrg., Tokyo, III, 1960, 1345–1363

9 Ambraseys, N. N. and Sarma, S. K. The response of earth dams to strong earthquakes, *Geotechnique* 1967, **17**(2), 181–213

10 Chopra, A. K. Earthquake response of earth dams, *J. Soil Mech. and Found. Div., ASCE* 1967, **93**, SM2

11 Clough, R. W. and Chopra, A. K. Earthquake stress analysis in earth dams, *J. Engrg. Mech., ASCE* 1966, **92**, EM2

12 Chopra, A. K., Dibaj, M., Clough, R. W., Penzien, J. and Seed, H. B. Earthquake analysis of earth dams, Proc. 4th World Conf. on Earthq. Engrg., Santiago, 1969

13 Chopra, A. K. and Perumalswami, P. R. Dam-foundation interaction during earthquakes, Proc. 4th World Conf. on Earthq. Engrg., Santiago, 1969

14 Castro, G. Liquefaction and cyclic mobility of saturated sands, *J. Geotech. Engrg., ASCE* 1975, **101**, GT6, 551–569

15 Castro, G. and Poulos, S. J. Factors affecting liquefaction and cyclic mobility, *J. Geotech. Engrg., ASCE* 1977, **103**, GT6, 501–516

16 Chen, A. T. F. Transmitting boundaries and seismic response, *J. Geotech. Engrg., ASCE* 1985, **111**(2), 174–180

17 Constantinou, M. C., Gazetas, G. and Tadjbakhsh, I. Stochastic seismic sliding of rigid mass supported through non-symmetric friction, *Earthq. Engrg. and Struct. Dyn.* 1985, **12**, 777–793

18 Constantopoulos, I. V. Amplification studies for a nonlinear hysteretic soil model, *Report R73-46*, MIT, 1973

19 Dakoulas, P. Contributions to seismic analysis of earth dams, PhD Thesis, Rensselaer Polytechnic Institute, 1985

20 Dakoulas, P. and Gazetas, G. A class of inhomogeneous shear models for seismic response of dams and embankments, *Soil Dyn. and Earthq. Engrg.* 1985, Vol. 4, No. 4, 166–182

21 Dakoulas, P. and Gazetas, G. Seismic shear strains and seismic coefficients in dams and embankments, *Soil Dyn. and Earthq. Engrg.* 1986, Vol. 5, No. 2, 75–83

22 Dakoulas, P. and Gazetas, G. Seismic lateral vibration of embankment dams in semi-cylindrical valleys, *Earthq. Engrg. and Struct. Dyn.* 1986, No. 14, 19–40

23 Dakoulas, P. and Gazetas, G. Nonlinear response of embankment dams, Proc. 2nd Int. Conf. Soil Dyn. and Earthq. Engrg., June/July, 1985, Springer-Verlag, 5/29–44

24 Dezfulian, H. Effects of silt content on dynamic properties of sandy soils, Proc. 8th World Conf. Earthq. Engrg., San Francisco, **III**, 63–70

25 Dibaj, M. and Penzien, J. Response of earth dams to travelling seismic waves, *J. Soil Mech. and Found. Div., ASCE* 196995, SM2

26 Dobry, R., Mohamad, R., Dakoulas, P. and Gazetas, G. Liquefaction evaluation of earth dams – a new approach, Proc. 8th World Conf. Earthq. Engrg., San Francisco, 1984, **III**, 33–340

27 Elgamal, A. W. M., Abdel-Ghaffar, A. M. and Prevost, J. H. Nonlinear earthquake response analysis of earth dams, Princeton Univ. Research Report, 1984

28 Frazier, G. A. Vibration characteristics of three dimensional solids with application to earth dams, PhD Thesis, Montana State University, 1969

29 Finn, W. D. L. Dynamic analysis of soil structures, Implementation of Computer Proced. Stress-Strain Laws in Geotech. Engrg., (Eds C. S. Desai and S. K. Saxena), Durham: Acron Press, 1981

30 Franklin, A. G. and Chang, F. K. Earthquake resistance of earth and rock-filled dams, rep. 5: permanent displacements of earth embankments by newmark sliding block analysis, Misc. Pap. S-71-17, Waterways Experimental Station, Vicksburg, 1977

31 Gazetas, G. 2-Dimensional lateral and longitudinal seismic stability of earth and rockfill dams, Proc. 7th World Conf. Earthq. Engrg., Instanbul, 1980, **8**, 109–116

32 Gazetas, G. A new dynamic model for earth dams evaluated through case histories, *Soils and Foundations* 1981, **21**(1), 67–68

33 Gazetas, G. Shear vibrations of vertically inhomogeneous earth dams, *Int. J. for Num. and Anal. Methods in Geomech.* 1982, **6**(1), 219–241

34 Gazetas, G. Longitudinal vibrations of embankment dams, *J. Geotech. Engrg., ASCE* 1981, **107**, GT1, 2–40

35 Gazeras, G. Vertical oscillation of earth and rockfill dams: analysis and field observation, *Soils and Foundations* 1981, **21**(4), 265–277

36 Gazetas, G., Debchaudhury, A. and Gasparini, D. A. Random vibration analysis of earth dam seismic response, *Geotechnique* 1981, **31**, 261–279

37 Gazetas, G., Debchaudhury, A. and Gasparini, D. A. Stochastic estimation of the nonlinear response of earth dams to strong earthquakes, *Soil Dyn. and Earthq. Engrg.* 1982, **1**, 39–46

38 Gazetas, G. and Abdel-Ghaffar, A. M. Earth dam characteristics from full-scale vibrations, Proc. X World Conf. Soil Mech. and Found. Engrg., Stockholm, 1981, **III**, 207–210

39 Ghaboussi, J. and Wilson, E. Seismic analysis of earth dam-reservoir systems, *J. Soil Mech. and Found. Div., ASCE* 1973, **99**, SM10, 849–862

40 Hardin, B. and Black, W. Sand stiffness under various triaxial stresses, *J. Soil Mech. and Found. Div., ASCE* 1966, **92**, SM2

41 Hatanaka, M. 3-Dimensional consideration on the vibration of earth dams, *J. Jap. Soc.: Civ. Engrs.* 1952, **37**, 10

42 Hatanaka, M. Fundamental consideration on the earthquake resistant properties of the earth dam, *Bull. No. 11*, Disaster Prevention Research Inst., Kyoto Univ., 1955

43 Hatano, T. and Watanabe, H. Seismic analysis of earth dams, Proc. 4th World Conf. on Earthq. Engrg., Santiago, 1969

44 Hayashi, M., Komada, H. and Fujiwara, Y. 3-Dimensional dynamic response and earthquake resistant design of rockfill dam against input earthquake in direction of dam axis, Proc. 5th World Conf. Earthq. Engrg., 1974

45 Hynes-Griffin, M. E. and Franklin, A. G. Rationalizing the seismic coefficient method, Waterways Experiment Station Report, Vicksburg

46 Idriss, I. M., Lysmer, J., Hwang, R. and Seed, H. B. QUAD-4 A computer program for evaluating the seismic response of soil structures by variable damping finite element procedures, *Report No. EERC 73-16*, Univ. of Calif., Berkeley, 1973

47 Ishizaki and Hatekeyama, Consideration on the dynamical behavior of earth dams, *Bull. No. 52*, Disaster Prevention Research Inst., Kyoto Univ., 1963

48 Joyner, W. B. and Chen, A. T. F. Calculation of nonlinear ground response in earthquakes, *Bull. Seism. Soc. Am.* 1975, **65**(5), 1315–1336

49 Kausel, E. and Roesset, J. M. Soil amplification: some refinements, *Soil Dyn. and Earthq. Engrg.* 1984, **3**(3), 116–123

50 Keightley, W. O. Vibration tests of structures, Earthquake Engineering Research Laboratory, Caltech, Pasadena, 1963

51 Keightly, W. O. Vibrational characteristics of an earth dam, *Bull. Seism. Soc. Am.* 1966, **56**(6), 1207–1226

52 Knox, D. P., Stokoe, K. H., II and Kopperman, S. E. Effect of state of stress on velocity of low amplitude shear waves propagating along principal stress directions in dry sand, Geotech. Engrg., *Rep. GR82-23*, The Univ. of Texas, Austin, 1982

53 Kokusho, T. and Esashi, Y. Cyclic triaxial test of sands and coarse materials, Proc. X World Conf. Soil Mech. and Found. Engrg., Stockholm, 1981

54 Kuribayashi, E., Iwasaki, T. and Tatsuoka, F. Effects of stress-strain conditions on dynamic properties of sands, Proc. Jap. Soc. Civ. Engrgs., 1975, No. 242

55 Makdisi, F. I. and Seed, H. B. Simplified procedure for estimating dam and embankment earthquake-induced deformations, *J. Geotech. Engrg., ASCE* 1978, **104**, GT7, 849–867

56 Makdisi, F. I. and Seed, H. B. Simplified procedure for evaluating embankment response, *J. Geotech. Engrg., ASCE* 1979, **105**, GT12, 1427–1434

57 Makdisi, F. I., Kagawa, T. and Seed, H. B. Seismic response of earth dams in triangular canyons, *J. Geotech. Engrg., ASCE* 1982, **108**, GT10, 1328–1337

58 Mansuri, T. A. and Nelson, J. D. Dynamic response and liquefaction of earth dams, *J. Geotech. Engrg., ASCE* 1983, **109**(1), 89–100

59 Martin, G. R. The response of earth dams to earthquakes, PhD Thesis, Univ. of Calif., Berkeley, 1965

60 Marcuson, W. F., III and Krinitzsky, E. L. Dynamic analysis of Fort Peck Dam, Waterways Experiment Station Report S-76-I, Vicksburg, 1976

61 Martinez, B. and Bielak, J. On the three-dimensional seismic response of earth structures, Proc. 7th World Conf. Earthq. Engrg., Instanbul, 1980, **8**, 523–528

62 Mathur, J. N. Analysis of the response of earth dams to earthquakes, PhD Thesis, Univ. of Calif., Berkeley, 1969

63 Medvedev, S. and Sinitsym, A. Seismic effects on earth fill dams, Proc. 3rd World Conf. Earthq. Engrg., New Zealand, 1965, Paper IV/M/18

64 Mejia, L. H., Seed, H. B. and Lysmer, J. Dynamic analysis of earth dam in three dimensions, *J. Geotech. Engrg., ASCE* 1982, **108**, GT12, 1586–1604

65 Mejia, L. H. and Seed, H. B. Comparison of 2-D and 3-D dynamic analyses of earth dams, *J. Geotech. Engrg., ASCE* 1983, **109**, GT11, 1383–1398

66 Mohamad, R., Dakoulas, P., Gazetas, G. and Dobry, R. Liquefaction flow failure evaluation of earth dams, Proc. XI Conf. Soil Mech. Found. Engrg., San Francisco, 1985

67 Mohamad, R. Evaluation of seismically induced liquefaction flow failure of earth dams, PhD Dissertation, Rensselaer Polytechnic Institute, 1985

68 Mononobe, H. A. *et al.* Seismic stability of the earth dam, Proc. 2nd Congress on Large Dams, Washington DC, IV, 1936

69 Mori, Y. *et al.* Dynamic properties of the Ainono and Ushino dams, *J. Jap. Soc. Civ. Engrs.* 1975, 240

70 Moriwaki, V. *et al.* Cyclic strength and properties of tailing slimes, Dynamic Stability of Tailing Dams, ASCE, 1982, 1–30

71 Newmark, N. M. Effects of earthquakes on dams and embankments, *Geotechnique* 1965, **15**(2), 139–160

72 Nose, M. and Baba, K. Dynamic behavior of rockfill dams, Design of Dams to Resist Earthquake, ICE, London, 1980, 55–64

73 Ohmachi, T. Analysis of dynamic shear strain distributed in 3-dimensional earth dam models, Proc. Int. Conf. on Recent advances in Geotech. Earthq. Engrg. and Soil Dyn., St. Louis, 1981, **1**, 459–464

74 Ohmachi, T. and Tokimatsu, K. Simplified method for 3-dimension dynamic analysis of embankment dams, Proc. 4th Int. Conf. Num. Meth. Geomech., 1982, **1**, 411–419

75 Ohmachi, T. and Soga, S. Practical method for dynamic interaction analysis of three dimensional dam-foundation system, Proc. 8th Worl Conf. on Earthq. Engrg., San Francisco, 1984, **III**, 1065–1072

76 Okamoto, S. *et al.* On the dynamical behavior of an earth dam during earthquakes, Proc. 4th World Conf. Earthq. Engrg., Santiago, 1969

77 Okamoto, S. Earthquake resistance of embankment dams, Chap. 15 in Introduction to Earthquake Engineering, John Wiley and Sons, 1973, 427–490

78 Oner, M. Estimation of the fundamental period of large earthfill dams, *Soils and Foundations* 1984, **24**, 1–10

79 Oner, M. Shear vibration of inhomogeneous earth dams in rectangular canyons, *Soil Dyn. and Earthq. Engrg.* 1984, **3**(1), 19–26

80 Papadakis, C. and Wylie, E. B. Seismic shear wave propagation through earth dams, *Soils and Foundations* 1975, **15**, 2

81 Petrovski, J., Paskalov, T. and Jurukovski, D. Dynamic full-scale test of an earthfill dam, *Geotechnique* 1974, **24**(2), 193–206

82 Poulos, S. J., Castro, G. and France, J. W. Procedure for liquefaction evaluation, *J. Geotech. Engrg., ASCE* 1985, **111**(6), 772–792

83 Prange, B. Resonant column testing of rail road ballast, Proc. X World Conf. Soil Mech. and Found. Engrg., Stockholm, 1981, **III**, 273–278

84 Prevost, J. H., Abdel-Ghaffar, A. M. and Elgamal, A. W. M. Nonlinear hysteretic dynamic response of soil systems, *J. Engrg. Mech., ASCE* 1985, **111**(7), 882–897

85 Prevost, J. H., Abdel-Ghaffar, A. M. and Lacy, S. J. 'Nonlinear Dynamic Analysis of Earth Dam: A Comparative Study', *J. Geotech. Engr., ASCE* 1985, **111**(7), 882–897

86 Richart, F. E., Hall, J. R. and Woods, R. D. Vibrations of Soils and Foundations, Prentice Hall, 1970

87 Richart, F. E. and Wylie, E. B. Influence of dynamic soil properties on response of soil masses, Structural and Geotechnical Mechanics, Prentice Hall, 1975, 141–162

88 Roesset, J. Soil amplification of earthquakes, Numerical Methods in Geot. Engrg., (Eds Desai and Christian), McGraw-Hill, 1977

89 Roesset, J. M. and Tassoulas, J. L. Nonlinear soil-structure interaction – an overview, Earthq. Ground Motion and Its Effects on Structures, Appl. Mech. Div., ASCE, 1982, 53
90 Romo, M. P., Ayala, G., Resendiz, D., Diaz, C. R. Response analysis of El Infiernillo and La Villita Dams, Chap. 6 in Performance of El Infiernillo and La Villita Dams Including the Earthquake of March 1979, Comision Federal de Electricidad, Mexico, 1980, 87–107
91 Sarma, S. K. Response and stability of earth dams during strong earthquakes, Paper GL-79-13, Waterways Experiment Station, Vicksburg, 1979
92 Sarma, S. K. Seismic stability of earth dams and embankments, *Geotechnique* 1975, **25**(4), 743–761
93 Seed, H. B. and Martin, G. R. The seismic coefficient in earth dam design, *J. Geotech. Engrg., ASCE* 1966, 92
94 Seed, H. B. Stability of earth and rockfill dams during earthquakes, in Embankment-Dam Engrg., Casagrande Vol., (Eds Hirschfeld and Poulos), John Wiley, 1973
95 Seed, H. B. Soil liquefaction and cyclic mobility evaluation for level ground during earthquakes, *J. Geotech. Engrg., ASCE* 1979 **105**, GT2, 210–255
96 Seed, B. Considerations in the earthquake design of earth and rockfill dams, *Geotechnique* 1979, **29**(3), 215–263
97 Seed, H. B., Lee, K. L. and Idriss, I. M. An analysis of Sheffield Dam failure, *J. Soil Mech. and Found. Div., ASCE* 1969, **95**, SM6, 1453–1490
98 Seed, H. B., Lee, K. L., Idriss, I. M. and Makdisi, F. I. Analysis of the slides in the San Fernando dams during the earthquake of Feb. 9, 1971, Report No. EERC 73-2, Univ. of Calif., Berkeley, 1973
99 Seed, H. B. Lessons from the performance of earth dams during earthquakes, Design of Dams to Resist Earthquake, ICE, London, 1980, 251–258
100 Singh, M. P. and Khatua, T. P. Stochastic seismic stability prediction of earth dams, Proc. Earthq. Engrg. and Soil Dyn. Spec. Conf., ASCE, Pasadena, 1978, **II**, 875–889
101 Stara-Gazetas, E. Method for inelastic response analysis of earth dams, PhD Thesis, Rensselaer Polytechnic Institute, 1986
102 Takahashi, T. *et al.* Study on dynamic behavior of rockfill dams, Proc. 6th World Conf. on Earthq. Engrg., New Delhi, 1977, **6**, 2238–2243
103 Terzaghi, K. Mechanics of landslides, The Geological Survey of America, Engineering Geology (Berkey) Volume, 1950
104 Tsiatas, G. and Gazetas, G. Plane-strain and shear beam free vibration of earth dams, *Soil Dyn. and Earthq. Engrg.* 1982, **1**, 150–160
105 Umehara, Y., Ohneda, H. and Matsumoto, K. In-situ soil investigation and evaluation of dynamic properties of sandy soils in very deep sea, Proc. 8th World Conf. Earthq. Engrg., San Francisco, 1984, **III**, 71–78
106 Vrymoed, J. Dynamic FEM Model of Oroville Dam, *J. Geotech. Engrg. Div., ASCE* 1981, **107**, GT8, 1057–1077
107 Zienkiewicz, O. C., Leung, K. H. and Hinton, E. Earth dam analysis for earthquakes: numerical solutions and constitutive relations for non-linear (damage) analysis, Design of Dams to Resist Earthquake, ICE, London, 1980, 141–156